The role of the neck linker and neck in kinesin velocity regulation

Dissertation

zur Erlangung des akademischen Grades
doctor rerum naturalium (Dr. rer. nat.)

vorgelegt dem Rat der Biologisch-Pharmazeutischen Fakultät
der Friedrich-Schiller-Universität Jena

von

Nikolina Kalchishkova

geboren am 10.05.1975
in Yambol, Bulgarien

Gutachter:

1. Prof. Dr. Frank Große
2. Prof. Dr. Reinhard Wetzker
3. Prof. Dr. William O. Hancock

Tag der öffentlichen Verteidigung: 09.02.2009

Table of Contents

Table of Contents I
Abbreviations III
Summary IV
Zusammenfassung VII
1. Introduction 1
1.1 Molecular motors 1
1.2 Kinesin superfamily 2
1.2.1 Conventional kinesin 4
1.2.1.1 Structure 4
1.2.1.1.1 Catalytic core 5
1.2.1.1.2 Neck linker and neck 7
1.2.1.2 Hand-over-hand model of kinesin motility 8
1.3 KIF5A kinesin 11
1.4 Eg5 kinesin 12
1.4.1 Model of dimeric Eg5 motility 13
1.5 Goals of the work 17
2. Materials and Methods 22
2.1 Materials 22
2.1.1 Vectors, cloning- and expression systems 22
2.1.2 Media and cultivation of E. coli 22
2.1.3 Media and cultivation of insect cells 22
2.2 Molecular biology methods 23
2.2.1 Agarose gel electrophoresis 23
2.2.2 DNA extraction from agarose gels 23
2.2.3 Determination of DNA concentration 23
2.2.4 Restriction of DNA by endonucleases 23
2.2.5 Ligation of DNA into plasmid vectors 23
2.2.6 Preparation of plasmid DNA 24
2.2.7 Preparation of competent E. coli cells using the calcium chloride method 24
2.2.8 Transformation of E. coli cells by heat shock 24
2.2.9 Identification of transformed clones 24
2.2.10 PCR 25
2.2.11 Oligonucleotides for PCR 26
2.2.12 Generation of kinesin constructs 28
2.2.12.1 Constructs for expression in E. coli 28
2.2.12.2 Full-length Eg5 construct for expression in insect cells 29
2.3 Biochemical methods 30
2.3.1 SDS-PAGE 30
2.3.2 Western blotting 31
2.3.3 Expression and purification of kinesin constructs 31
2.3.3.1 Proteins expressed in E. coli 31
2.3.3.2 Proteins expressed in insect cells 32
2.3.4 Preparation of microtubules 33
2.3.5 Determination of protein concentration 33
2.4 Activity measurements 33
2.4.1 Motility assay 33
2.4.2 Microscopy 34
2.4.2.1 Light microscopy 34
2.4.2.1 Transmission electron microscopy 34
2.4.3 ATPase activity measurement 34
2.4.4 Kinesin-microtubule binding assay 35

3. Results ... 36
3.1 Construct design ... 36
3.1.1 Full-length and truncated control KIF5A and Eg5 constructs ... 36
3.1.2 Truncated and chimeric constructs to study the role of strand β8 and helix α6 ... 37
3.1.2.1 Truncated KIF5A and Eg5 motor domain constructs ... 37
3.1.2.2 Chimeric KIF5A and Eg5 constructs with β8, α6, neck linker and neck interchanged ... 37
3.1.3 KIF5A and Eg5 chimeras with neck linker and/or neck regions interchanged to study velocity regulation ... 38
3.1.3.1 Chimeras with neck linker and neck regions interchanged ... 38
3.1.3.2 Chimeras with neck regions interchanged ... 39
3.1.4 KIF5A truncated and chimeric constructs to study the role of the neck linker ... 39
3.1.4.1 KIF5A constructs without neck linker, with the half and complete native linker ... 39
3.1.4.2 KIF5A-based chimera with half native linker fused to the Eg5 linker and neck ... 40
3.2 Purification of recombinant kinesins ... 41
3.2.1 Purification from E. coli ... 41
3.2.2 Purification of the full-length Eg5 from insect cells ... 44
3.3 ATPase activity, microtubule binding and motility ... 45
3.3.1 Full-length KIF5A ... 46
3.3.2 Full-length Eg5 ... 47
3.3.3 Control KIF5A and Eg5 constructs ... 48
3.3.4 KIF5A and Eg5 constructs to study the role of strand β8 and helix α6 ... 50
3.3.4.1 Truncated KIF5A and Eg5 motor domains ... 50
3.3.4.2 Chimeric KIF5A and Eg5 proteins with β8, α6, neck linker and neck interchanged ... 52
3.3.5 KIF5A and Eg5 chimeras with neck linker and/or neck regions interchanged ... 53
3.3.5.1 Chimeric KIF5A and Eg5 with neck linker and neck interchanged ... 53
3.3.5.2 Chimeric KIF5A and Eg5 with neck interchanged ... 54
3.3.6 KIF5A proteins to study the role of the linker in motility generation ... 56
3.3.6.1 Truncated KIF5A with either the half or the full neck linker ... 56
3.3.6.2 Chimeric KIF5A construct with half native linker fused to the Eg5 linker and neck ... 56
3.3.7 Summary of the results ... 58
4. Discussion ... 62
4.1 Control KIF5A and Eg5 constructs ... 62
4.2 KIF5A and Eg5 motor domains ... 63
4.2.1 The role of strand β8 and helix α6 in activity generation ... 63
4.2.2 The role of the half linker in KIF5A activity ... 65
4.3 The role of KIF5A and Eg5 C-terminal regions in the regulation of motor activity ... 66
4.4 The role of the neck linker and neck in KIF5A and Eg5 velocity regulation ... 67
4.4.1 The effect of the neck linker on KIF5A and Eg5 velocity ... 69
4.4.2 The effect of the neck on KIF5A and Eg5 velocity ... 72
4.4.3 The effect of the first half of KIF5A linker on velocity ... 72
4.5 Conclusions ... 74
5. References ... 75
Acknowledgements ... 84
Curriculum vitae ... 85
Selbstständigkeitserklärung ... 87

Abbreviations

ADP	adenosine-5’-diphosphate
AMP-PNP	adenosine-5’-[β,γ-imido]-triphosphate
ATP	adenosine-5’-triphosphate
AVEC-DIC	Allen video-enhanced differential interference contrast microscopy
BSA	bovine serum albumin
DMSO	dimethylsulfoxide
DTT	dithiothreitol
EDTA	ethylene diamine tetraacetic acid
EGTA	ethylene glycol tetraacetic acid
GST	glutathione S-transferase
IPTG	isopropyl-β-thiogalactopyranoside
MT	microtubules
PAGE	polyacrylamide gel electrophoresis
PBS	phosphate-buffered saline
PIPES	piperazine-N,N’-bis-[2-ethanesulfonic acid]
SDS	sodium dodecyl sulfate
TAE	TRIS-acetate-EDTA
TRIS	tris(hydroxymethyl)-aminomethan

Summary

Kinesins are microtubule-associated motor proteins that perform a wide range of motility functions within cells using the energy released from ATP hydrolysis. They participate in the intracellular transport of different cargoes like cell organelles, vesicles, protein complexes, and additionally, in regulation of microtubule dynamics (Goldstein 2001; Miki *et al.* 2005). Kinesins are also involved in bipolar spindle formation, chromosome transport, and cytokinesis (Sharp *et al.* 2000).

Kinesin molecules represent long-stretched structures revealing distinct globular motor domains. The motor domains are composed of a conserved catalytic core containing the microtubule- and ATP-binding sites, and a so-called mechanical element comprising the neck linker and the neck (Vale & Fletterick 1997).

The present study deals with human neuron-specific kinesin-1 (KIF5A) and human mitotic kinesin-5 (Eg5). Both proteins are plus-end-directed kinesins with conserved motor domains, revealing an about 40% identity in amino acid sequence. In addition, there is a very high level of similarity in their crystal structures (Turner *et al.* 2001). Regardless, the Eg5 moves about 25 times slower than kinesin-1 (Krzysiak *et al.* 2006; Korneev *et al.* 2007). Considering the high level of structural similarity of kinesin-1 and Eg5 on the one hand and the similar strategies in motility generation on the other hand, it has been still unclear which structures or mechanisms are involved in velocity regulation.

It is known that there is a major structural difference in the neck linkers of kinesin-1 and Eg5 (Turner *et al.* 2001). In ADP state, the linkers are undocked, whereby the linker of Eg5 is in a stabile position perpendicular to the core and that of kinesin-1 is disordered and flexible. Upon ATP binding, the linkers of both proteins transit into a docked-to-core position (Kull *et al.* 1996; Turner *et al.* 2001; Yan *et al.* 2004; Sindelar *et al.* 2002).

Using chimeric proteins derived from minus-end-directed and plus-end-directed motors, it has been demonstrated that the neck linker and neck determine kinesin directionality (Case *et al.* 1997; Henningsen & Schliwa 1997; Hirose *et al.* 2000).

An important step towards understanding mechanisms of velocity regulation was made by Case *et al.* (2000) who replaced the neck linker of kinesin-1 by randomly designed, artificial coils which resulted in practically immotile motor constructs

(velocities of 1-4 nm s^{-1}). The question arises whether the insertion of a natural kinesin-related sequence might change the result.

In the present study, a natural wild-type human KIF5A is described, which has been produced together with a set of KIF5A-derived constructs by heterologous expression in *E. coli* without tag and any other artificial sequences. Parallel, diverse kinesin constructs were expressed based on the slowly moving Eg5. Comparing their ATPase, microtubule-binding, and motility activities, it has become possible to deepen the knowledge on molecular mechanisms of kinesin-mediated motility and in particular on structural motifs contributing to velocity regulation.

First, C-terminally truncated KIF5A and Eg5 proteins were expressed and comparatively studied to find out the minimal structural requirements of the catalytic cores to generate ATPase activity. The results demonstrated that to generate activity the catalytic core up to helix α6 has to be preserved and must not be altered.

Moreover, chimeric proteins were produced in which the neck linker and/or the neck of the fast KIF5A and the slow Eg5 motor were interchanged. Motility measurements performed with these proteins demonstrated that the neck linker and neck are involved not only in motility generation in general, but additionally in tuning the velocity of movement. Compared to the neck region, the neck linker was found to affect velocity stronger, but both structures are crucial in kinesin motility cycle.

Recently, a new model on the kinesin mechanochemical cycle has been proposed using molecular dynamics simulations with available kinesin crystal structures (Hwang *et al.* 2008). These simulations indicated that kinesin passes steps of forming and breaking so-called cover-neck bundles during its mechanochemical cycle. It has been suggested that, upon ATP binding, a nine amino acid-long N-terminal region of kinesin-1, termed cover strand, forms a β-sheet with the first half of the linker (strand β9), resulting in a so-called cover-neck bundle. This cover-neck bundle is considered to be a special conformation leading to the kinesin power stroke.

To corroborate this hypothesis experimentally, KIF5A C-terminally truncated motor proteins containing either the half or the full linker were constructed and their ATPase activity was compared with that of a KIF5A construct lacking the linker. It became evident that the first half of the linker (strand β9) is an obligate structural element that essentially affects the ATP hydrolysis cycle.

Finally, a chimera composed of the KIF5A core with its natural half linker (strand β9), fused to Eg5 linker and neck was constructed to study the role of the half linker on motility generation. This construct was ATPase-active and able to move. As the control chimera lacking the half KIF5A linker was found to be immotile, it is concluded that the strand β9 is critical for KIF5A-based motility generation.

The present study provides first evidence that the neck linker and neck elements are involved in determination and regulation of the velocity at which kinesin motors move. The neck linker and neck seem to be evolved to adapt the great variety of cellular motors to different biological functions.

Zusammenfassung

Kinesine sind Motorproteine, welche die aus ATP-Hydrolyse gewonnene Energie nutzen, um sich entlang von Mikrotubuli zu bewegen und dabei verschiedenartige zelluläre Lasten wie z.B. Zellorganellen, Vesikel oder Proteinkomplexe transportieren. Neben ihrer Funktion als cytoplasmatische Transporter sind Kinesine auch an der Regulation der Mikrotubulusdynamik beteiligt (Goldstein 2001; Miki *et al.* 2005) sowie in die Bildung der bipolaren Mitosespindel und in den Transport von Chromosomen involviert (Sharp *et al.* 2000).

Kinesinmoleküle sind langgestreckte filamentöse Strukturen, die in der Regel am N-Terminus zwei globuläre Köpfe (Motordomänen) aufweisen. Jede dieser Motordomänen umfasst einen konservierten katalytischen Kern und ein sogenanntes mechanisches Element. Der katalytische Kern enthält die Mikrotubulus- und ATP-Bindungsstellen. Das mechanische Element wird aus dem Neck-Linker und Neck gebildet (Vale & Fletterick 1997).

In der vorliegenden Arbeit wurden das humane neuronenspezifische KIF5A (Kinesin-1) und das humane mitotische Eg5 (Kinesin-5) untersucht. Beide Proteine sind anterograde Motoren, d.h. sie bewegen sich zum *plus*-Ende der Mikrotubuli. Die Motordomänen von KIF5A und Eg5 weisen eine etwa 40-prozentige Identität in der Aminosäuresequenz sowie eine starke Ähnlichkeit in ihrer strukturellen Organisation auf (Turner *et al.* 2001). Trotz der ausgeprägten Analogie in der Kristallstruktur von Kinesin-1 und Eg5 und damit prinzipiell gleicher Mechanismen der Bewegungserzeugung, bewegt sich Eg5 rund 25-mal langsamer als Kinesin-1 (Krzysiak *et al.* 2006; Korneev *et al.* 2007). Es erhebt sich die Frage, wodurch die Unterschiede in den Geschwindigkeiten auf molekularer Ebene bedingt sind.

Es wurde berichtet, dass sich die Strukturen der Neck-Linker-Region von Kinesin-1 und Eg5 auffällig unterscheiden (Turner *et al.* 2001). Im ADP-gebundenen Zustand sind die Neck-Linker Regionen beider Proteine nicht am katalytischen Kern gebunden (undocked), wobei sich der Eg5 Linker in stabiler senkrechter Position zum Kern befindet, während der Linker von Kinesin-1 ungeordnet und flexibel ist. Nach ATP-Bindung nehmen die Linker-Elemente der beiden Proteine einen am Kern gebundenen (docked) Zustand ein (Kull *et al.* 1996; Turner *et al.* 2001; Yan *et al.* 2004; Sindelar *et al.* 2002).

Anhand chimärer Proteine, die aus Teilen von *plus*-Ende und *minus*-Ende gerichteten Motorproteinen konstruiert wurden, ist gezeigt worden, dass Neck-Linker und Neck-Elemente die Bewegungsrichtung der Kinesine beeinflussen (Case *et al.* 1997; Henningsen & Schliwa 1997; Hirose *et al.* 2000).

Ein wichtiger Schritt zur Aufklärung der Mechanismen der Geschwindigkeits-regulation wurde von Case *et al.* (2000) gemacht. Dabei wurde die Kinesin-1 Neck-Linker-Region durch eine zufällig konstruierte, artifizielle Sequenz (Coil) ersetzt. Das resultierende Motorprotein-Konstrukt war praktisch unbeweglich (es wurden Geschwindigkeiten von 1-4 nm s^{-1} gegenüber 400 nm s^{-1} für das Kontrollprotein gemessen). Eines der Ziele der hier vorliegenden Arbeit war zu prüfen, ob durch Einfügen natürlicher, Kinesin-spezifischer Sequenzen die Geschwindigkeit von KIF5A und Eg5 reguliert werden kann.

Im Gegensatz zu den ubiquitären Mitgliedern der Kinesin-1 Familie (z.B. KIF5B) liegen bislang keine biochemischen oder biophysikalischen Daten zu dem neuronen-spezifischen KIF5A vor. Das in der vorliegenden Arbeit beschriebene humane KIF5A, wurde zusammen mit einer Serie von KIF5A-abgeleiteten Konstrukten durch heterologe Expression aus *E. coli* ohne Tag- oder andere artifizielle Sequenzen gewonnen. Parallel dazu wurden verschiede Eg5-abgeleitete Konstrukte exprimiert. Durch Vergleich von ATPase-, Mikrotubulusbindungs- und Bewegungsaktivität konnten neuartige Erkenntnisse zu den molekularen Mechanismen der Kinesin-vermittelten Motilität gewonnen werden. Insbesondere wurde eine Beziehung von Strukturelementen der Neck-Linker und Neck-Region für die Regulation der Geschwindigkeit von Kinesinen herausgearbeitet.

Um die minimale strukturelle Organisation des katalytischen Kerns von KIF5A und Eg5 zu definieren, wurden zunächst verkürzte KIF5A und Eg5 Proteine exprimiert und bezüglich ihrer ATPase-Aktivität charakterisiert. Es stellte sich heraus, dass für die Ausprägung der vollen Aktivität alle Strukturelemente des katalytischen Kerns bis einschließlich Helix α6 vorhanden sein müssen. Dabei sind Helix α6 und Strand β8 Kinesintyp-spezifisch und können nicht zwischen Eg5 und KIF5A ausgetauscht werden.

Desweiteren wurden chimäre KIF5A und Eg5 Proteine mit vertauschten Neck-Linker und/oder Neck-Elementen exprimiert. Anhand von Bewegungsexperimenten konnte gezeigt werden, dass der Neck-Linker und zu einem gewissen Teil auch der Neck nicht nur an der Bewegungserzeugung im Allgemeinen, sondern auch an der

Regulation der Geschwindigkeit beteiligt sind. Damit wurde zum ersten Mal experimentell nachgewiesen, dass durch Einbau von Neck-Linker und Neck-Elementen aus dem schnelleren KIF5A die Geschwindigkeit von Eg5 erhöht werden kann.

Mit Hilfe von molekulardynamischen Simulationsstudien auf der Basis von Kinesin-Kristallstrukturen wurde vor kurzem ein neues Modell zum mechanochemischen Zyklus des Kinesins vorgeschlagen (Hwang *et al.* 2008). Aus den Simulationen konnte abgeleitet werden, dass die Bewegung von Kinesin durch Bildung und Lösen sogenannter Cover-Neck Bündel generiert wird. Es wurde diskutiert, dass nach ATP-Bindung die neun Aminosäuren lange β0-Region am Kinesin-1 N-Terminus (genannt Cover Strand) ein β-Faltblatt mit dem halben Neck-Linker (β9) bildet und dadurch ein sogenanntes Cover-Neck Bündel entsteht. Die Cover-Neck Bündel-Konformation, in der die halbe Linker-Region involviert ist, wird als spezifisch für die Kinesin-vermittelte Bewegungsgeneration (Power Stroke) diskutiert.

Um dieses Modell experimentell zu bestätigen, wurden im Rahmen dieser Arbeit zusätzlich KIF5A-verkürzte Proteine produziert, die entweder die volle oder nur die halbe Neck-Linker Region beinhalten. Die ATPase-Aktivität dieser Proteine wurde mit einem verkürzten KIF5A, das keine Linker-Sequenz in seiner Struktur enthält, verglichen. Die gewonnenen Ergebnisse zeigen, dass die N-terminale Hälfte der Linker-Region (β9) obligatorisch für die Ausprägung der ATPase-Aktivität ist.

Darüber hinaus wurde die Wirkung des halben Neck-Linker auf der Motilität von KIF5A untersucht. Dazu wurde ein chimäres Protein hergestellt, in dem der KIF5A-Kern mit dem halben Neck-Linker an die Eg5-spezifischen Neck-Linker und Neck-Sequenzen fusioniert wurde. Dieses Protein war ATPase- und bewegungsaktiv. Da das entsprechende Protein ohne den halben KIF5A-spezifischen Neck-Linker bewegungsunfähig war, wird abgeleitet, dass diese Sequenz, die dem β9-Strand entspricht, eine entscheidende Rolle in der KIF5A-vermittelten Bewegungsgeneration ausübt.

Die vorliegende Arbeit liefert erste Hinweise, dass die Geschwindigkeit von Kinesinen durch den Neck-Linker und der Neck-Region vorbestimmt und reguliert wird. Beide Strukturelemente scheinen sich evolutionär entwickelt zu haben, um die verschiedenen Kinesine an die Vielfalt der von ihnen auszuführenden biologischen Funktionen anzupassen.

1. Introduction

1.1 Molecular motors

Motility is a crucial feature of living matter. To maintain motility on different organization levels of life nature has evolved highly specialized motor proteins, which are able to convert chemical into mechanical energy. One main group of motor proteins is working in close association with the cytoskeleton. These motors are involved in diverse processes, including the movement of whole cells, the cell surface transport, cell contraction, the intracellular transport of membranous vesicles and macromolecules, the alignment and segregation of chromosomes, and cytokinesis.

There are three main types of cytoskeleton-associated motors generating active movement: the myosins, kinesins, and dyneins (Figure 1.1). They bind to and move along polarized cytoskeletal filaments in unidirectional fashion. The energy necessary for their movement is supplied by ATP hydrolysis. The energy released is taken to induce large-scale conformational changes within the motor protein, which are followed by pushing the motor protein molecule along its filamentous rail.

The structure of an individual motor protein is optimized to perform its specific function in accordance to the temporal requirements within a cell. The members of the myosin, dynein or kinesin superfamilies share a structurally similar globular motor domain, binding to the corresponding cytoskeletal filaments. The motor domain is followed by a more or less long stalk and/or tail, responsible for cargo binding.

The first cytoskeleton-associated motor protein identified was the skeletal muscle myosin which is basically involved in generating the force for muscle contraction. All motor proteins known to move on actin microfilaments are members of the myosin superfamily. Those ones moving along microtubules are members of either the kinesin superfamily or the dynein family.

The numbers of motors widely vary not only between different organisms, but also between different cell types of one and the same organism. In yeast, for example, 6 kinesins, 5 myosins and 1 dynein have been found, while mammals have genes for more than 40 kinesins, 40 myosins, and over a dozen dyneins (Schliwa & Woehlke 2003). Despite the fact that many motors are not yet characterized, remarkable insights into the motor mechanochemistry and function have been gained.

The velocities at which the motor proteins move vary: from about 0.2 to 60 μm s^{-1} for myosins, and about 0.02 to 2 μm s^{-1} for kinesins, respectively. These differences are

supposed to arise from fine-tuning of the mechanochemical cycle. But, it has been still unknown what detailed mechanism or which structures are involved in velocity regulation.

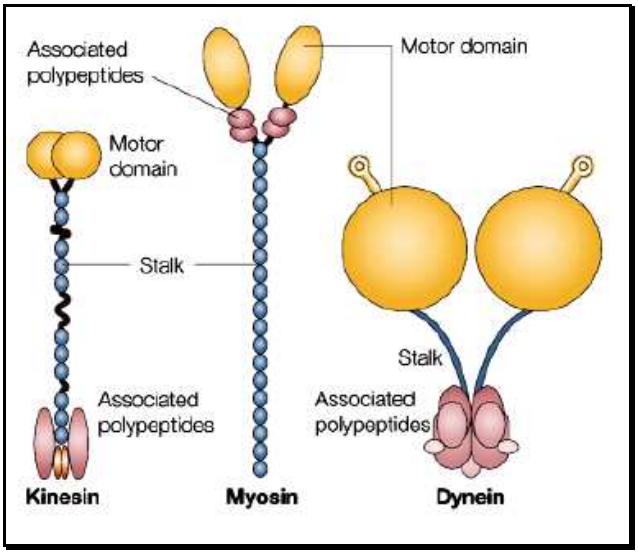

Figure 1.1 *Cytoskeleton-associated motor proteins.*
Conventional kinesin, muscle myosin, and cytoplasmic dynein are dimeric proteins with two distinct globular motor domains shown in yellow. The stalks which form extended coiled-coils are depicted in blue. Within cells, the dimeric motors are accompanied by associated polypeptides, or light chains (two for kinesin, four for myosin and a complex set of intermediate, light-intermediate and light chains for dynein), purple coloured. Dynein motor domains contain antennae-like extensions with the microtubule-binding sites, which are in kinesin and myosin incorporated within their motor domains. The Figure is taken from Woehlke & Schliwa 2000.

1.2 Kinesin superfamily

The first member of the kinesin superfamily, the conventional kinesin was identified in fractions of squid and mammalian nervous tissue as a novel brain ATPase (Brady 1985; Vale *et al.* 1985).

Later on, using molecular-biological approaches the search for genes coding for proteins containing ATP- and microtubule-binding sequences resulted in the discovery of many kinesin superfamily (KIF) proteins (Aizawa *et al.* 1992; Hirokawa *et al.* 1998; Cole *et al.* 1992; Hirokawa 1993; Nakagawa *et al.* 1997; Tabish *et al.* 1995; Yang *et al.* 1997). Up-to-date, more than 40 kinesin family members have been identified in the human and mouse genome (Miki *et al.* 2001; Hirokawa & Noda 2008) and classified into three major types based on the position of their motor domains.

Most of the members of the kinesin superfamily have their motor domain at the N-terminus (N-kinesins) and walk towards the plus end of the microtubule. There is a

smaller number of kinesin family members with motor domains in the center of the molecule (M-kinesins), or at the C-terminus (C-kinesins). C-kinesins walk in the opposite direction, *i.e.* from microtubule plus to the minus end.

Kinesin molecules are composed in general of two identical heavy chains. Each heavy chain can be divided into a globular motor domain, a coiled-coil stalk, and a globular tail domain (Figure 1.2 A). The motor domain represents the force-producing element which comprises the catalytic core with the ATP- and microtubule-binding sites, and the mechanical element, composed of the neck linker and neck. The catalytic core is conserved throughout the kinesin superfamily, while the neck linker and neck are conserved within certain kinesin classes, only (Vale & Fletterick 1997). Whereas the neck linker is a flexible structure which communicates with the catalytic core via hydrogen bonds, the neck region is important for dimerization of the heavy chains. The motor domain of kinesin is usually followed by a long α-helical coiled-coil stalk region and finally by the unique tail, which is involved in targeting a particular cargo, *e.g.* a membrane-enclosed organelle, another microtubule, or DNA (chromokinesins) (Vale & Fletterick 1997). The direction in which a kinesin motor moves is dependent upon the neck linker and neck sequences (Case *et al.* 1997; Henningsen & Schliwa 1997; Endow 1999; Hirose *et al.* 2000).

Kinesins occur in different oligomerization states. Beside the homodimeric kinesins (Figure 1.2 B), consisting of two identical protein chains and the heterodimeric kinesins (consisting of two distinct chains), the chains of some kinesin-related proteins lack a coiled-coil sequence and seem to function as monomers. The protein chains of another class of kinesins, (kinesin-5), self-associate through the tail domain, forming a bipolar tetrameric motor (Figure 1.2 C), able to slide anti-parallel microtubules apart.

The fact that microtubules are polar structures, whose plus ends point towards the cell periphery, as well as the ability of kinesins to move unidirectionally allow to transport a given cargo to predetermined compartments within the cell. Moreover, many of the kinesin superfamily members have specific roles in mitotic and meiotic spindle formation and chromosome separation. Thus, depending on their biological function and correspondingly on the cargo they transport, the kinesins can be divided into two groups - cytosolic and spindle kinesins. Cytosolic kinesins transport vesicles organelles and mRNA, whereas the spindle kinesins participate in spindle assembly and chromosome segregation.

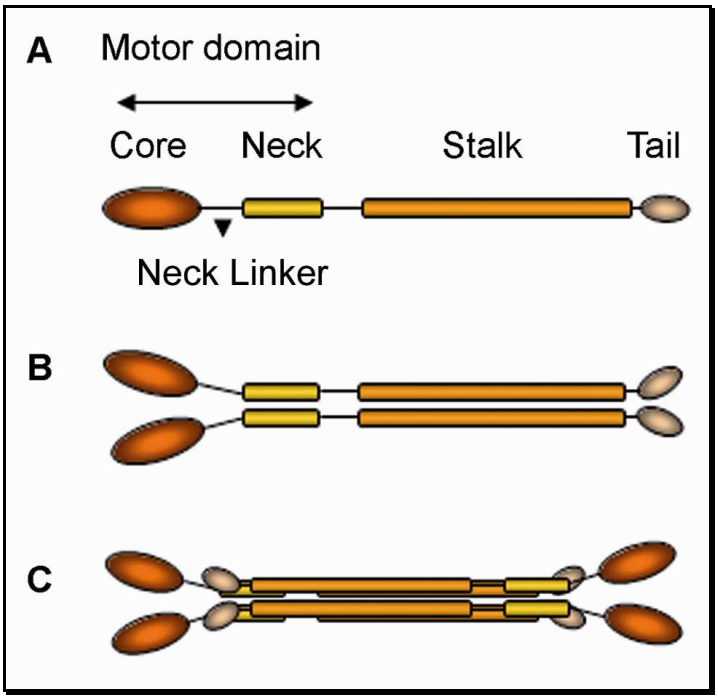

Figure 1.2 *Domain organization of kinesin members.*
A) a single kinesin chain; B) a homodimeric kinesin molecule (conventional kinesin) and C) a bipolar homotetrameric (kinesin-5) molecule.

1.2.1 Conventional kinesin

1.2.1.1 Structure

The conventional kinesin (kinesin-1 family member) as the founding member of the kinesin superfamily is the best studied kinesin. It represents an N-terminal (related to motor domain localization) motor, consisting of two identical 120-kD protein heavy chains (Figure 1.3), which are found to be associated with two 64-kD light chains within the cells (Brady 1985; Vale *et al.* 1985; Bloom *et al.* 1988). The light chains bind to the heavy chains at the coiled-coil tail region (Diefenbach *et al.* 1998), and are not essential for motility (Yang *et al.* 1990). Most probably, the light chains have regulatory and cargo-binding functions (Stenoien & Brady 1997; Vale & Fletterick 1997; Gindhart *et al.* 1998; Verhey *et al.* 1998).

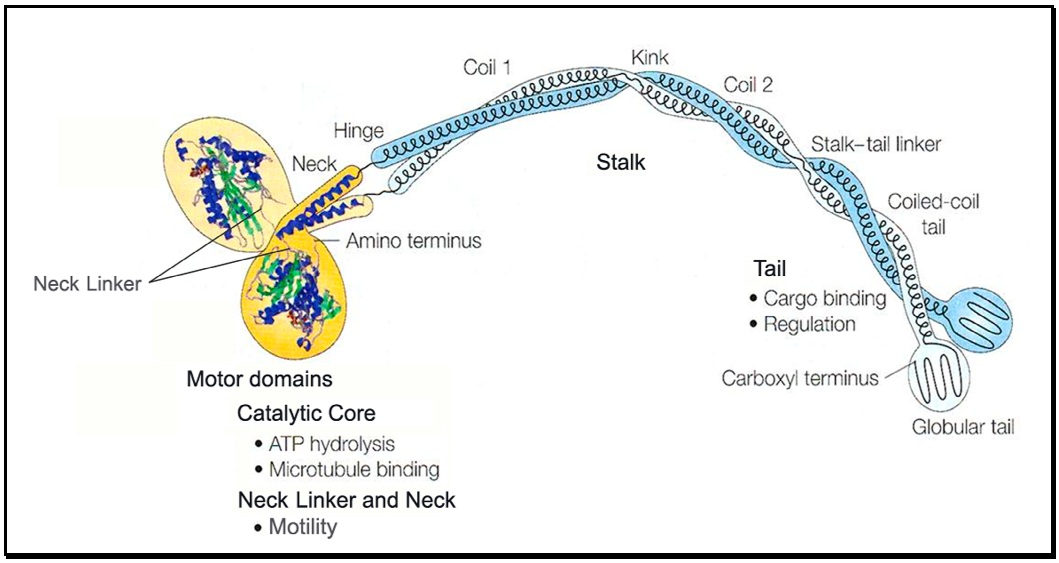

Figure 1.3 *Domain organization of the conventional kinesin heavy-chain dimer.*
The Figure is adapted from Woehlke & Schliwa 2000.

The motor domain of the kinesin-1 is composed of ~350 amino acids. The crystal structure, solved by Kull *et al.* (1996), reveals the catalytic core and the mechanical element.

1.2.1.1.1 Catalytic core

The catalytic core of conventional kinesin comprises a central β-sheet consisting of eight β-strands surrounded by six α-helices, three on either side (Figure 1.4). It includes the ATP- and microtubule-binding sites.

The nucleotide-binding site is formed by the four structural elements N1-N4 (Table 1.1), including highly conserved residues, essential for correct binding of ATP and consequently hydrolysis (Sablin *et al.* 1996).

Protein	Nucleotide	N1 (P-loop)	N2 Switch I	N3 Switch II	N4 base
Kinesin	ATP	G_{86}QTxxGKS/T	N_{199}xxSSR	D_{232}xxGxE	R_{14}xRP

Table 1.1 *Nucleotide-binding motifs in kinesin.* x depicts not conserved residues.

N1 or the **P-Loop** is a common phosphate-binding motif. Within this motif, a positively charged conserved lysine residue ensures the proper electrical environment for the negatively-charged phosphate. The serine or threonine in the motif (Table 1.1) coordinates the Mg^{2+} cofactor. The P-loop is essential for nucleotide binding and is highly conserved among ATP and GTP-binding proteins.

N2 or the **switch I** region includes the helix α3, loop L9, and α3a (Figure 1.4). Since the lengths in α3 and α3a differ in the different kinesin family members, this region shows a higher variability (Sack *et al.* 1999; Song *et al.* 2001).

N3 or the **switch II** region includes the conserved DLAGSE motif, which belongs to loop L11 (Figure 1.4). This loop is closely located to both ATP- and microtubule-binding region that is involved in conformational changes during ATP turnover.

N4 motif participates in nucleotide binding by interacting with the adenine base moiety. The proline in the motif interacts with the adenosine ring, whereas the aliphatic side chain of arginine makes a hydrophobic interaction.

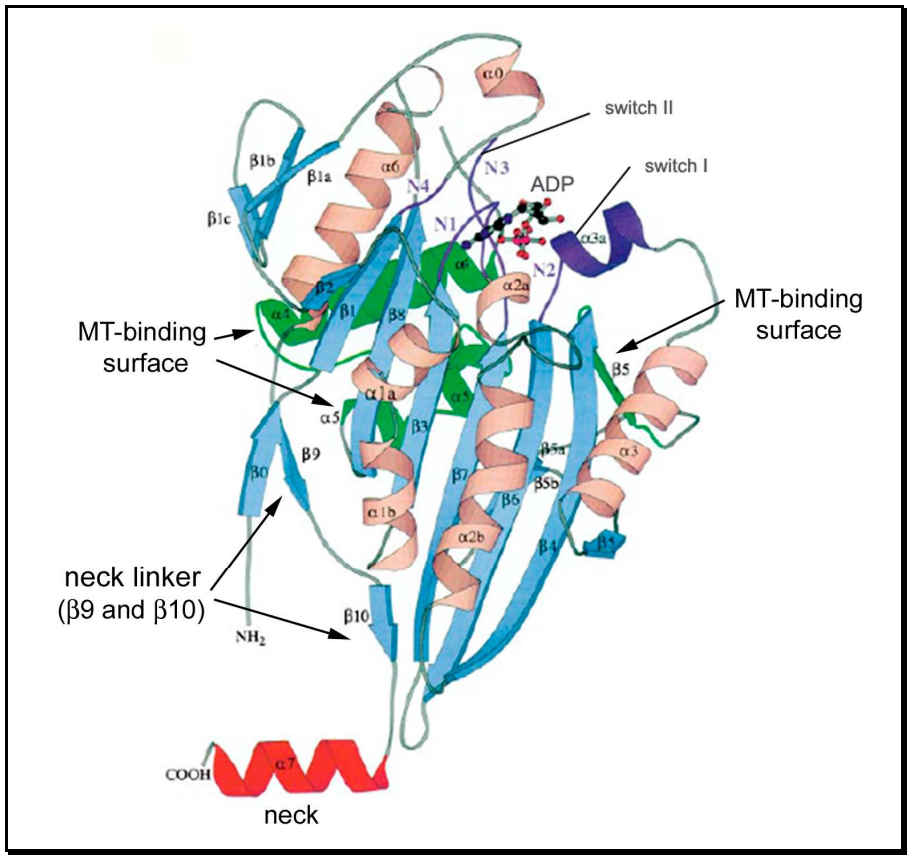

Figure 1.4 *Structure of rat brain kinesin (monomer, residues 1-354).*
The microtubule-binding (MT-binding) region is coloured green (α4-L12-α5). The nucleotide-binding region is coloured purple, the nucleotide (ADP) is shown as a ball-and-stick model. The neck-linker region (β9 and β10) connects the core and the neck region formed by helix α 7 (red). The Figure is adapted from Sack *et al.* 1999.

The **microtubule-binding surface** is diametrically opposed to the nucleotide-binding site and includes the β5-L8 lobe, the α4-loop12-α5-loop13 cluster and loop L11 (shown in green on Figure 1.4) (Woehlke *et al.* 1997; Hoenger *et al.* 1998; Hoenger *et al.* 2000; Song *et al.* 2001; Grant *et al.* 2007). Helix α5 and its neighbouring loops undergo ATP-dependent internal movements. Manipulations in this part of the motor domain have been shown to prevent the interaction with microtubules (Turner *et al.* 2001). In addition to these elements, the neck region (helix α7) may contribute to microtubule binding via interaction with the C-terminus of the microtubule β-tubulin subunit.

1.2.1.1.2 Neck linker and neck

An important property of conventional kinesin is its high processivity. An individual kinesin molecule can move continuously along microtubules taking hundreds of steps without dissociating, thus transporting its cargo over long distances to the proper cellular location. Processive motility appears to be an adaptation to kinesin´s function as organelle transporter. The processive motion requires a dimeric molecule, in which two motor domains are tightly connected and acting in coordinated fashion (Hancock & Howard 1998; Hancock & Howard 1999; Kaseda *et al.* 2003). The coiled-coil neck region (helix α7) links the two kinesin chains which results in formation of stable dimers.

The neck linker, positioned at the end of the helix α6 (Figure 1.4), connects the catalytic core to the neck coiled-coil of the kinesin molecule. It is an extended, flexible region composed of the β9 and β10 strands and is highly conserved among plus-end-directed kinesins (Vale & Fletterick 1997). The neck linker provides the necessary compliance for the individual motor domains ensuring that they find their correct forward microtubule-binding site. This region undergoes large conformational changes depending on the nucleotide-bound state, which has been used to explain the mechanism of kinesin motility. The catalytic cycles of the motor domains pass phases of weak and strong microtubule affinity, whereby the interaction of the linkers guarantees that at each given time point at least one of the motor cores is bound to the microtubule.

1.2.1.2 Hand-over-hand model of kinesin motility

The kinesin-1 moves processively along microtubules in discrete steps corresponding to the distance between adjacent tubulin dimers (Svoboda *et al.* 1993). Each single motor domain of the kinesin dimer moves alternatingly in 16-nm steps. The center-of-mass migration for the whole motor molecule is 8 nm (Mandelkow & Johnson 1998).

Per step, kinesin hydrolyses one ATP molecule (Hua *et al.* 1997; Schnitzer & Block 1997). It is commonly accepted that during movement along the microtubule a kinesin molecule follows the axis of a single protofilament (Ray *et al.* 1993).

It has been shown that the unidirectional movement of kinesin is based on a large conformational change within the neck linker (Rice *et al.* 1999). To coordinate the work of both motor domains their affinity to the microtubule is nucleotide-dependent (Hackney 1994; Ma & Taylor 1997; Gilbert *et al.* 1998). Kinesin binds to microtubules in the ADP or nucleotide-free state. In solution, a kinesin dimer contains one ADP molecule per head. Binding to the microtubule lattice causes ADP to be released from the catalytic core of the one (leading) motor domain, whereafter it locks to the microtubule and is ready to accept one ATP molecule. Upon ATP binding, a cascade of conformational changes takes place within the core. To change conformation between ATP- and ADP-bound states, the kinesin has to sense the presence or absence of a single phosphate group. This is realized by a so-called nucleotide-state sensor, comprised of switch I and switch II loops (Figure 1.4), which form hydrogen bonds with the γ-phosphate of ATP. Additionally, a salt bridge is formed between switch I and II loops to stabilize the ATP-bound state. The resulting small movements of the γ-phosphate sensor are transmitted to other regions within the core, such as helix α4 (switch II helix) and consequently the neck linker. The helix α4, which is also interacting with the microtubule-binding site, is the key region within the communication pathway linking the nucleotide site, the microtubule-binding site, and the neck linker.

Movement of kinesin-1 along a microtubule can be well explained by a so-called hand-over-hand model (Figure 1.5).

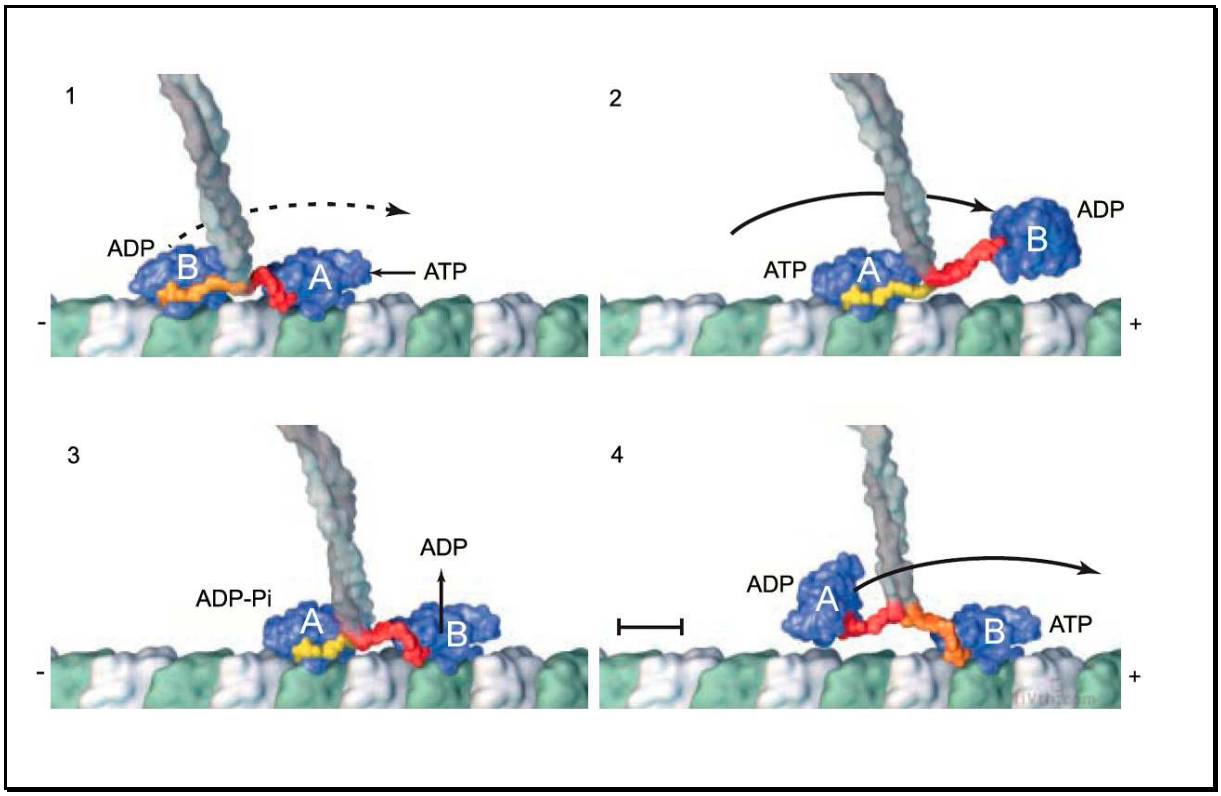

Figure 1.5 *Model of hand-over-hand motility cycle of conventional kinesin.*
Alternating tubulin subunits (α and β) of a protofilament are coloured in white and green, respectively. The two motor domains of the kinesin dimer work in a coordinated manner to move processively along the microtubule. The kinesin dimer is depicted only up to its coiled-coil neck (grey). The neck linker undergoes a series of conformational changes during ATP turnover (partly docked - depicted in orange, docked - depicted in yellow and undocked - depicted in red) (adapted from Vale & Milligan 2000). Detailed explanations see in the text.

When the core of the leading motor domain (depicted with A in Figure 1.5, frame 1) is binding ATP, the C-terminus of the neck linker is pointing rearward to the microtubule minus end (Figure 1.5 – frame 1, red linker). The aroused conformational changes upon ATP binding (a so-called upstroke of switch II helix) result in neck-linker docking to the catalytic core with the C-terminus pointing towards the microtubule plus end (frame 2, yellow coloured linker). Upon this rapid process (>800 s^{-1} at room temperature; Rosenfeld *et al.* 2002) the linker is becoming immobilized (docked) onto the catalytic core. ATP binding causes an efficient forward motion of the neck linker and any object attached to its C-terminus. The neck-linker movement (docking) in the one motor domain is transmitted to its partner domain to enable processive motion. Docking of the linker of the leading motor domain (domain A) leads to detachment of the second (trailing) motor domain from the microtubule. The docked linker of the leading domain pulls the trailing domain (domain B) forward by 16 nm to the next free

tubulin binding site. Thus, the kinesin step is initiated by the ATP-driven swing of the neck linker of the leading motor domain. The tight binding of the trailing motor domain to its new tubulin site stabilizes the step and produces a force that pulls the attached cargo forward by 8 nm (the distance between adjacent tubulin dimers). At this point, both motor domains have exchanged their roles (the trailing domain B has became leading). This is an intermediate state, in which the cores of both motor domains are bound to adjacent tubulin binding sites. Binding of the leading motor domain (B) to microtubules accelerates the ADP release (frame 3). During this time, the trailing motor domain (A) hydrolyses the ATP to ADP-Pi. ATP binding to the core of the leading motor domain induces neck linker docking conformation (frame 4, orange coloured partly docked linker). In the trailing motor domain, which has released the Pi, the contacts between switch I and switch II are lost and the consequent conformational changes (called downstroke of the switch II helix) result in undocking of the neck linker (frame 4, neck linker shown in red). The trailing motor domain (A) in this model is arranged in a position of being thrown forward.

During the ATP hydrolysis cycle, the microtubule-binding surface of kinesin is pulled towards the nucleotide during the upstroke of the switch II helix and is pushed away during the downstroke. These motions seem to affect microtubule-binding affinity of kinesin.

During kinesin motility cycle, the upstroke of helix α4 upon ATP binding results in formation of a pocket, which provides a docking site for conserved residues from the neck linker (isoleucine Ile^{325} in human kinesin and Ile^{327} and asparagine Asn^{329} in rat kinesin) (Vale & Milligan 2000). The interaction between these residues and the core (via hydrogen bonds) initiates a “zippering” of the rest of the neck linker onto the catalytic core. The downstroke of the switch II helix induces an occlusion of the binding pocket, which pushes the conserved residues out and the neck linker becomes disordered (undocked).

Some authors have proposed alternative models. The most prominent is the inchworm model, in which only one of the motor domains of dimeric kinesin hydrolyses ATP and moves forward in “inchworm” fashion, thereby dragging the partner motor domain along the microtubule (Hua *et al.* 2002). Though this model is able to explain certain features of kinesin behaviour, the hand-over-hand model is the most widely accepted one to illustrate the processive movement of conventional

kinesin-1 (Schief & Howard 2001; Endow & Barker 2003; Asbury *et al.* 2003; Kaseda *et al.* 2003; Yildiz *et al.* 2004; Schief *et al.* 2004; Shao & Gao 2006; Mori *et al.* 2007).

1.3 KIF5A kinesin

In contrast to some lower species including *Drosophila melanogaster* and *Caenorhabditis elegans* where only one conventional kinesin-1 gene has been found, mammals have three kinesin-1 genes encoding KIF5A, KIF5B and KIF5C proteins. KIF5B appears to be ubiquitously expressed, whereas both KIF5A and KIF5C are expressed exclusively in neurons (Navone *et al.* 1992; Niclas *et al.* 1994; Kanai *et al.* 2000). Alignment of the amino acid sequences between the three kinesin-1 family members has shown more than 70% identity and more than 90% homology.

In humans, some neurons such as spinal motor and sensory neurons form axons of 1 m or more to reach postsynaptic targets at the periphery. Such an enormous extension requires an efficiently working transport mechanism. Nerve impulses are transmitted from a neuron by release of neurotransmitters from the terminal of the axon. The neuron must constantly supply new materials such as proteins and membranes to the terminal to replenish those lost by exocytosis at the junction (synapse) with another cell. Axons and synaptic terminals lack a protein synthesis machinery. Therefore, proteins and membranes that are synthesized and assembled in the cell body have to be transported the axon down to the synaptic regions. Membranous organelles, mitochondria, and other vesicles are transported by the fast axonal transport, while cytoskeletal proteins like neurofilament proteins (NF) are moved by the slow axonal transport. Although KIF5A, KIF5B, and KIF5C have been shown to be involved in the fast axonal transport, there is evidence that KIF5A is also involved in the slow axonal transport of neurofilaments (Xia *et al.* 2003).

The kinesin-1 members have been found to move along microtubules with a velocity at about 0.8-1 μm s^{-1} (see *e.g.*, Hancock & Howard 1998; Blasius *et al.* 2007). Recent studies have suggested a mechanism explaining the controversy between the velocity of KIF5A and the slow transport of neurofilaments. It has been proposed that the decreased velocity during KIF5A-mediated slow axonal transport may be caused by long pauses of KIF5A movement (Xia *et al.* 2003).

Mutations in the KIF5A gene have been found to cause a form of hereditary spastic paraplegia in humans, a disorder characterized by progressive spastic weakness of the lower extremities (Reid *et al.* 2002; Fichera *et al.* 2004; Blair *et al.* 2006; Lo

Guidice *et al.* 2006). These findings underscore the importance of KIF5A and the proper axonal transport for normal functioning of the human nervous system. Accumulations of neurofilaments observed in many neurodegenerative diseases might be caused by impaired KIF5A transport, but the molecular basis of such mechanism is still unknown.

1.4 Eg5 kinesin

Eg5 belongs to kinesin-5 family and plays an essential role in mitosis. At least one kinesin-5 homologue has been found in every eukaryote, called BimC in *Aspergillus* (Enos & Morris 1990), cut7 in *Schizosaccharomyces pombe* (Hagan & Yanagida 1990), cin8p in *Saccharomyces cerevisiae* (Hoyt *et al.* 1992), Klp61F in *Drosophila* (Heck *et al.* 1993) and Eg5 in *Xenopus* (LeGuellec *et al.* 1991; Swain *et al.* 1992) and humans (Blangy *et al.* 1995). All these motors share slow, plus-end-directed movement (Lockhart & Cross 1996; Crevel *et al.* 1997) and a unique homotetrameric structure (Kashina *et al.* 1996). The activity of kinesin-5 members is controlled, at least in part, by phosphorylation at a conserved C-terminal region by $p34^{cdc2}$ kinase (Blangy *et al.* 1995; Swain & Mitchison 1995).

Eg5, like kinesins in general, can be structurally divided into three main subunits: an N-terminal motor domain, a coiled-coil stalk, and a C-terminal tail domain. Unlike most other kinesins characterized so far, Eg5 is homotetramer with a pair of identical motor domains, positioned at each end of a central rod (Figure 1.2 C). Like conventional kinesin, two heavy chains of Eg5 form a dimer via association of their coiled-coil regions. Both dimers then align in anti-parallel fashion to form the bipolar structure, enabling microtubule crosslinking and antiparallel sliding. Based on its structure, Eg5 has been suggested to contribute to centrosome separation and to the assembly of the bipolar mitotic spindle (Figure 1.6) (Kashina *et al.* 1996; Sharp *et al.* 1999). Recent *in vitro* studies have shown that Eg5 first packs microtubules into aligned bundles and subsequently sorts them apart (Kapitein *et al.* 2005).

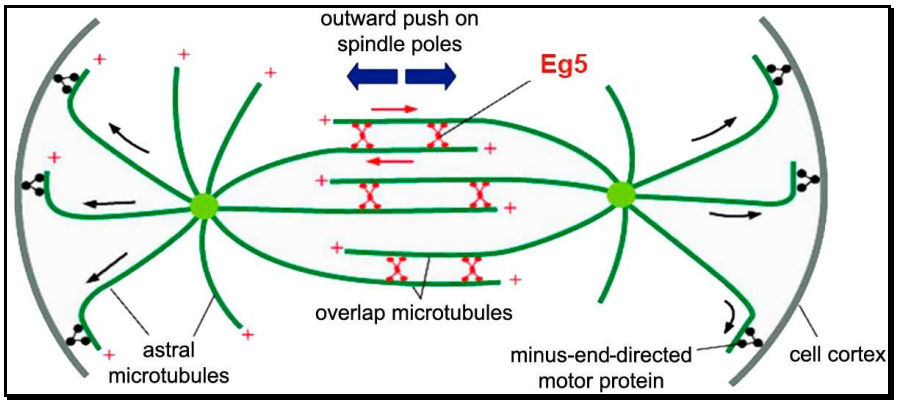

Figure 1.6 *Model of Eg5 function in mitotic spindle morphogenesis.*
The plus-end-directed motor protein Eg5 cross-links the overlapping, anti-parallel microtubules and slides them past each other, thereby pushing the spindle poles apart. The red arrows indicate the direction of microtubule sliding. Minus-end-directed motor proteins bind to the cell cortex and to those astral microtubules that point away from the spindle and pull the poles apart. Blue arrows indicate the direction in which the centrosomes are pushed apart. The Figure is adapted from Molecular Biology of the Cell, Alberts *et al.* 4th edition.

Eg5 expression is most abundant in proliferating human tissues (thymus, tonsils, testis, oesophageal epithelium, bone marrow). Failure in Eg5 function has been shown to lead to cell cycle arrest with monopolar mitotic spindles and cell dead (Blangy *et al.* 1995). These findings have favoured Eg5 in the last years as a highly promising target in tumour therapy with reduced side effects than known microtubule-binding antimitotics (taxanes, *Vinca* alkaloids). A number of small molecule inhibitors has been identified that specifically and reversibly inhibits Eg5 function leading to monoaster formation and arrested cell division (Mayer *et al.* 1999; Duhl & Renhowe 2005). Up-to-date several successful approaches exist to screen for Eg5 inhibitors (Kozielski *et al.* 2007).

1.4.1 Model of dimeric Eg5 motility

Extensive studies have been performed to understand the mechanochemical cycle of Eg5 using recombinant truncated monomeric and dimeric proteins (Cochran *et al.* 2004; Cochran *et al.* 2006; Rosenfeld *et al.* 2005; Valentine *et al.* 2006; Krzysiak & Gilbert 2006; Krzysiak *et al.* 2008). Dimeric Eg5 was found to move along microtubules at a velocity of about 0.04 µm s^{-1} (Krzysiak *et al.* 2006; Korneev *et al.* 2007).

The mechanochemical cycle of dimeric Eg5 is very similar to that of conventional kinesin. While conventional kinesin can take hundreds of steps, the Eg5 dimer takes only 8-10 steps on average (Valentine *et al.* 2006; Valentine & Gilbert 2007).

In contrast to kinesin-1, whose neck linker is flexible in ADP-bound state, the neck linker of Eg5 has been found to take a unique position in ADP-bound state. Crystal structure analysis revealed that the Eg5 linker is well ordered and hold in a stable position perpendicular to the long axis of the catalytic core (Figure 1.7) (Turner *et al.* 2001).

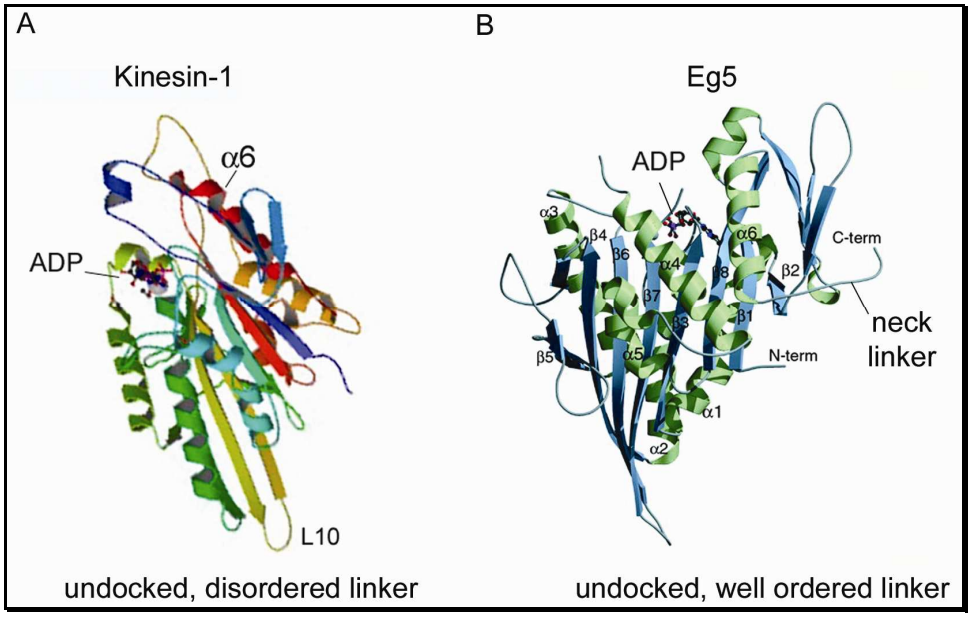

Figure 1.7 *Comparison of the crystal structures of human kinesin-1 and Eg5 motor domains.* A) kinesin-1 motor domain (residues 1-349) in ADP-bound state. The neck linker is undocked and disordered (and cannot be visualized). Helix α6 which connects the linker to the core is shown in dark red (PDB: 1BG2; Kull *et al.* 1996); B) structure of Eg5 motor domain (residues 1-368) in ADP-bound state with β-sheets shown in blue and α-helices shown in green. The linker is undocked, well ordered and stabilized in position perpendicular to the long axis of core (PDB: 1II6; Turner *et al.* 2001).

During its mechanochemical cycle kinesin-1 steps processively as soon as the one motor domain contacts the microtubule and releases the ADP. To step, Eg5 performs a small conformational change in its motor domain upon microtubule binding. It has been recently shown that dimeric Eg5 has two distinct phases in its cycle - the first one includes the intermediate Eg5 dimer competent for processive run length and the second one the processive run length itself (Krzysiak *et al.* 2008).

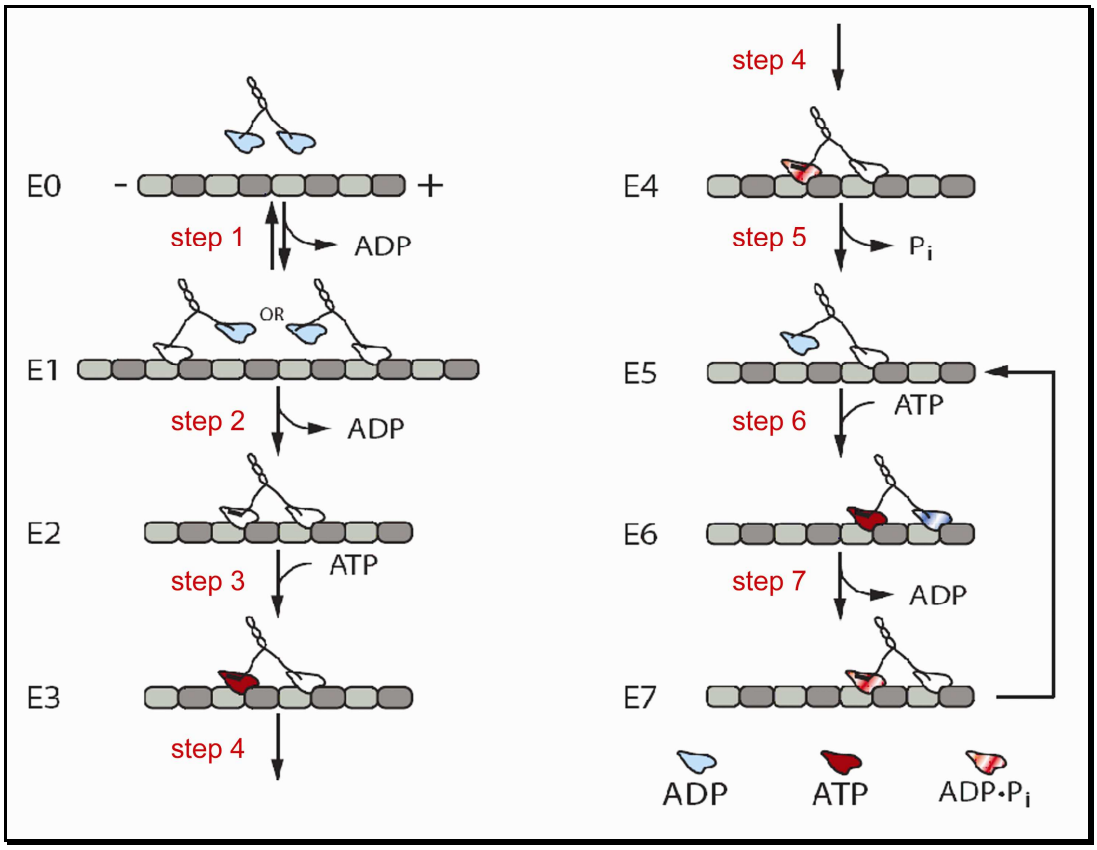

Figure 1.8 *Model of dimeric Eg5 stepping***.**
By contrast to kinesin-1, binding to microtubules triggers ADP release from both Eg5 motor domains. In this process, the one Eg5 motor domain releases its ADP rapidly, whereas the second one releases it after a slow conformational change. As a result, Eg5 starts its stepping cycle with both motor domains bound to microtubules and nucleotide-free (steps 1 and 2). E1-E7 depict the different states of the Eg5 dimer during ATP turnover. Blue-coloured motor domain represents the ADP-bound state; red-coloured the ATP-bound state. The ADP-Pi state is illustrated by red-white striated motor domain, the nucleotide-free motor domain is coloured in white and the motor domain prior to release its ADP is coloured in blue-white (Figure taken from Krzysiak *et al.* 2008). For detailed description of the motility mechanism see the text.

In solution one motor domain of the Eg5 dimer has a tightly bound ADP molecule whereas the other one is weakly bound (Figure 1.8, E0 dimer). According to the model of Krzysiak *et al*. (2008), the motility cycle starts with collision of the weak motor domain with the microtubule and rapid release of the bound ADP (Step 1, Figure 1.8), followed by a slow conformational change of about 1 s^{-1}, which is most probably related to the reorientation of the Eg5 neck linker from a position perpendicular to the core into a docked position. At this step, the detached motor domain in the intermediate Eg5 dimer (E1) may have two possible orientations: a forward one searching for the next microtubule-binding site, and a rearward one. As

a result of changing conformation the partner motor domain (with tightly bound ADP) binds to the microtubule followed by ADP release (step 2) and formation of an intermediate Eg5 dimer (E2) in which both motor domains lack the nucleotide and are bound to microtubule. Eg5 starts to move (step 3) upon ATP binding to the rearward motor domain, which has a docked neck linker. ATP hydrolysis (step 4) and phosphate release (step 5) weaken the ADP binding and the rearward motor domain detaches from the microtubule (E5). In order to allow the rearward motor domain to advance forward towards the microtubule plus end, ATP should bind and be hydrolysed at the forward motor domain. ATP hydrolysis in the forward motor domain (steps 6 and 7) is needed to complete the advance of the rearward motor domain. Upon ADP release, the rearward motor domain binds to the microtubule and becomes forward. Phosphate release from the rearward motor domain (E7 intermediate Eg5 dimer) closes this cycle and induces to start the next one from the Eg5 dimer state E5 (Figure 1.8 step 6).

The question why Eg5 processivity is limited to a relatively small number of steps has been unsolved, so far. It cannot be ruled out that the geometry or the structural state of the neck linker might be responsible for the loss of coordination between the motor domains and, consequently, for motor detachment (Krzysiak *et al.* 2006). It was concluded that the communication between both Eg5 motor domains accounts for the short run length, which seems to be essential for correct functioning of the Eg5 tetramer during mitosis (Krzysiak *et al.* 2008).

1.5 Goals of the work

Though the kinesin members share a conserved motor domain structure and generate motility in a similar manner, each of them has optimized its mechanochemical cycle to perform different motility tasks within cells. This is reflected by the broad range of velocities at which individual representatives of the kinesin superfamily move along microtubules (~0.02-2.0 µm s^{-1}).

Despite the key advances that have been made in elucidation of kinesin motility generation, the molecular mechanisms and the detailed events, which take place during motility generation in general, in controlling the direction of movement, and in the fine-tuning of the velocity, are still unknown.

Manipulations in the neck-linker region were found to disrupt the native switch between the docked and undocked conformational stage of the linker, thus preventing motility (Tomishige & Vale 2000; Case *et al.* 2000; Hahlen *et al.* 2006). Earlier reports on chimeric proteins constituted by parts of minus-end-directed *Drosophila* kinesin Ncd (non claret disjunctional) and either human kinesin-1 (Case *et al.* 1997), or *Neurospora* kinesin Nkin (Henningsen & Schliwa 1997; Hirose *et al.* 2000) showed that the neck linker and neck determine kinesin directionality. The question what regulates the velocity is still open.

Alignment of kinesin-1 and Eg5 has shown that their motor domains share about 40% identity in the amino acid sequences (Figure 1.9) and a high similarity in the crystal structures. This similarity is the highest among kinesins from different families (Figure 1.10) (Turner *et al.* 2001). Nevertheless, Eg5 moves about 25-fold slower than kinesin-1.

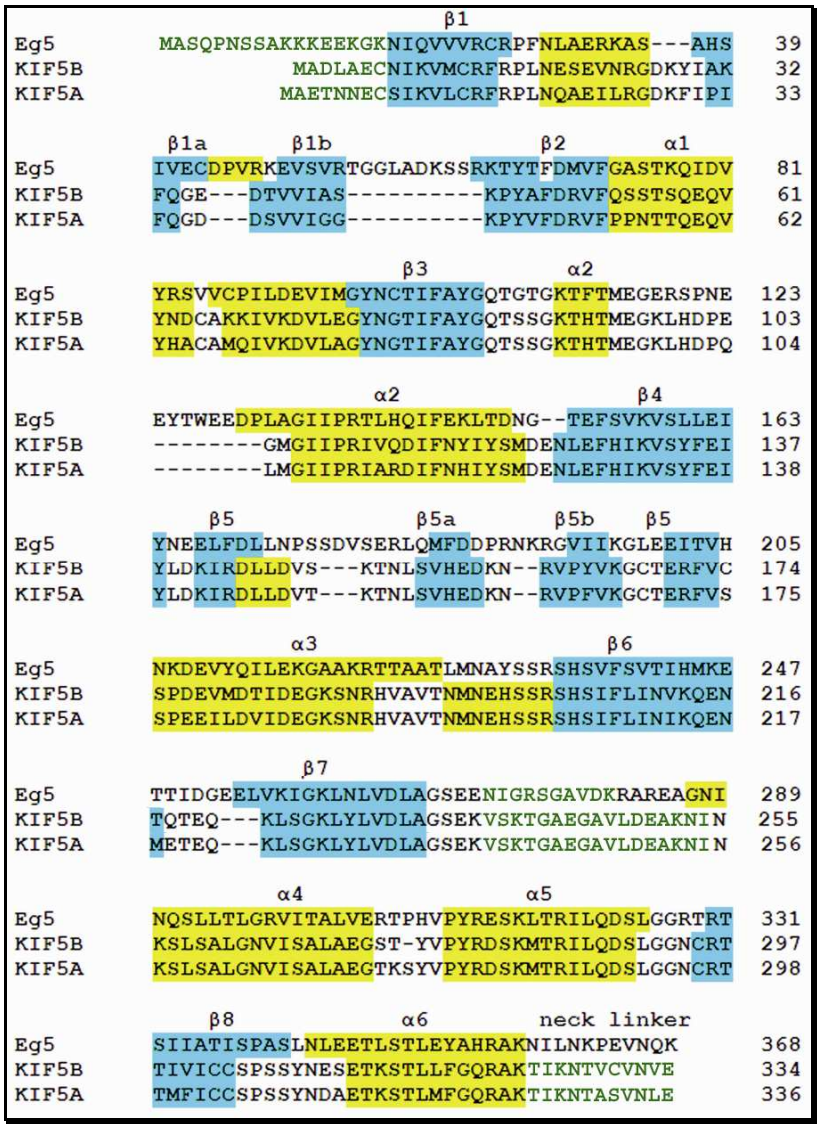

Figure 1.9 *Alignment of the amino acid sequences of the motor domains of Eg5 and the kinesin-1 members KIF5B and KIF5A.*
The major β-sheets and α-helices are highlighted in blue and yellow, respectively. The green-coloured amino acids represent flexible regions. The Figure is adapted from Turner *et al.* 2001.

Excepting some minor deviations, such as the elongation of loop L10 at the tip of Eg5 core (Figure 1.10 A) and the enlargement of the Eg5 loop L5 between α2a and α2b (Figure 1.10 B), the most evident difference in the crystal structure between Eg5 and kinesin-1 motor domains in ADP-bound state has been found in the neck linker (Figure 1.10 F) (Turner *et al.* 2001). The Eg5 neck linker is well ordered and extends roughly perpendicular to helix α6, while in kinesin-1 the linker is flexible. This unusual conformation of Eg5 linker is stabilized by internal hydrogen bonds (Turner *et al.* 2001).

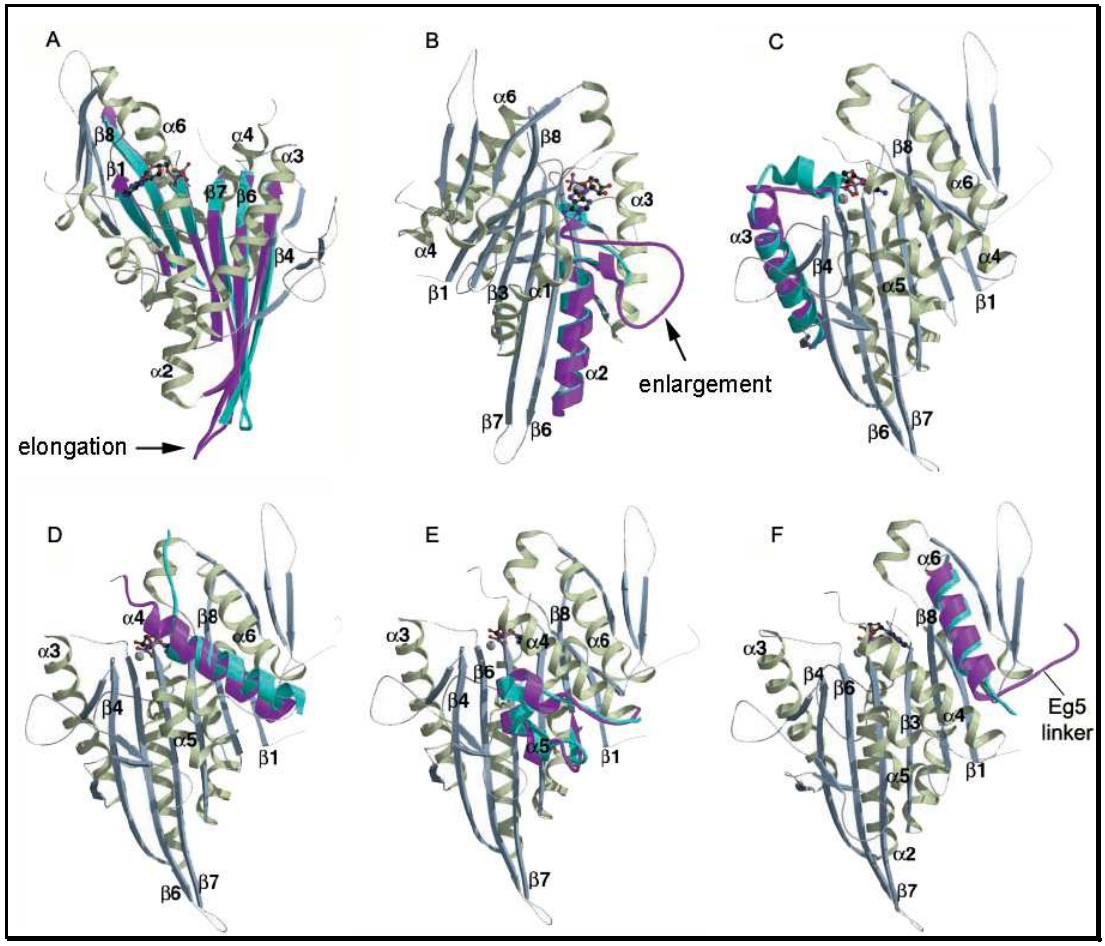

Figure 1.10 *Alignment of the crystal structures of Eg5 and kinesin-1 motor domains.*
A) overlay of the β-sheets of Eg5 (pink) and kinesin-1 (blue). The remainder of the structure is Eg5; B) overlay of helix α2, showing an enlargement of the Eg5 loop L5; C) overlay of helix α3 and the switch I regions of Eg5 and kinesin-1. In Eg5, switch I is found as a coil, whereas in kinesin-1 it is a short α-helix; D) overlay of helix α4 (switch II helix), which is slightly longer in Eg5 than in kinesin-1; E) overlay of helix α5; F) overlay of helix α6, showing the unique position of the Eg5 neck linker. In kinesin-1, the neck linker is disordered and invisible. The Figure is adapted from Turner *et al.* 2001.

Considering the very high structural similarity of kinesin-1 and Eg5 motor domains, on the one hand, and the similar strategies in their motility generation on the other hand, it has been still unclear which structures or mechanisms are involved in the velocity regulation of both motors.

To advance the understanding of motility generation and velocity regulation, a main goal of the present work was to test the hypothesis that the neck linker and neck of kinesin motors might be involved in velocity regulation. C-terminally truncated KIF5A and Eg5 proteins were first expressed and their activities were compared to find out if

the catalytic core of both kinesins requires the same minimal organization. Thereafter, based on the results obtained for the truncated proteins, chimeric proteins constituted by parts of the “fast” KIF5A motor and the “slow” Eg5 motor were expressed and characterized.

Using molecular dynamics simulations with available kinesin crystal structures Hwang and co-workers (2008) presented a new model on kinesin motility generation. They suggested that upon ATP binding the N-terminal part (strand β0) of kinesin-1, termed cover strand (CS), forms a β-sheet called cover-neck bundle (CNB) with the first half (strand β9) of the linker. Formation of the cover-neck bundle (Figure 1.11) is suggested to lead to the kinesin power stroke. The authors concluded that linker subdivision into strands β9 and β10 is functional. Upon ATP binding the β9 interacts weakly with the core and generates the force crucial for forward motion through cover-neck bundle formation. The strand β10 stabilizes the docked state of the linker through a stronger and more specific binding to the core (latch-like mechanism). Once this interaction is disrupted (upon hydrolysis of the nucleotide), the cover-neck bundle breaks because of the weakly formed β-sheet between β9 and β0. So far, no experimental data have been available to proof this model.

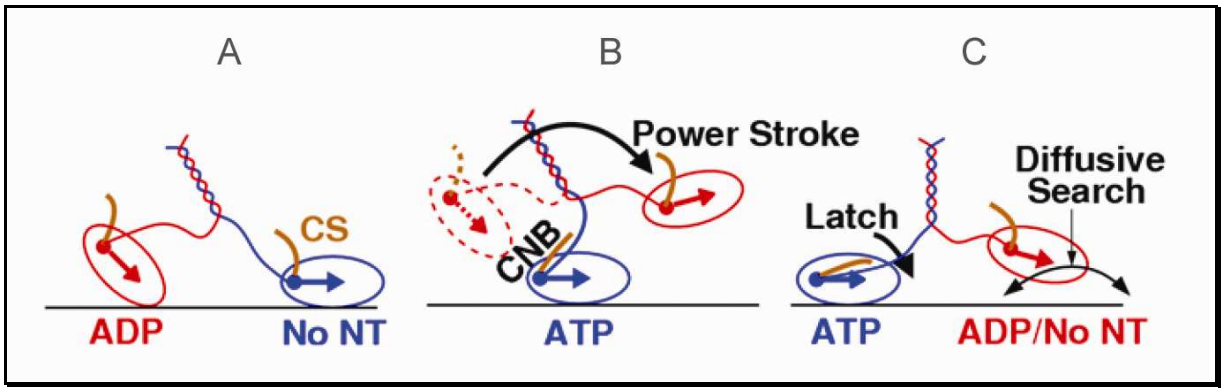

Figure 1.11 *Cover-neck bundle dependent stepping mechanism of kinesin.*
A) Pi release in the trailing motor domain (red) leads to either its dissociation or to weak binding to the microtubule. The N-terminal part of the core, termed cover strand (CS, brownish coloured) is free; B) ATP binding to the leading motor domain (blue) results in interaction between the CS and the first half of the linker and finally in formation of a β-sheet, termed cover-neck bundle (CNB). Formation of the CNB leads to power stroke, stronger binding (latch mechanism shown in C) of the linker to the core to stabilize the docked state and to move the trailing motor domain forward; C) the now becoming leading motor domain (depicted in red) starts either diffusive search for its microtubule-binding site, or is weakly bound in a mobile state until ADP release. NT: nucleotide. The Figure is taken from Hwang *et al.* 2008.

A further goal of the present work was to investigate the role of the first half of the KIF5A linker (strand β9) in ATPase and motility activity. Truncated KIF5A proteins containing either the half linker or the full linker were expressed and compared to a truncated KIF5A protein lacking the linker. Additionally, a chimeric protein composed of the KIF5A core and the first half of its natural linker fused to the complete Eg5 linker and neck has been expressed to investigate the role of the half KIF5A linker in motility generation.

2. Materials and Methods

2.1 Materials

2.1.1 Vectors, cloning- and expression systems

For expression of kinesin constructs in *E. coli* pTYB2 and pTYB4 (New England Biolabs, Germany) were used as parental vectors.

E. coli strains XL1-Blue (Stratagene Europe, Netherland) and ER2566 (New England Biolabs, Germany) were applied for cloning and protein expression, respectively.

Full-length Eg5 protein was expressed in *Spodoptera frugiperda* Sf9 insect cells (BD Biosciences Clontech, Germany) using the pAcG2T baculovirus transfer vector (BD Biosciences Clontech, Germany).

2.1.2 Media and cultivation of E. coli

According to standard methods (Sambrook *et al.* 1989) *E. coli* cells were grown on LB agar plates (Carl Roth, Germany), or in suspension by shaking at 225 rpm at 37℃ in LB medium (1% tryptone, 0.5% yeast extract, 0.5% NaCl), containing 50 µg/ml carbenicillin.

To start protein expression, which was performed in culture medium containing 0.1% N-Z-amine, 94.2 mM NaCl, 72 mM Na_2HPO_4, 2.2 mM KH_2PO_4, 8.6 mM NaCl, 18.6 mM NH_4Cl, 1 mM $MgSO_4$, 0.4% glucose and 50 µg/ml carbenicillin, the temperature was reduced to 16℃.

2.1.3 Media and cultivation of insect cells

Sf9 cells were cultivated in TNM-FH media (BD Biosciences Clontech, Germany) supplemented with 10% fetal bovine serum (Invitrogen, Germany). The cells were grown as monolayers in culture flasks at 27℃ witho ut CO_2.

To store cell lines, logarithmically grown cells were sedimented at 2000 rpm for 10 min (Labofuge 400R centrifuge with an angle-fixed rotor; Heraeus, Germany) and resuspended in 90% TNM-FH medium, supplemented with 10% DMSO. The cells were slowly frozen at -20℃ for one hour, placed at -80℃ overnight and transferred to liquid nitrogen.

Cells were rethawed quickly at 37℃ in a waterbath, diluted in TNM-FH medium, sedimented, resuspended in fresh medium, and seeded into fresh cell culture dishes.

2.2 Molecular biology methods

2.2.1 Agarose gel electrophoresis

DNA fragments were mixed with loading dye (5% glycerol, 0.04% bromphenol blue, 0.04% xylene cyanol) and separated using 0.8%-1% agarose gels, supplemented with 0.05 µg/ml ethidium bromide in TAE buffer (40 mM TRIS, 20 mM acetic acid, 1 mM EDTA, pH 8.0).

Gels were run at 75 V. Bands were detected by UV illumination (Biostep GmbH, Germany) and documented with Argus X1 software (Biostep GmbH, Germany).

2.2.2 DNA extraction from agarose gels

DNA bands were excised from the agarose gel with a scalpel and transferred to sterile tubes. The DNA was purified in the presence of high concentrations of chaotropic salts, using silica membrane columns (Qiagen, Germany).

2.2.3 Determination of DNA concentration

DNA concentrations were determined by measuring the extinction at 260 nm (E_{260}) after calibration of the photometer (BioPhotometer Eppendorf, Germany) with a buffer control. An E_{260} of 1.0 corresponds to 50 µg/ml of double-strand DNA (Sambrook *et al.* 1989).

2.2.4 Restriction of DNA by endonucleases

Restriction reactions were performed using 1-5 units enzyme per µg DNA using the protocol recommended by the manufacturer (Fermentas GmBH, Germany). The minimal reaction volume was 15 µl and the incubation time ≥1 h. Completion of the digestion reaction was proved by agarose gel electrophoresis (2.2.1).

2.2.5 Ligation of DNA into plasmid vectors

Plasmid vectors were first cleaved with appropriate endonucleases (2.2.4), separated on agarose gel by electrophoresis (2.2.1), and extracted from the gel (2.2.2). Insert-DNA (PCR products) was cleaved with the necessary endonucleases and purified using the DNA-cleanup-kit (Qiagen, Germany), following the manufacturer instructions. The vector and insert fragments were ligated with T4 DNA ligase (New England Biolabs, Germany) in a volume of 15 µl at 16℃ overnight using the buffer system supplied by the manufacturer. An insert-to-vector ratio of 3:1 was fixed

corresponding to a total amount of DNA of 200 ng. As a religation control, vector DNA was incubated without the insert. 5 µl of each reaction mixture were transformed into competent *E. coli* cells (2.2.8).

2.2.6 Preparation of plasmid DNA

Plasmid DNA was prepared from bacterial overnight cultures using a plasmid kit (Qiagen, Germany) and according the instructions of the manufacturer. Small scale preparations (3 ml) were done with the plasmid miniprep kit and large scale preparations (100-200 ml) with the plasmid midiprep kit, respectively.

2.2.7 Preparation of competent E. coli cells using the calcium chloride method

100 ml of LB medium were inoculated with 1 ml of an *E. coli* (ER 2566) overnight culture and grown at 37℃ under vigorous shaking to an early log phase (OD_{600} of 0.2-0.4). All flasks and solutions subsequently used were sterilized and cooled to 4℃. Cells were harvested by centrifugation (4000 r pm, 5 min, 4℃, using an angle-fixed conical rotor C0650 and a Beckman Avanti^{TM} 30 centrifuge), resuspended in 1/10 of the culture volume of 0.1 M ice-cold $CaCl_2$ and hold on ice for 30 min. Following another centrifugation step (4000 rpm, 5 min, 4℃, using an angle-fixed conical rotor C1015 and a Beckman Avanti^{TM} 30 centrifuge) the cells were gently resuspended in 1/50 culture volume of ice-cold 0.1 M $CaCl_2$/10% glycerol solution. Thereafter, 100 µl aliquots of the cell suspension were frozen in liquid nitrogen and stored at -80℃.

2.2.8 Transformation of E. coli cells by heat shock

For transformation, competent cells were thawed on ice. 5 µl of the ligation mixture were added to a volume of 100 µl cells and incubated on ice for 10-30 min, transferred at 42℃ in waterbath for 45 s and again on ice for 2 min, respectively. After adding 900 µl LB medium (Carl Roth, Germany), the cells were incubated at 37℃ under shaking for 1h. 50 µl of the transformed *E. coli* cells were plated on LB agar containing 50 µg/ml carbenicillin.

2.2.9 Identification of transformed clones

For DNA identification in the transformed *E. coli* cells, small scale plasmid DNA preparations (3 ml) were performed (2.2.6), cleaved with appropriate restriction

endonucleases and analyzed by agarose gel electrophoresis (2.2.1). Plasmids with the expected restriction fragments were sequenced (MWG-Biotech AG, Germany) before protein expression.

2.2.10 PCR

DNA amplification was carried out by polymerase chain reaction (PCR) with the PfuUltra high-fidelity DNA polymerase (Stratagene). The reactions (50 µl final volume) contained 1 ng/µl template (final concentration), 200 µM of each dNTP, 0.5 µM 5'- and 3'-primer, and 2.5 units PfuUltra high-fidelity DNA polymerase. The number of cycles, temperature and duration of denaturation, annealing and elongation phases were chosen according to the Stratagene instructions.

The PCR products were purified from the nucleotides and the polymerase by the Qiaquick PCR purification kit (Qiagen, Germany).

2.2.11 Oligonucleotides for PCR

Construct	Primer	Restriction site	Primer sequence (with restriction site underlined)
$KIF5A_{1-295}$	for. rev.	*NheI* *SmaI*	5´ - ttt aag cta gca tgg cgg aga cca aca acg - 3´ 5´ - ttt aac ccg ggg ttt ccc ccg aga gag tcc - 3´
$KIF5A_{1-304}$	for. rev.	*NheI* *SmaI*	5´ - ttt aag cta gca tgg cgg aga cca aca acg - 3´ 5´ - ttt aaa ccc ggg gca aca gat gaa cat agt cg - 3´
$KIF5A_{1-325}$	for. rev.	*NheI* *SmaI*	5´ - ttt aag cta gca tgg cgg aga cca aca acg - 3´ 5´ - ttt aaa ccc ggg ctt tgc ccg ctg ccc aaa cat c - 3´
$KIF5A_{1-330}$	for. rev.	*NheI* *SmaI*	5´ - ttt aag cta gca tgg cgg aga cca aca acg - 3´ 5´ - ttt aaa ccc ggg agtgttcttaatggtctttgcc - 3´
$KIF5A_{1-336}$	for. rev.	*NheI* *SmaI*	5´ - ttt aag cta gca tgg cgg aga cca aca acg - 3´ 5´ - ttt aaa ccc ggg ctc caa att tac tga ggc - 3´
$KIF5A_{1-560}$	for. rev.	*NheI* *XhoI*	5´ - ttt aag cta gca tgg cgg aga cca aca acg - 3´ 5´ - ttt aaa ctc gag ctc gct cag atc ctt cat - 3´
$Eg5_{1-329}$	for. rev.	*NcoI* *SmaI*	5´ - ttt aac cat ggc gtc gca gcc aaa t - 3′ 5´ - agt ccc ggg tgt acg ccc tcc aag aga - 3´
$Eg5_{1-341}$	for. rev.	*NcoI* *SmaI*	5´ - ttt aac cat ggc gtc gca gcc aaa t - 3′ 5´ - ttt ccc ggg aga tgc agg aga aat tgt tgc - 3´
$Eg5_{1-357}$	for. rev.	*NcoI* *SmaI*	5´ - ttt aac cat ggc gtc gca gcc aaa t - 3′ 5´ - agt ccc ggg ctt tgc tct atg agc ata ttc - 3´
$Eg5_{1-513}$	for. rev.	*NcoI* *SmaI*	5´ - ttt aac cat ggc gtc gca gcc aaa t - 3′ 5´ - ttt aaa ccc ggg gag acc aga tac atc ttt tgt agt ttc-3´
$Eg5_{1-1057}$ (full-length Eg5 for bacterial expression)	for. rev.	*NcoI* *SmaI*	5´ - aac cat ggc gtc gca gcc aaa ttc - 3´ 5´ - aac ccg gga agg ttg atc tgg gct cgc aga gg - 3´
$Eg5_{1-1057}$ (full-length Eg5 for insect cell expression)	for. rev.	*SmaI* *SmaI*	5´ - aaa ccc ggg cgc gtc gca gcc aaa ttc - 3´ 5´ - aaa ccc ggg cca agt gaa tta aag gtt gat ctg ggc tc - 3´

Table 2.1 *Primers for the construction of C-terminally truncated KIF5A and Eg5 motor domains, as well as primers for the construction of the full-length Eg5 for expression in bacterial cells and insect cells.*

Construct	Primer	Restriction site	Primer sequence (with restriction site underlined)
$Eg5_{1-325}$ - $KIF5A_{293-450}$ termed: E-K(β8α6-linker-neck)	external.for. external.rev. internal.for. internal.rev.	*NcoI* *SmaI*	5´ - ttt aac cat ggc gtc gca gcc aaa t - 3´ 5´ - aaa ttt ccc ggg cag cat ttg ctg ctt gag c - 3´ 5´ - gga aac tgc cgg acg act atg - 3´ 5´ - cat agt cgt ccg gca gtt tcc tcc aag aga atc ctg gag gat tc - 3´
$KIF5A_{1-294}$ - $Eg5_{328-513}$ termed: K-E(β8α6-linker-neck)	external.for. external.rev. internal.for. internal.rev.	*NheI* *SmaI*	5´ - ttt aag cta gca tgg cgg aga cca aca acg - 3´ 5´ - ttt aaa ccc ggg gag acc aga tac atc ttt tgt agt ttc - 3´ 5´ - ggg cgt aca aga aca tct ata att g - 3´ 5´ - caa tta tag atg ttc ttg tac gcc ccc cga gag agt cct gga gaa tcc - 3´
$Eg5_{1-357}$ - $KIF5A_{326-450}$ termed: E-K(linker-neck)	external.for. external.rev. internal.for. internal.rev.	*NcoI* *SmaI*	5´ - ttt aac cat ggc gtc gca gcc aaa t - 3´ 5´ - aaa ttt ccc ggg cag cat ttg ctg ctt gag c - 3´ 5´ - acc att aag aac act gcc tc - 3´ 5´ - gag gca gtg ttc tta atg gtc ttt gct cta tga gca tat tcc aat g - 3´
$KIF5A_{1-325}$ - $Eg5_{358-513}$ termed: K-E(linker-neck)	external.for. external.rev. internal.for. internal.rev.	*NheI* *SmaI*	5´ - ttt aag cta gca tgg cgg aga cca aca acg - 3´ 5´ - ttt aaa ccc ggg gag acc aga tac atc ttt tgt agt ttc - 3´ 5´ - cat att gaa taa gcc tga ag - 3´ 5´ - cat att gaa taa gcc tga ag - 3´
$Eg5_{1-368}$ - $KIF5A_{337-450}$ termed: E-K(neck)	external.for. external.rev. internal.for. internal.rev.	*NcoI* *SmaI*	5´ - ttt aac cat ggc gtc gca gcc aaa t - 3´ 5´ - aaa ttt ccc ggg cag cat ttg ctg ctt gag c - 3´ 5´ -ttg act gct gag cag tgg aag aag - 3´ 5´ - ctt ctt cca ctg ctc agc agt caa ttt ctg att cac ttc agg c - 3´
$KIF5A_{1-336}$ - $Eg5_{369-513}$ termed: K-E(neck)	external.for. external.rev. internal.for. internal.rev.	*NheI* *SmaI*	5´ - ttt aag cta gca tgg cgg aga cca aca acg - 3´ 5´ - ttt aaa ccc ggg gag acc aga tac atc ttt tgt agt ttc - 3´ 5´ - ctc acc aaa aaa gct ctt att aag g - 3´ 5´ - cct taa taa gag ctt ttt tgg tga gct cca aat tta ctg agg cag tg - 3´
$KIF5A_{1-330}$ - $Eg5_{358-513}$ termed: K(5aa linker)-E(linker-neck)	external.for. external.rev. internal.for. internal.rev.	*NheI* *SmaI*	5´ - ttt aag cta gca tgg cgg aga cca aca acg - 3´ 5´ - ttt aaa ccc ggg gag acc aga tac atc ttt tgt agt ttc - 3´ 5´ - cat att gaa taa gcc tga ag - 3´ 5´ - ctt cag gct tat tca ata tgg cag tgt tct taa tgg tct tt - 3´

Table 2.2 *Primers for the construction of Eg5- and KIF5A-based chimeric proteins using SOE-PCR method.*

2.2.12 Generation of kinesin constructs

2.2.12.1 Constructs for expression in E. coli

The kinesins, with exception of the full-length Eg5, were expressed in *E. coli* by the means of the IMPACT protein fusion and purification system (New England Biolabs, Germany). This system contains pTYB expression vectors (pTYB1, 2, 3 and 4) which allow the fusion of a bi-functional tag, containing both an intein- and chitin-binding domain, to the C-terminus of the target protein. The pTYB vectors use a T7 promoter and the *lac I* gene to provide stringent control of the fusion gene expression.

For the C-terminally truncated KIF5A constructs, as well as for the chimeric proteins containing KIF5A motor domain elements, the pTYB2 was used as vector (Figure 2.1). The parental pTYB2 vector encoding for the full-length KIF5A protein was cloned by Susana Kushnir (present address: Max Planck Institute for Molecular Physiology, Dortmund, Germany) using the KIF5A cDNA kindly provided by Ronald D. Vale (University of California, San Francisco, USA). The PCR primers and the restriction enzymes applied for ligation in pTYB vectors are shown in Table 2.1 and 2.2.

To obtain C-terminally truncated Eg5 constructs and the chimeric constructs containing Eg5 motor domain elements, the pTYB4-Eg5 parental vector was generated by insertion of the gene for the full-length Eg5, amplified from human placenta cDNA (BD Biosciences Clontech, Germany) in the pTYB4 (Figure 2.1). The primers as well as the restriction enzymes used for ligation are shown in Table 2.1 and 2.2.

Standard PCR method was used to amplify the DNA encoding for the full-length Eg5 and for all C-terminally truncated KIF5A and Eg5 proteins.

To generate the KIF5A- and Eg5-based chimeras the splicing by overlap extension (SOE)-PCR method was used (Ho *et al.* 1989).

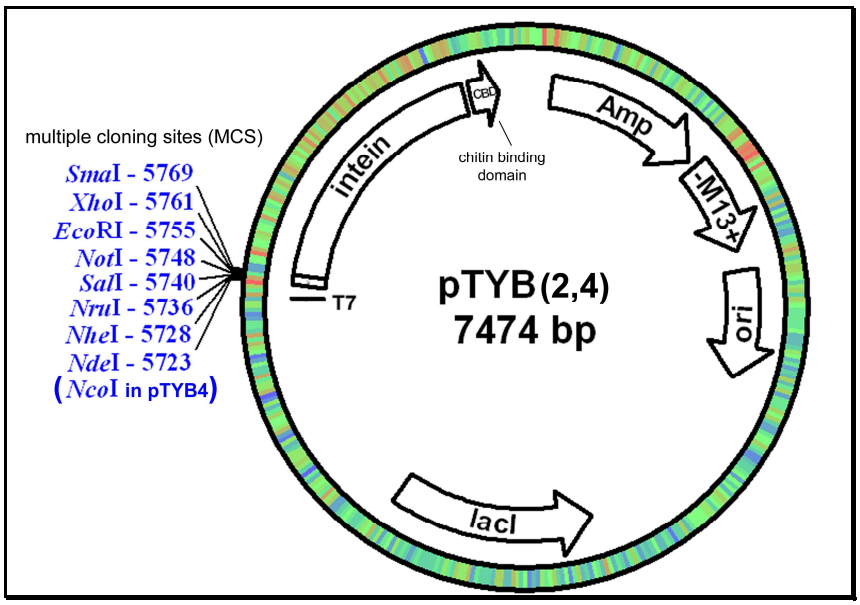

Figure 2.1 *Map of the pTYB2 and pTYB4 vectors used for expression of recombinant KIF5A and Eg5 in E. coli.*
The multiple cloning sites (MCS) of both vectors allow translational fusion of the intein tag to the C-terminus of the cloned target protein. The chitin binding domain (CBD), fused to the C-terminus of intein allows purification of the intein-target protein precursor. Transcription of the fusion gene is controlled by the inducible T7 promoter, requiring *E. coli* strains containing integrated copies of the T7 RNA polymerase gene [e.g., ER2566, C2833 or BL21(DE3)] for expression. Basal expression from the T7 promoter is minimized by binding of the Lac repressor (encoded by the *lacI* gene) to the *lac* operator, which is positioned immediately downstream of the T7 promoter. The vectors contain the pMB1 (ori) and M13 origin of replication, as well as the bla (Amp^R) gene encoding for ampicillin (or carbenicillin) resistance.

2.2.12.2 Full-length Eg5 construct for expression in insect cells

To express the full-length Eg5 protein in insect cells, the Eg5 gene was amplified from pTYB2-Eg5 vector using the standard PCR and introduced into the pAcG2T baculovirus transfer vector (BD Biosciences Clontech, Germany) using the *SmaI* restriction enzyme site (Figure 2.2). The primers for cloning are shown in Table 2.1. The Eg5 gene, cloned into the pAcG2T vector, is expressed as a fusion protein with N-terminal GST tag under the control of the strong polyhedrin promoter.

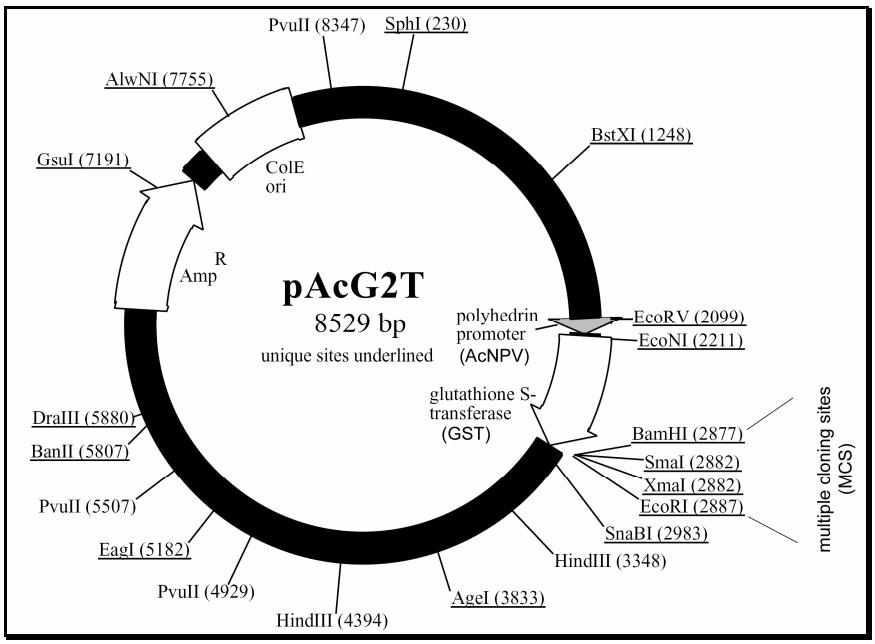

Figure 2.2 *pAcG2T baculovirus expression vector.*
Using pAcG2T vector, foreign genes of interest may be expressed as glutathione S-transferase (GST) fusion proteins when cloned into one of the multiple cloning sites. The GST fusion protein expression is controlled by the strong AcNPV polyhedrin promoter. GST has a high affinity for reduced glutathione, which allows a single-step purification of the target protein using glutathione beads. The vector contains the ColE origin of replication and the bla (Amp^R) gene encoding for ampicillin resistance. Unique restriction sites are underlined.

2.3 Biochemical methods

2.3.1 SDS-PAGE

Proteins were characterized by electrophoresis using 7.5%-10% SDS-polyacrylamide (Carl Roth, Germany) gels. The samples were mixed with Laemmli sample buffer (50 mM TRIS-HCl, pH 6.8, 2.5 mM EDTA, 2% SDS, 5% glycerol, 2.5% β-mercaptoethanol, 0.01% bromphenol blue) (Laemmli 1970) and incubated at 95℃ for 5 min. After loading onto the gel, the proteins (6 µg per lane) were separated in running buffer (2.5 mM TRIS-HCl, 0.01% SDS, 19.2 mM glycine) at 25 mA for at least 1 h. A broad range protein standard (covering the range between 6.5 kD and 205 kD) was used (Sigma-Aldrich, Germany).

Gels were stained for 30 min in 0.2% Coomassie blue R solution (Carl Roth, Germany), rinsed with distilled water and destained with a solution of 10% acetic acid and 20% ethanol. Before drying (20 min incubation in 10% glycerine and 20% methanol), the gels were documented by a Duoscan T1200 scanner (AGFA).

2.3.2 Western blotting

After separation by SDS-PAGE, the proteins were transferred to PVDF membrane by semi-dry blotting transfer system. For KIF5A-based constructs Western blotting was performed using mouse monoclonal anti-kinesin heavy chain antibody (Sigma-Aldrich, Germany) at a 1:500 dilution and HRP (horseradish peroxidase)-conjugated anti-mouse secondary antibody (Jackson Immunoresearch, USA) at a 1:2000 dilution. Eg5-based constructs were detected with rabbit anti-Eg5 antibody (Cytoskeleton Inc. USA) at 1:2000 dilution followed by HRP-conjugated mouse anti-rabbit secondary antibody (Promega) at 1:2000 dilution. Western blots were developed by enhanced chemiluminescence (ECL) using ECL Plus™ Western Blotting Detection Reagents (Amersham Biosciences).

2.3.3 Expression and purification of kinesin constructs

2.3.3.1 Proteins expressed in E. coli

The pTYB vectors encoding either the C-terminally truncated or chimeric proteins were transformed in *E. coli* strain ER 2566 (New England Biolabs) and expressed as fusion proteins with a C-terminal chitin-binding intein tag. *E. coli* cells were grown first in LB-medium with 50 µg/ml carbenicillin at 37℃ overnight and sedimented (5000 rpm, 5 min, 4℃ in a Sorvall centrifuge, using an angle-fixed rotor SLA-1000). The pellet was resuspended in culture medium, containing 0.1% N-Z-amine, 94.2 mM NaCl, 72 mM Na_2HPO_4, 2.2 mM KH_2PO_4, 18.6 mM NH_4Cl, 1 mM $MgSO_4$, 0.4% glucose, and 50 µg/ml carbenicillin, and grown at 37℃ until reaching an optical density of ~0.8 at 600 nm. Protein expression was induced by adding 0.1 mM isopropyl-β-thiogalactopyranoside (IPTG). After growing for 16 h at 16℃, the cells were harvested (5000 rpm, 5 min, 4℃ in a Sorvall centrifuge, using an angle-fixed rotor SLA-3000) and resuspended in lysis buffer (PBS, with additional 360 mM NaCl, 0.1 mM EDTA, 0.1% TritonX-100, pH 7.4), supplemented with 1 mM Pefabloc (Roche, Germany), 1 mM sodium ATP, and 40 ng/ml DNase I. A crude extract was obtained by a triple passage through a French Press. After obtaining a clear extract by a high speed centrifugation (35 000 rpm, 45 min, 4℃, using a Beckman Optima ultracentrifuge and an angle-fixed Ti 50.2 rotor), the fusion protein was bound to chitin beads (New England Biolabs) by 1 h incubation at 4℃. The beads were incubated after washing with lysis buffer in elution buffer (20 mM NaH_2PO_4, 500 mM NaCl, 1 mM EDTA, 0.1% Triton X-100, pH 7.4) containing 1 mM Pefabloc and 50 mM

dithiothreitol (DTT) for 40 h at 4℃ under rotation . At this step, the DTT induces the release of the intein tag from the motor protein construct, which thereafter can be easily separated from the chitin beads by high speed centrifugation (25 000 rpm, 45 min, 4℃ in a Beckman Optima ultracentrifuge, us ing an angle-fixed Ti 50.2 rotor). The proteins were concentrated by centrifugation (6000 rpm, 45 min, 4℃ in an angle-fixed rotor 8 x 50 ml, Sigma 3K30 centrifuge; Sigma Laborzentrifugen GmbH, Germany) in Amicon ultra filter units (Millipore) with different pore diameters according to their molecular weight and stored in motility buffer (50 mM imidazol, 0.5 mM $MgCl_2$, 0.5 mM EGTA, 0.5 mM DTT, pH 6.8) supplemented with 150 mM NaCl and 1 M glycerol at -80℃.

2.3.3.2 Proteins expressed in insect cells

Spodoptera frugiperda (Sf9) cells were routinely cultivated as described by manufacturer (BD Biosciences Clontech, Germany). The recombinant baculovirus was generated and amplified also according to protocols of BD Biosciences, Clontech. To obtain the full-length Eg5, the Sf9 cells were infected with recombinant baculovirus at a multiplicity of infection of 3-10. The Sf9 cells were pelleted (2500 rpm, 5 min using angle-fixed rotor; Labofuge 400R centrifuge, Heraeus Germany) 72 h after infection. The pellet was resuspended in ice-cold insect cell lysis buffer (BD Biosciences Clontech, Germany) containing protease inhibitor cocktail (16 µg/ml benzamidine HCl, 10 µg/ml phenantroline, 10 µg/ml aprotinin, 10 µg/ml leupeptin, 10 µg/ml pepstatin A, 1 mM PMSF) and hold for 45 min on ice. The lysate was cleared by centrifugation (40 000 rpm, 45 min, 4℃ in a Beckman Avanti ^{TM} 30 centrifuge using conical angle-fixed F2402 rotor) and the supernatant was incubated in batch with glutathione agarose beads overnight at 4℃ on a rocking platform. After twice washing in PBS, the Eg5 was eluted using GST elution buffer (5 mM glutathione, 50 mM Tris-HCl, pH 8.0), concentrated using 100K Amicon ultra filter units (Millipore) and stored in motility buffer (50 mM imidazol, 0.5 mM $MgCl_2$, 0.5 mM EGTA, 0.5 mM DTT, pH 6.8) supplemented with 150 mM NaCl and 1 M glycerol at -80℃.

2.3.4 Preparation of microtubules

The tubulin was purified from porcine brain homogenates by two cycles of temperature-dependent disassembly/reassembly (Shelanski *et al.* 1973) followed by phosphocellulose column chromatography (Weingarten *et al.* 1975). Microtubules were formed by Taxol-promoted self assembly of 5 mg/ml tubulin in 20 mM PIPES, 80 mM NaCl, 0.5 mM $MgCl_2$, 1 mM EGTA, 0.2 mM GTP, 50 µM Taxol at 37℃, pH 6.8.

2.3.5 Determination of protein concentration

The total protein concentration was determined by the Lowry method (Lowry *et al.* 1951) using bovine serum albumin (BSA, Sigma-Aldrich, Germany) as reference. To distinguish between the kinesin construct and possible protein contaminations, and consequently to get exact information of the kinesin content in each single preparation, the band intensities from corresponding SDS-PAGE were analyzed by Phoretix 1D advanced measurements (Nonlinear dynamics, USA) using pure tubulin as standard.

2.4 Activity measurements

2.4.1 Motility assay

The kinesin constructs were 100-fold diluted in distilled water and allowed to bind to 20-nm beads at a ratio of about 100 motor molecules per bead (colloidal gold, Sigma-Aldrich, Germany). After adding 10-fold concentrated motility buffer to restore normal motility buffer conditions, 10 µl of this bead suspension were mixed with casein (5 mg/ml final concentration), and MgATP (5 mM final concentration; Sigma-Aldrich, Germany) and transferred onto the microtubules, previously immobilized to glass slides by 1% poly(diallyldimethylammonium) chloride (Sigma-Aldrich, Germany) (model of the assay is shown in Figure 2.3).

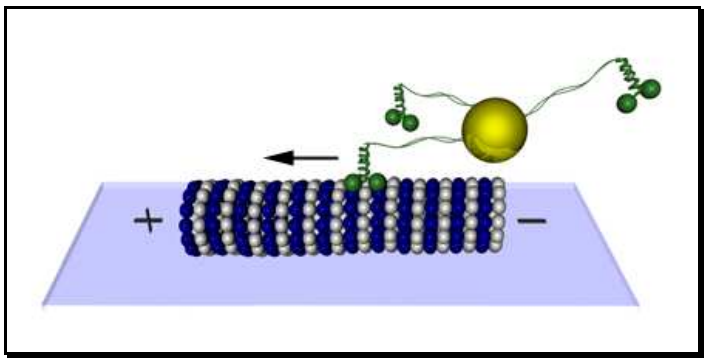

Figure 2.3 *Model of kinesin motility assay (bead assay).*
In the bead assay, the microtubules [polymers composed of α-tubulin (grey) and β-tubulin (blue)] are immobilized on a glass surface. The kinesin bound to the cargo moves towards the microtubule plus end. The arrow indicates the direction of the kinesin-driven cargo transport. The Figure is designed by Kerstin Dreblow, FLI Jena.

2.4.2 Microscopy

2.4.2.1 Light microscopy

The movement of the kinesin-coated gold beads along the microtubules was visualized by Allen video-enhanced differential interference contrast microscopy (AVEC-DIC) using an Axiophot microscope (Zeiss, Germany) with an oil immersion objective (100x/1.30), equipped with a Chalnicon video camera (Hamamatsu Photonics GmbH, Germany) and the image processing system Argus 20 (Hamamatsu), which enables background subtraction, electronic contrast enhancement, and online velocity measurement. Bead movement was documented on a digital hard-disk recorder (JVC SR-DVM 70 Recorder).

2.4.2.1 Transmission electron microscopy

For electron microscopy, either full-length Eg5 or full-length KIF5A (as control) were allowed to bind to taxol-stabilized microtubules in the presence of MgATP. Thereafter, a small portion of the microtubule-kinesin suspension was transferred onto formvar/carbon-coated 400-mesh copper grids and negatively stained with 1% uranyl acetate. Electron micrographs were taken by a ZEISS CEM 902 microscope.

2.4.3 ATPase activity measurement

The enzymatic activities of the recombinant kinesins were determined by measuring the free inorganic phosphate released during ATP hydrolysis, using a Malachite green staining technique (Martin *et al.* 1985) (Biomol, Germany).

Taxol-stabilized microtubules at different concentrations were mixed with the kinesin constructs at concentrations of 50-300 nM. ATP hydrolysis was initiated by adding MgATP (Sigma-Aldrich) at final concentrations of 3-5 mM. After incubation (20-30 min) at 37℃, the reaction was stopped by ad dition of HCl (0.1 N final concentration). Triple aliquots of the mixtures were assayed for their phosphate content at 650 nm. The values obtained were plotted against the microtubule (tubulin) concentration. Exponential fitting the plot, using Microcal Origin 7.5 software (Additive GmbH, Germany) provided the k_{cat} value at conditions of microtubule saturation.

2.4.4 Kinesin-microtubule binding assay

The different kinesin constructs were directly dotted (total amounts of 1 µg per dot) onto nitrocellulose membrane and allowed to dry completely. The membrane was blocked by 1 h incubation in 5% non-fat dry milk/PBS. After three 10-min washing steps with PBS the membrane was incubated for 30 min with microtubules (40 µM tubulin) in motility buffer containing 10 µM Taxol and 2 mM AMP-PNP (a non-hydrolysable ATP analogue, causing a strong binding of kinesin to microtubules) (Sigma-Aldrich, Germany). After microtubule binding, the membrane was briefly washed twice in motility buffer with Taxol and AMP-PNP. The microtubules bound to the protein dots were fixed by 0.1% glutardialdehyde in PBS for 20 min. The free aldehyde groups were blocked by incubation of the membrane in PBS containing 1 mg/ml $NaBH_4$ for 20 min. After washing with PBS, the membrane was incubated for 1 h with monoclonal mouse anti-alpha-tubulin antibody (dilution 1:3000) (Sigma-Aldrich, Germany) in PBS containing 0.05% Tween 20 (PBS-Tween) and 5% non-fat dry milk. After washing with PBS-Tween, the membrane was incubated for 1 h with goat anti-mouse IgG-HRP (dilution 1:3000) in PBS-Tween with 5% non-fat dry milk. The membrane was washed triple with PBS-Tween and once with PBS, and finally developed by enhanced chemiluminescence. A control membrane with the same order of dotted proteins was prepared. However, in this case the incubation step in taxol-stabilized microtubules was replaced by incubation in taxol-containing buffer, only.

3. Results

3.1 Construct design

3.1.1 Full-length and truncated control KIF5A and Eg5 constructs

The full-length Eg5, composed of 1057 amino acids, is known to represent a homotetramer with pairs of identical motor domains positioned at both ends of a central rod (Figure 1.2 C). Recent *in vitro* studies have shown that Eg5 can bundle and subsequently sort apart anti-parallel microtubules (Kapitein *et al.* 2005).

In the present work, a full-length and a truncated variant of Eg5 (N-terminal 1-513 amino acids) were expressed (Figure 3.1) as control proteins.

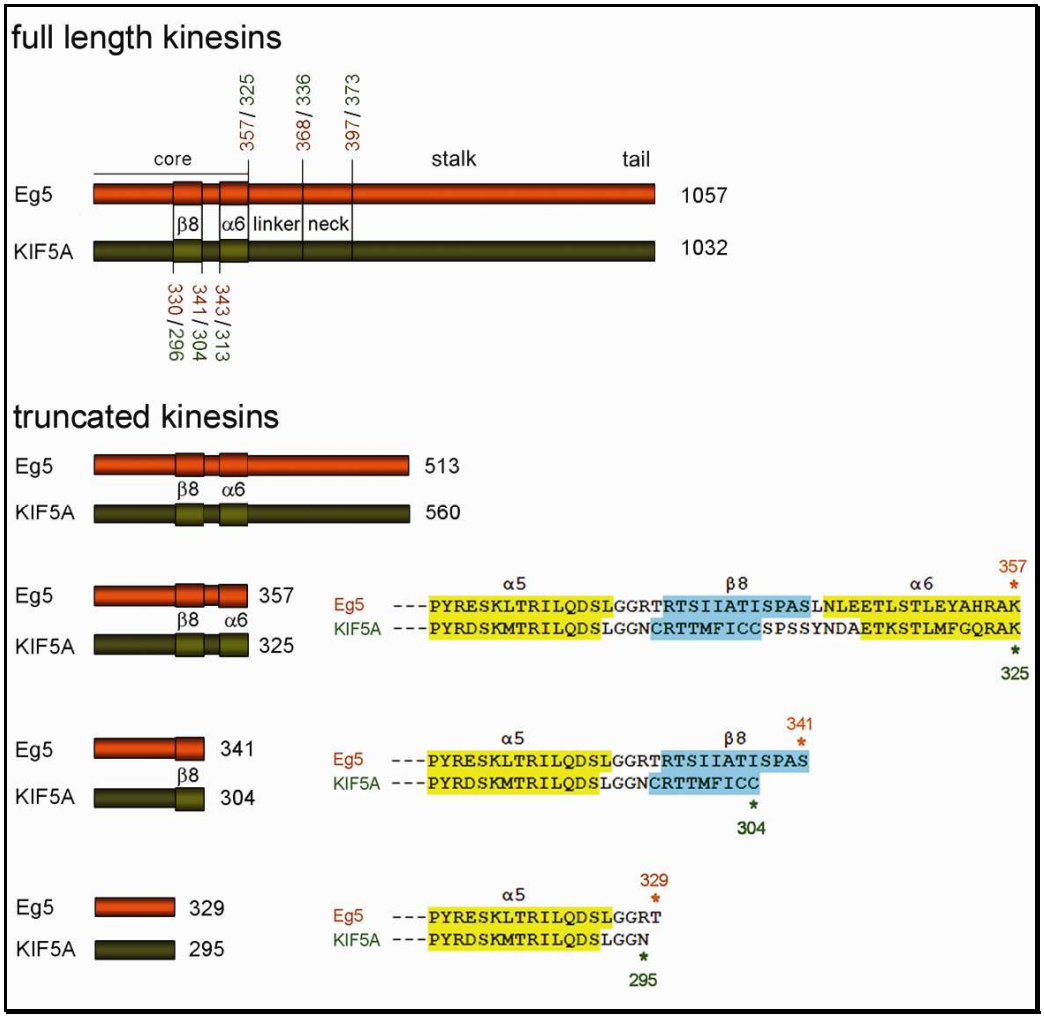

Figure 3.1 *Bar diagrams of C-terminally truncated Eg5 and KIF5A proteins.*
The positions at which strand β8 and helix α6 end and at which the linker and neck terminate are indicated by numbers (orange for Eg5 and green for KIF5A, respectively). The amino acids sequence and the positions at which the C-terminally truncated motor domains of Eg5 and KIF5A terminate are indicated by asters and numbers. The α5 and α6 are highlighted in yellow, strand β8 in blue.

Full-length KIF5A is composed of 1032 amino acids. It represents a dimeric protein with two motor domains at one and the same end. As control proteins a full-length and a truncated KIF5A (amino acids 1-560) were expressed. $KIF5A_{1-560}$ was terminated to the first coiled-coil of its stalk (hinge-2 region) (Figure 3.1).

3.1.2 Truncated and chimeric constructs to study the role of strand β8 and helix α6

3.1.2.1 Truncated KIF5A and Eg5 motor domain constructs

The catalytic core of both KIF5A and Eg5 comprises a central β-sheet consisting of eight β-strands surrounded by six α-helices (Figure 1.4) and does not include the neck linker and neck sequences. The catalytic core contains the nucleotide-binding loop (P-loop), formed by N1-N4 structural elements (Sablin *et al.* 1996) (see 1.2.1.1.1), and the microtubule-binding surface. Strand β8 and helix α6 (the last elements of the core) are structures which are not a part of either the P-loop or the microtubule-binding surface. Their exact role in the mechanochemical cycle of KIF5A and Eg5 is still not fully understood.

To investigate whether KIF5A and Eg5 require the same minimal catalytic core to generate activity (microtubule binding and ATP hydrolysis) C-terminally truncated KIF5A and Eg5 motor domain proteins were constructed.

First, the $KIF5A_{1-325}$ and $Eg5_{1-357}$ motor domains (Figure 3.1), containing the N-terminal part of the catalytic core up to the end of helix α6 were expressed.

Additionally, to answer the question of whether β8 and α6 contribute to the activity of the catalytic cores of both KIF5A and Eg5, or whether they are only structures to maintain proper core conformation, truncated motor domains lacking either α6 only ($Eg5_{1-341}$ and $KIF5A_{1-304}$) or both β8 and α6 ($Eg5_{1-329}$ and $KIF5A_{1-295}$) were expressed (Figure 3.1). Since these four constructs lack the neck linker and neck they are considered to exist as monomers (Jiang *et al.* 1997).

3.1.2.2 Chimeric KIF5A and Eg5 constructs with β8, α6, neck linker and neck interchanged

To extend the knowledge on the molecular mechanisms of microtubule binding and ATPase and motility activity it was tested if strand β8 and helix α6 can be interchanged between KIF5A (referred as K) and Eg5 (referred as E), or if they are kinesin type-specific.

Two chimeric proteins were generated - the first one, K-E(β8α6-linker-neck) (residues $KIF5A_{1-294}$-$Eg5_{328-513}$) contains the catalytic core of KIF5A up to the end of helix α5 fused to Eg5 starting with the strand β8, proceeding with helix α6, neck linker and neck and terminating at the initial brake in the coiled-coil of the Eg5 stalk. Parallel, the complementary chimera E-K(β8α6-linker-neck) (residues $Eg5_{1-325}$-$KIF5A_{293-450}$) has been constructed (Figure 3.2). The chimeras were generated using the splicing by overlap extension (SOE) PCR method (Ho *et al.* 1989).

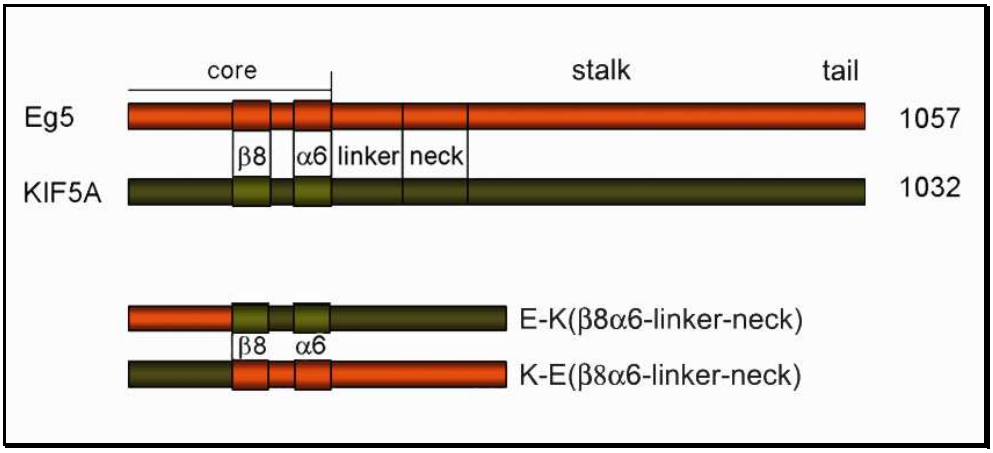

Figure 3.2 *Construction of Eg5- and KIF5A-based chimeric proteins.*
The Eg5 and KIF5A elements are shown in orange and green, respectively.

3.1.3 KIF5A and Eg5 chimeras with neck linker and/or neck regions interchanged to study velocity regulation

3.1.3.1 Chimeras with neck linker and neck regions interchanged

In contrast to kinesin-1, the neck linker of Eg5 was found in ADP-bound state in a unique position perpendicular to the core (Turner *et al.* 2001). As the neck linker is a flexible element that docks and undocks to the core during ATP turnover, it was hypothesized that the linker might be involved in velocity regulation. To confirm this hypothesis, chimeric proteins consisting of elements of the fast-moving KIF5A and the slow-moving Eg5 were constructed and expressed (Figure 3.3).

In the chimera K-E(linker-neck) (residues $KIF5A_{1-325}$-$Eg5_{358-513}$) the catalytic core of KIF5A was fused to the Eg5 neck linker and neck and a part of the stalk. The complementary chimera E-K(linker-neck) (residues $Eg5_{1-357}$-$KIF5A_{326-450}$) contains the Eg5 catalytic core fused to the KIF5A neck linker, neck and part of the stalk.

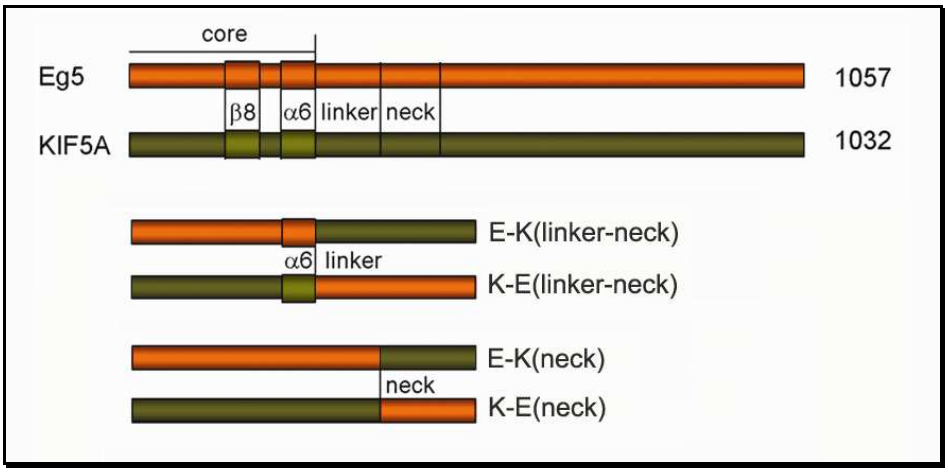

Figure 3.3 *Construction of Eg5- and KIF5A-based chimeric proteins.*
The Eg5 and KIF5A elements are shown in orange and green, respectively.

3.1.3.2 Chimeras with neck regions interchanged

The neck region as a part of the mechanical element might also play a role in velocity regulation. To confirm this assumption, two KIF5A- and Eg5-based chimeras with interchanged neck coiled-coils were generated. In the first one, K-E(neck) (residues $KIF5A_{1-336}$-$Eg5_{369-513}$), the KIF5A core and the linker were fused to the neck coiled-coil and a part of the stalk of Eg5. The second one, E-K(neck) (residues $Eg5_{1-368}$-$KIF5A_{337-450}$), contains the Eg5 catalytic core and linker fused to the KIF5A neck (Figure 3.3).

3.1.4 KIF5A truncated and chimeric constructs to study the role of the neck linker

3.1.4.1 KIF5A constructs without neck linker, with the half and complete native linker

Recently, molecular dynamics simulations with kinesin crystal structures have demonstrated that a so-called cover strand (strand β0), which comprises a nine-amino-acid-long sequence at the N-terminus, is crucial for kinesin force generation (Hwang *et al.* 2008). Upon ATP binding, the cover strand creates a cover-neck bundle by forming a β-sheet with the first half (strand β9) of the linker. This bundle is discussed to be a special conformation which forces the linker to dock to the core.

To test the effect of the linker on KIF5A ATPase activity, C-terminally truncated constructs with either the full linker or its first half, have been generated ($KIF5A_{1-336}$ and $KIF5A_{1-330}$, respectively). The ATPase activity of these proteins was compared with the activity of the $KIF5A_{1-325}$ protein, which does not contain linker sequences (Figure 3.4).

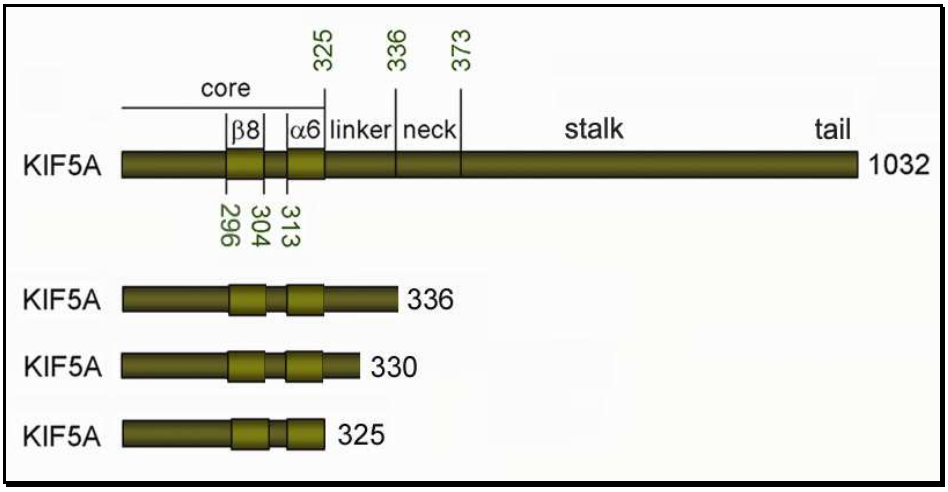

Figure 3.4 *Bar diagrams of C-terminally truncated KIF5A proteins.*
$KIF5A_{1-325}$ lacks the linker sequence, while $KIF5A_{1-330}$ and $KIF5A_{1-336}$ contain the half and the complete linker, respectively.

3.1.4.2 KIF5A-based chimera with half native linker fused to the Eg5 linker and neck

To study the role of KIF5A half linker (strand β9) on velocity, a chimeric protein very similar in its structure to the K-E(linker-neck) construct (3.1.3.1) was generated. This chimera, termed K(5aa linker)-E(linker-neck) (residues $KIF5A_{1-330}$-$Eg5_{358-513}$), contained the KIF5A core with the first five amino acids of its native linker fused to Eg5 linker, neck and part of the stalk (Figure 3.5).

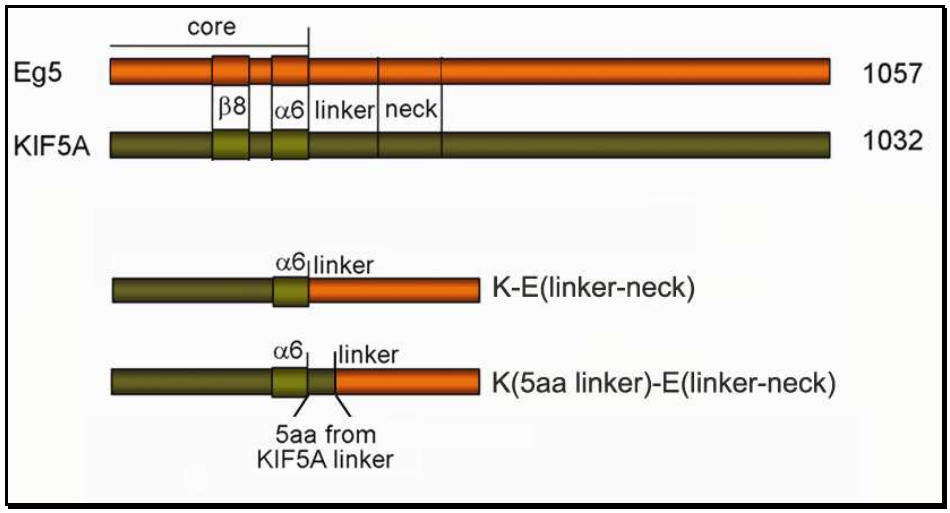

Figure 3.5 *Construction of K(5aa linker)-E(linker-neck) chimeric protein.*
The chimera contains the native half linker of KIF5A fused to the linker and neck of Eg5. The structures of the full-length Eg5 and KIF5A, as well as the structure of the control K-E(linker-neck) chimera are shown.

3.2 Purification of recombinant kinesins

All proteins used in the study were expressed in *E. coli*, excepting the full-length Eg5. Often, the expression of recombinant proteins in bacterial cells is limited by the size of the protein (<100 kD) (Marston 1986) or the proteins expressed are insoluble, aggregated or incorrectly folded. Therefore, recombinant proteins with a high molecular mass or proteins which require post-translational modifications are usually expressed in eukaryotic systems. These systems allow to produce recombinant proteins properly folded and revealing normal disulfide bond formation and oligomerization ability. Additionally, the system is capable of performing post-translational modifications, which leads to proteins both structurally and functionally similar to their native counterparts.

3.2.1 Purification from E. coli

When the bacterial expression system was used, the kinesins (listed in Table 3.1) were obtained as fusion proteins containing a C-terminal tag, composed of an intein followed by a chitin binding domain (New England Biolabs, Germany). This tag undergoes specific DTT-induced self-cleavage as a result of which the target protein separates from the intein tag. This one-step purification procedure yields proteins (Figure 3.6) without additional sequences.

Name	Amino acids	Molecular mass (kD)
	truncated	
$KIF5A_{full\text{-}length}$	1-1032	120
$KIF5A_{1\text{-}560}$	1-560	63.8
$KIF5A_{1\text{-}336}$	1-336	37.5
$KIF5A_{1\text{-}330}$	1-330	36.9
$KIF5A_{1\text{-}325}$	1-325	36.2
$KIF5A_{1\text{-}304}$	1-304	34.0
$KIF5A_{1\text{-}295}$	1-295	33.0
$Eg5_{1\text{-}513}$	1-513	57.6
$Eg5_{1\text{-}357}$	1-357	39.7
$Eg5_{1\text{-}341}$	1-341	37.8
$Eg5_{1\text{-}329}$	1-329	36.5
	chimeric	
K-E(β8α6-linker-neck)	$K_{1\text{-}294}$ - $E_{328\text{-}513}$	54.6
E-K(β8α6-linker-neck)	$E_{1\text{-}325}$ - $K_{293\text{-}450}$	54.3
K-E(linker-neck)	$K_{1\text{-}325}$ - $E_{358\text{-}513}$	54.2
E-K(linker-neck)	$E_{1\text{-}357}$ - $K_{326\text{-}450}$	54.2
K(5aa linker)-E(linker-neck)	$K_{1\text{-}330}$ - $E_{358\text{-}513}$	54.8
K-E(neck)	$K_{1\text{-}336}$ - $E_{369\text{-}513}$	54.2
E-K(neck)	$E_{1\text{-}368}$ - $K_{337\text{-}450}$	54.4

Table 3.1 *Overview of proteins expressed in E. coli.*
The amino acids, at which the C-terminally truncated proteins terminate, as well as the amino acids of the parts by which the chimeric proteins are composed, are indicated by numbers. The Table represents also the theoretical molecular mass of the proteins.

Since overexpression of the proteins with deleted or interchanged α6 and β8 structures was not high (Figure 3.6 C), the corresponding protein preparations were additionally characterized by Western blotting (Figure 3.6 D). The expression products are found at positions corresponding to their theoretically calculated molecular mass.

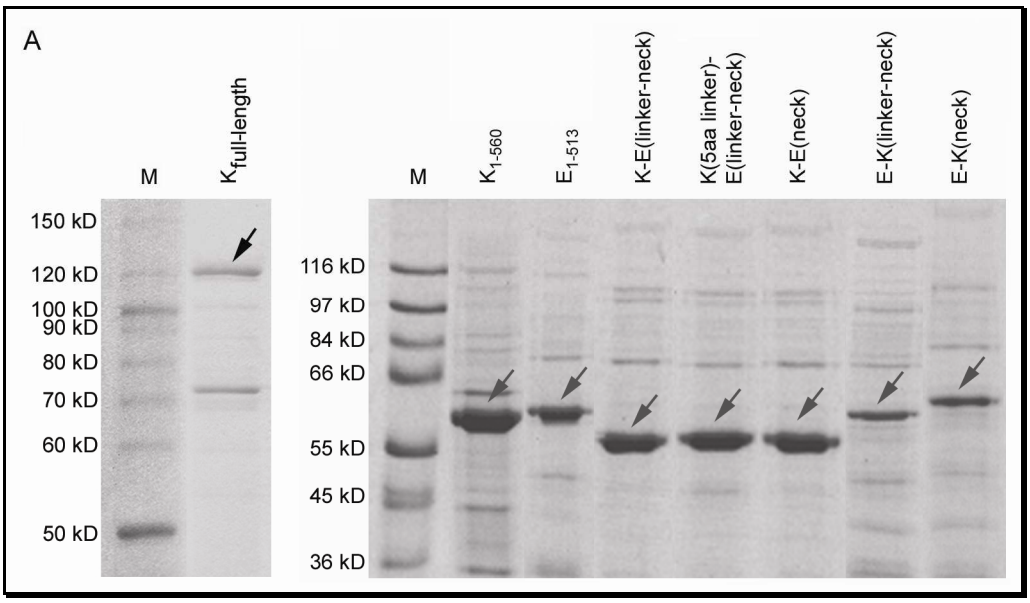
A
M
K full-length
150 kD
120 kD
100 kD
90 kD
80 kD
70 kD
60 kD
50 kD
M
K 1-560
E 1-513
K-E(linker-neck)
K(5aa linker)-E(linker-neck)
K-E(neck)
E-K(linker-neck)
E-K(neck)
116 kD
97 kD
84 kD
66 kD
55 kD
45 kD
36 kD

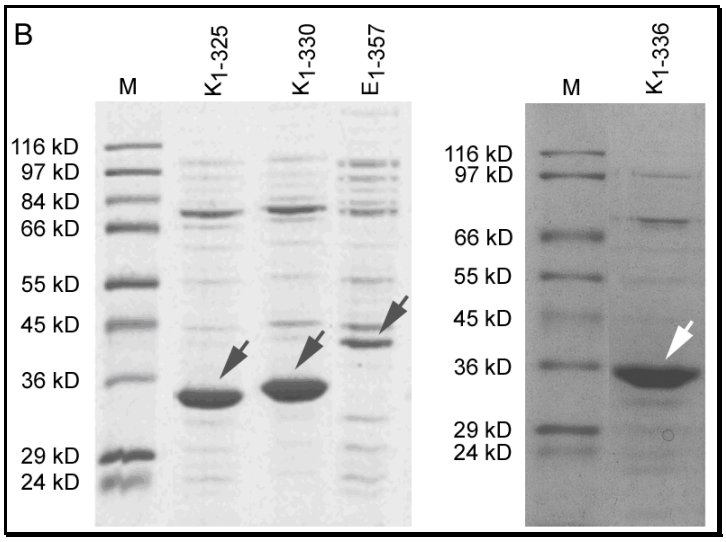
B
M
K 1-325
K 1-330
E 1-357
116 kD
97 kD
84 kD
66 kD
55 kD
45 kD
36 kD
29 kD
24 kD
M
K 1-336
116 kD
97 kD
66 kD
55 kD
45 kD
36 kD
29 kD
24 kD

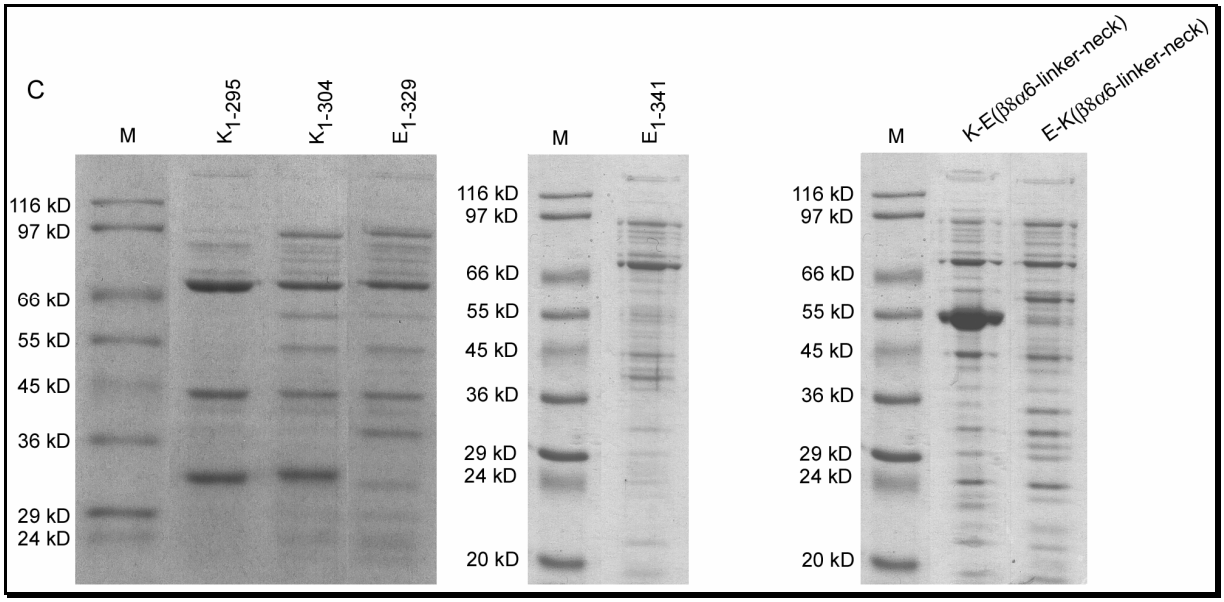
C
M
K 1-295
K 1-304
E 1-329
116 kD
97 kD
66 kD
55 kD
45 kD
36 kD
29 kD
24 kD
M
E 1-341
116 kD
97 kD
66 kD
55 kD
45 kD
36 kD
29 kD
24 kD
20 kD
M
K-E(β8α6-linker-neck)
E-K(β8α6-linker-neck)
116 kD
97 kD
66 kD
55 kD
45 kD
36 kD
29 kD
24 kD
20 kD

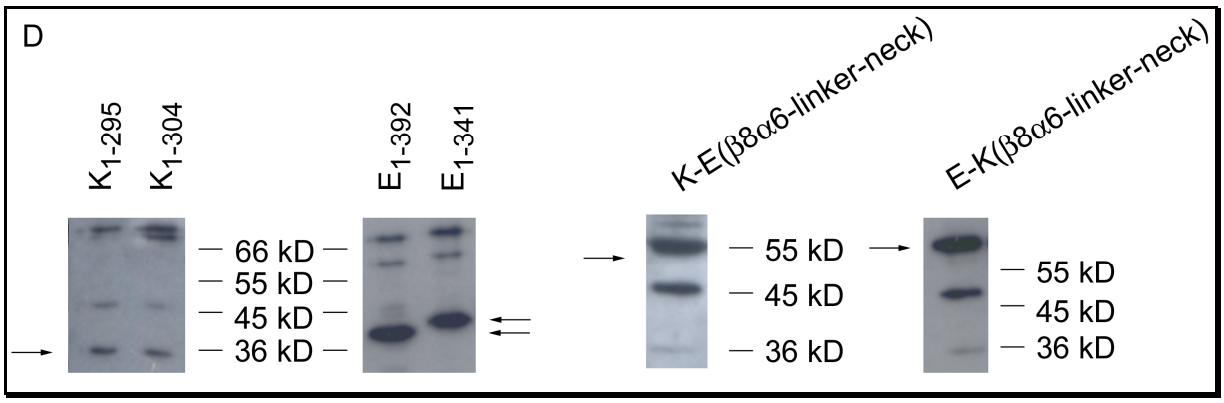

Figure 3.6 *Electropherograms of KIF5A (labelled by K) and Eg5 (E) truncated and chimeric proteins.*
A) coomassie stained 7.5 % SDS-gels of full-length KIF5A and control $KIF5A_{1-560}$ and $Eg5_{1-513}$, and chimeras with neck linker and/or neck regions interchanged.
B) coomassie stained 10% SDS-gel of the $Eg5_{1-357}$ motor domain without linker and KIF5A motor domains lacking the linker ($KIF5A_{1-325}$), or containing either half linker ($KIF5A_{1-330}$) or full linker ($KIF5A_{1-336}$).
C) coomassie stained 10% SDS-gels of truncated KIF5A and Eg5 motor domains lacking either helix α6 ($KIF5A_{1-304}$ and $Eg5_{1-341}$) or both helix α6 and strand β8 ($KIF5A_{1-295}$ and $Eg5_{1-329}$), and of the K-E(β8α6-linker-neck) and E-K(β8α6-linker-neck) chimeras.
D) Western blot of the proteins shown in C. KIF5A-derived proteins were detected with mouse monoclonal anti-kinesin heavy chain antibody, and Eg5-based proteins with rabbit anti-Eg5 antibody, respectively. Control reactions performed without primary antibody were negative. Positions of the KIF5A- and Eg5-derived constructs are indicated by arrows. Protein bands below the specific ones most probably represent degradation products. Protein bands above 60 kD might represent aggregations, or fusion constructs with uncut intein tag (intein tag is ~50 kD). M: molecular mass standard.

3.2.2 Purification of the full-length Eg5 from insect cells

The full-length Eg5 has a molecular mass of 120 kD. Four Eg5 heavy chains can oligomerize and form tetrameric structures, crucial for Eg5 activity. The bacterially expressed recombinant protein was found to be inactive (its ATPase activity could not be stimulated by microtubules), which is most probably due to incorrect folding. Therefore, full-length Eg5 protein was produced in insect cells as a fusion protein with an N-terminal GST (glutathione-S-transferase) tag, using the baculovirus vector expression system. The tag was fused to the N-terminus since any additional sequence to the C-terminal part of the Eg5 could disturb protein tetramerization. The GST tag enables affinity purification using glutathione agarose beads (2.3.3.2). The amount of contaminations after purification was very low (Figure 3.7, line 3). For further purification the GST tag was designed to contain a thrombin cleavage site which enables proteolytic cutting of the recombinant protein from the tag. Unfortunately, the cleavage of the GST tag from the purified Eg5-GST fusion protein

led to Eg5 degradation (Figure 3.7, line 4). Therefore, the full-length Eg5 was used without separating the GST tag.

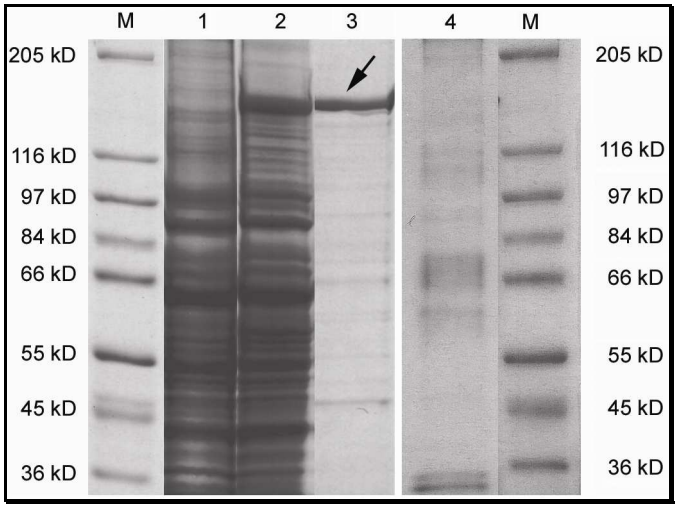

Figure 3.7 *SDS-gel of purification steps of the full-length Eg5 protein.*
1: total insect cell lysate from non-infected cells; 2: total insect cell lysate from cells infected with Eg5-GST-expressing virus; 3: purified Eg5-GST protein; 4: purified Eg5 after thrombin cleavage; M: molecular mass standard.

3.3 ATPase activity, microtubule binding and motility

For each kinesin construct, the ATP turnover rates were measured in the presence of microtubules and given as k_{cat} values (ATP molecules hydrolyzed per catalytic core per second, measured at 37℃). Plotting the k_{cat} values against the microtubule concentration (tubulin dimer concentration) reveals a Michaelis-Menten-like behavior. To compare the activities, the characteristic k_{cat} values were calculated for each construct under conditions of microtubule saturation (plateau level of exponential fitting).

Constructs lacking ATPase activity were additionally checked for their ability to bind to microtubules, using a kinesin-microtubule binding assay based on ligand blotting (2.4.4).

For the dimeric constructs the transport velocities were determined using a bead motility assay (2.4.1). Motility assays with C-terminally truncated motor domain constructs were not possible as these constructs lack the neck region crucial for dimerization and processive movement, as well as they lack the stalk region which is necessary to bind the motor to the cargo (gold bead).

3.3.1 Full-length KIF5A

In the absence of microtubules kinesins hydrolyse ATP slowly (basal ATPase activity). As commonly known, the ATPase activity of kinesin motors is stimulated by microtubules (Figure 3.8). The maximal KIF5A hydrolysis rate (k_{cat}) in the presence of microtubules was 1.82 s^{-1}. KIF5A hydrolysis rate in the absence of microtubules was 0.04 s^{-1} (Table 3.2).

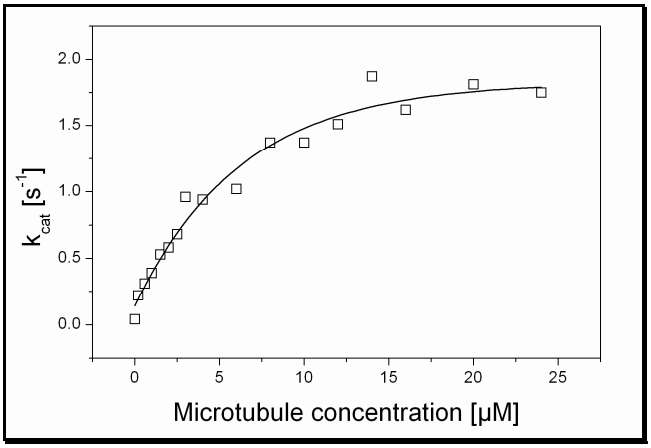

Figure 3.8 *ATPase activity of full-length KIF5A in dependence on microtubule concentration.*

The transport velocity of the full-length KIF5A was ~0.8-1.0 µm s^{-1}, comparable to the motility of other kinesin-1 members (see *e.g.*, Hancock & Howard 1998; Blasius *et al.* 2007).

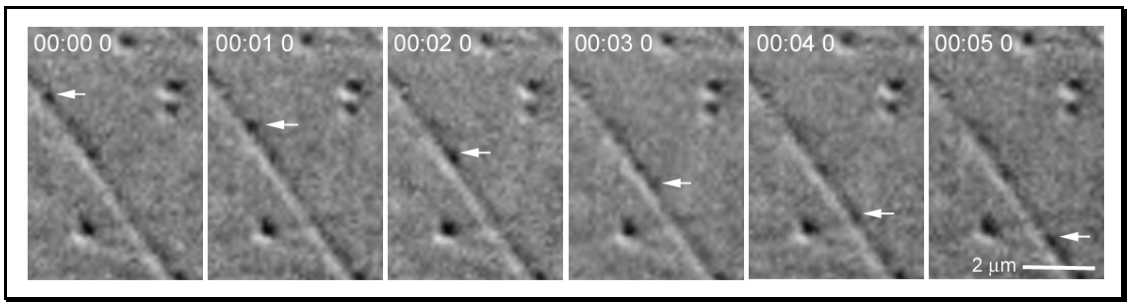

Figure 3.9 *Video sequence of bead transport by the full-length KIF5A.*
The moving bead is indicated by an arrow; the time scale indicates minutes, seconds, and tenths of a second.

Since the bacterial expression of the truncated $KIF5A_{1-560}$ led to higher expression levels of protein functionally undistinguishable from the full-length KIF5A (see section 3.3.3), the $KIF5A_{1-560}$ was used as control protein throughout this study.

3.3.2 Full-length Eg5

The ATP turnover of the full-length Eg5 in the presence of microtubules was ~0.02 s^{-1} (Figure 3.10). Up to now, no data on the ATPase activity of full-length Eg5 have been available.

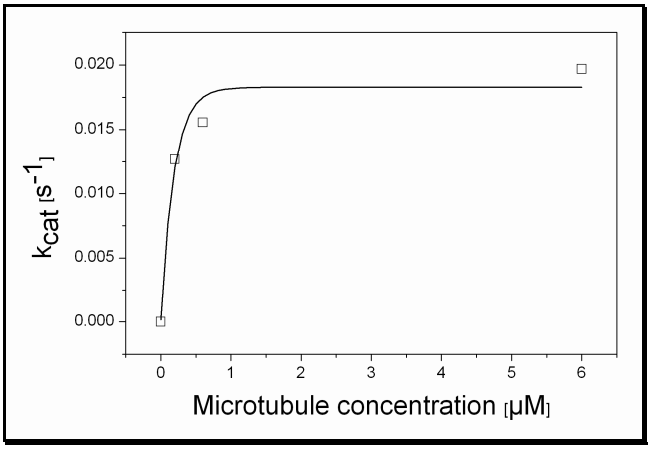

Figure 3.10 *ATPase activity of full-length Eg5 in dependence on microtubule concentration.*

The human full-length Eg5, obtained in this study, has been shown to be able to transport cargoes along immobilized microtubules at ~10 ± 3 nm s^{-1} (Figure 3.11). This velocity is comparable to that published for the full-length Eg5 protein from *Xenopus laevis* (14 nm s^{-1}) (Kwok *et al.* 2006), but lower compared to *Xenopus* Eg5 measured by Kapitein *et al.* 2005, and Korneev *et al.* 2007 (20 nm s^{-1} and 35 nm s^{-1}, respectively). The lower velocity, measured for the human full-length Eg5, could be due to the presence of the relatively large N-terminal GST tag which might affect the binding of the Eg5 to the next free tubulin dimer.

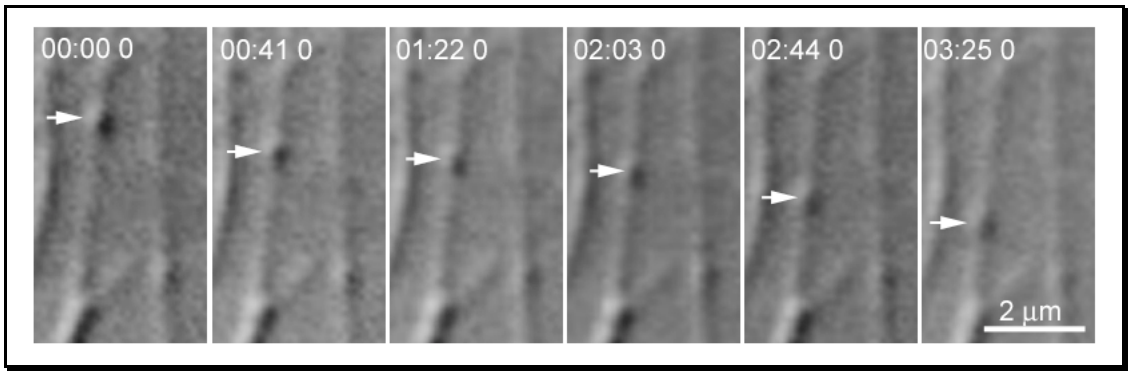

Figure 3.11 *Video sequence of bead transport by the slow-moving full-length Eg5.*
The moving bead is indicated by an arrow; the time scale indicates minutes, seconds, and tenths of a second.

Due to its bipolar tetrameric structure, *i.e.*, due to the presence of motor domains with microtubule-binding sites at both ends, full-length Eg5 was found to bundle microtubules (Figure 3.12). Under the same conditions, KIF5A which forms monopolar dimers with the motor domains at one end, only, did not support microtubule bundling (data not shown).

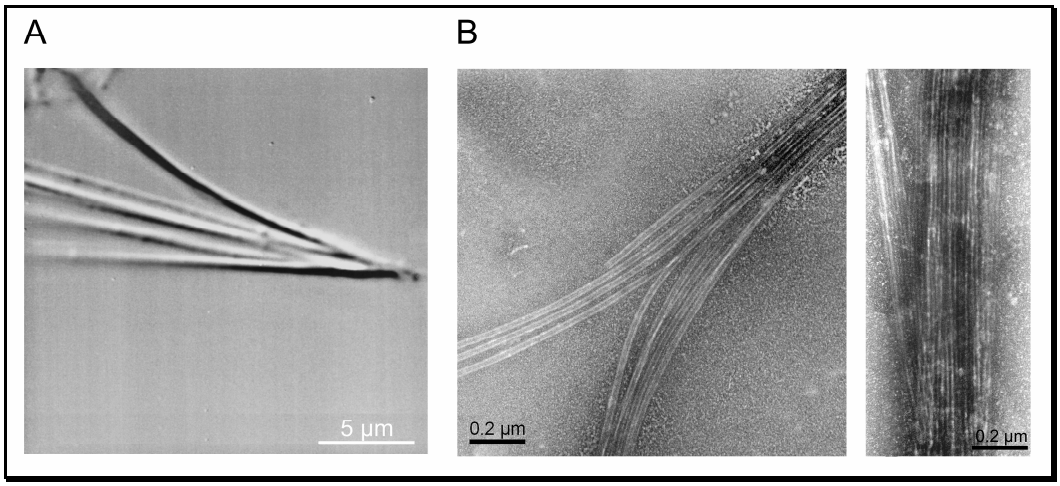

Figure 3.12 *Eg5 induced microtubule bundling.*
Microtubule bundling in the presence of full-length Eg5 using: A) AVEC-DIC and B) electron microscopy.

As all Eg5-based constructs described in this study were expressed in *E. coli* without artificial tag, $Eg5_{1-513}$ was used as control protein instead of the full-length Eg5, containing the GST tag, obtained from insect cells.

3.3.3 Control KIF5A and Eg5 constructs

The ATPase activity of the control $KIF5A_{1-560}$ and $Eg5_{1-513}$ has been measured as a function of microtubule concentration. The resulting k_{cat} (s^{-1}) values are shown in the Figure 3.13 and Table 3.2.

The ATP turnover rate of $KIF5A_{1-560}$ was 9.8 s^{-1} in the presence of microtubules and 0.1 s^{-1} in the absence of microtubules (basal activity).

The basal k_{cat} for the dimeric $Eg5_{1-513}$ was 0.04 s^{-1} and the k_{cat} value in the presence of microtubules was 0.8 s^{-1}.

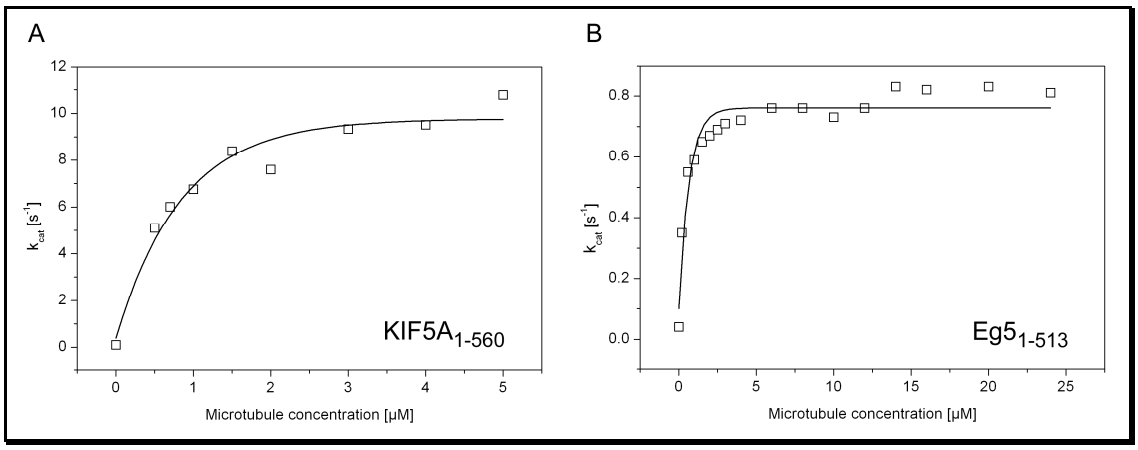

Figure 3.13 *ATPase activity of control KIF5A$_{1-560}$ (A) and Eg5$_{1-513}$ (B) proteins in dependence on microtubule concentration.*

The motility activity of both KIF5A$_{1-560}$ and Eg5$_{1-513}$ control proteins was determined by measuring the transport velocity of 20-nm gold particles driven by these motors along immobilized microtubules (Figure 3.14).

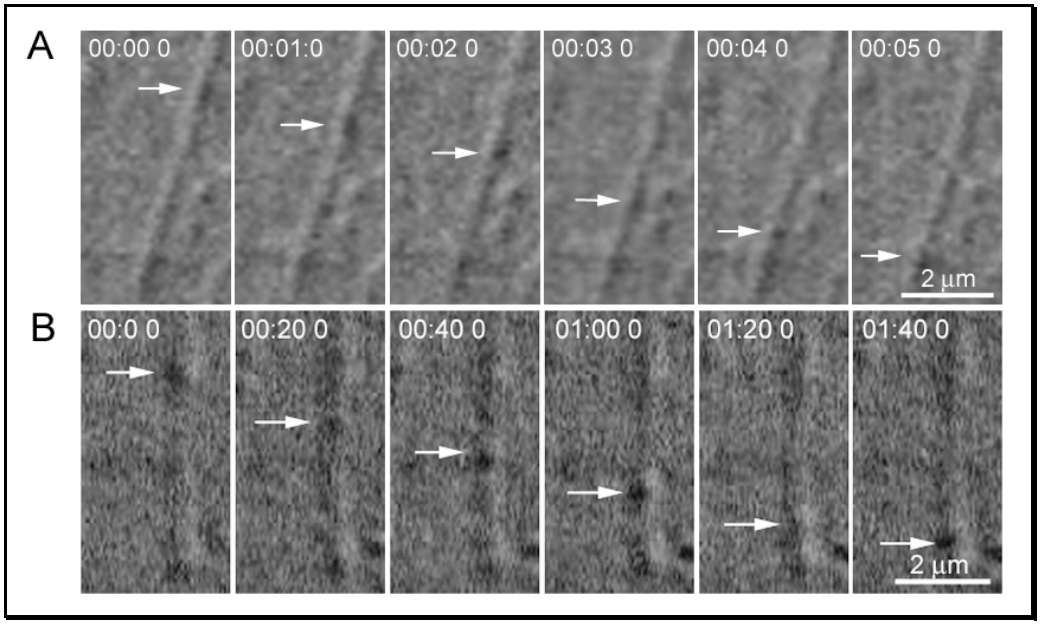

Figure 3.14 *Video sequences of the bead transport by the fast-moving KIF5A$_{1-560}$ (A) and the slow-moving Eg5$_{1-513}$ (B).*
The moving beads are indicated by arrows; the time scale indicates minutes, seconds, and tenths of a second.

The velocity of $KIF5A_{1-560}$ was ~1.0 ± 0.3 µm s^{-1}, which is comparable to that of the full-length KIF5A (Figure 3.15), or to that of other kinesin-1 members (see *e.g.*, Hancock & Howard 1998; Blasius *et al.* 2007).

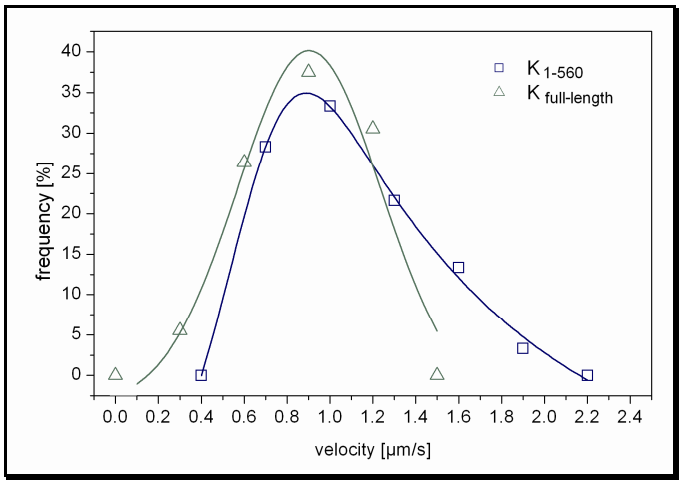

Figure 3.15 *Frequency diagram of velocity distributions of 20-nm gold beads moved by full-length KIF5A and truncated $KIF5A_{1-560}$.*
Each single data point represents the percentage of beads moving at a velocity corresponding to the value indicated at the x-axis with: ± 0.15 µm s^{-1} (number of beads n = 72 for the full-length KIF5A and n = 60 for the truncated protein, respectively).

It became evident that the control $Eg5_{1-513}$ moved at a velocity which was lower than that of the control $KIF5A_{1-560}$ by a factor of ~25. The value of 0.04 µm s^{-1} (Table 3.2) corresponds to the velocity of human $Eg5_{1-513}$ with C-terminal His tag (Krzysiak *et al.* 2006) and to spindle pole separation rates measured *in vivo* in *Drosophila* embryos (Brust-Mascher & Scholey 2002).

3.3.4 KIF5A and Eg5 constructs to study the role of strand β8 and helix α6

3.3.4.1 Truncated KIF5A and Eg5 motor domains

The $KIF5A_{1-325}$ and $Eg5_{1-357}$ constructs contain the complete catalytic core but lack the neck linker and neck sequences. As expected, their ATPase activity was stimulated upon microtubule binding (Figure 3.16 and Table 3.2).

$KIF5A_{1-325}$ ATPase activity was about ten-fold lower than that of the control $KIF5A_{1-560}$ (k_{cat} = 1.0 s^{-1} versus k_{cat} = 9.8 s^{-1} for $KIF5A_{1-560}$). Its basal ATP hydrolysis rate was 0.3 s^{-1}.

Compared to the control $Eg5_{1-513}$, the $Eg5_{1-357}$ showed two-fold higher ATP turnover (k_{cat} = 1.9 s^{-1} versus k_{cat} = 0.8 s^{-1} for $Eg5_{1-513}$). The basal ATPase activity of $Eg5_{1-357}$ was 0.07 s^{-1} and is comparable to that of the $Eg5_{1-513}$.

The higher ATPase activity observed for the monomeric $Eg5_{1-357}$ in comparison to the dimeric $Eg5_{1-513}$ control protein suggests cooperative interactions between the motor domains of the dimer which slow the overall reaction rate. Such behaviour has been documented also for kinesin-1 members, myosin-V, and myosin-VI (Moyer *et al.* 1996; Moyer *et al.* 1998; Rosenfeld *et al.* 1996; De La Cruz *et al.* 2001; Sakamoto *et al.* 2003; Cross 2004). In contrast, the ATPase activity of the monomeric $KIF5A_{1-325}$ was lower than that of the dimeric $KIF5A_{1-560}$ control protein, suggesting different mechanism of the control of the KIF5A ATP hydrolysis.

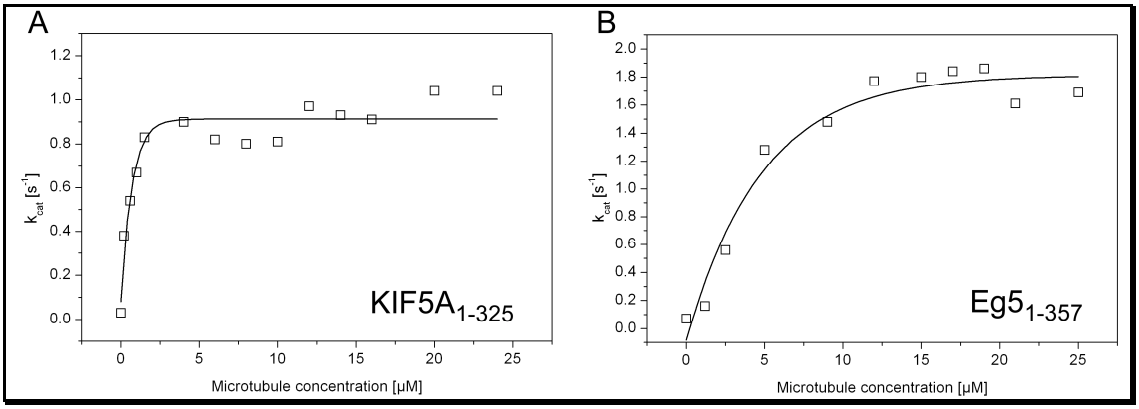

Figure 3.16 *ATPase activities of the truncated $KIF5A_{1-325}$ (A) and $Eg5_{1-357}$ (B) proteins in dependence on microtubule concentration.*

Unlike $KIF5A_{1-325}$ and $Eg5_{1-357}$, the $KIF5A_{1-304}$ and $Eg5_{1-341}$ (lacking helix α6), and $KIF5A_{1-295}$ and $Eg5_{1-329}$ (lacking both helix α6 and strand β8) were not ATPase-active (Table 3.2). The question arises if the truncations led to distortion of the microtubule-binding surface. Using a ligand blot, it has been demonstrated that removal of helix α6, or both α6 and strand β8 did not prevent microtubule binding (Figure 3.17).

It has to be mentioned that the reaction intensities for $KIF5A_{1-304}$, $KIF5A_{1-295}$ and $Eg5_{1-329}$ were relatively low. Nevertheless, when they were compared with those of the negative controls it becomes evident that the reaction was specific.

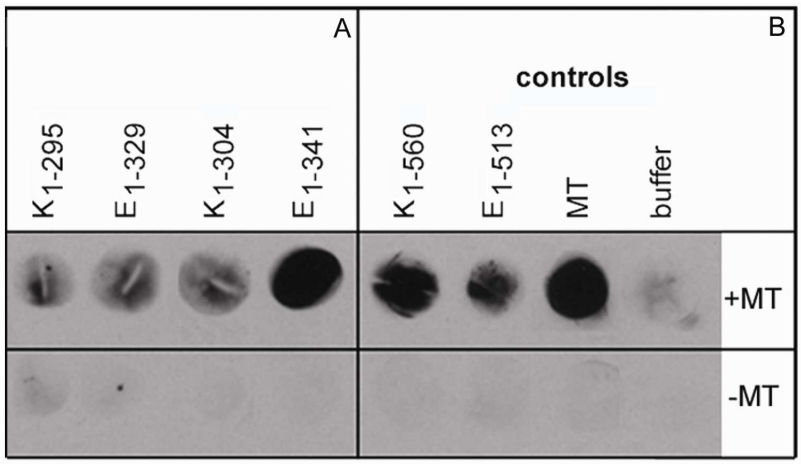

Figure 3.17 *Interaction of truncated KIF5A and Eg5 constructs with microtubules, analyzed by ligand blotting.*
A) truncated KIF5A and Eg5 motor domains (termed K and E, respectively); B) $KIF5A_{1-560}$ (K_{1-560}) and $Eg5_{1-513}$ (E_{1-513}) used as positive controls, microtubules (MT) used as control for the anti-tubulin antibody, motility buffer used as negative control. During preparation of the control membrane (-MT) the reaction step of the kinesin constructs with microtubules was omitted. In this case, the membrane was incubated in motility buffer, only.

3.3.4.2 Chimeric KIF5A and Eg5 proteins with β8, α6, neck linker and neck interchanged

KIF5A and Eg5 chimeras with interchanged strands β8, helices α6, neck-linker and neck regions (Figure 3.1) have been produced and characterized concerning their ATPase activity.

The basal ATP turnover rates were 0.01 s^{-1} for K-E(β8α6-linker-neck) and 0.02 s^{-1} for the E-K(β8α6-linker-neck), respectively. The ATPase was not stimulated by microtubules (Table 3.2). Correspondingly, the K-E(β8α6-linker-neck) and E-K(β8α6-linker-neck) chimeras did not generate motility.

Ligand blotting revealed that interchanging the β8, α6, neck linker and neck between KIF5A and Eg5 did not affect microtubule binding (Figure 3.18).

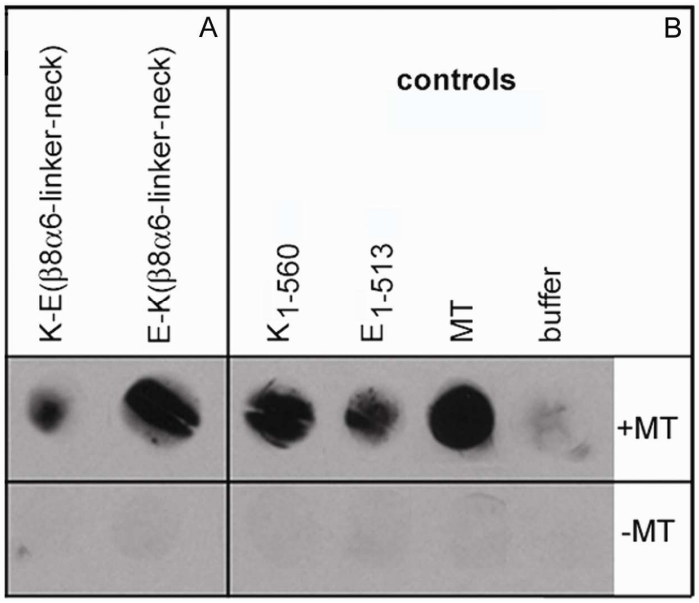

Figure 3.18 *Interaction of chimeric KIF5A- and Eg5-based constructs with microtubules, analyzed by ligand blotting.*
A) chimeric K-E(β8α6-linker-neck) and E-K(β8α6-linker-neck) proteins; B) $KIF5A_{1-560}$ (K_{1-560}), $Eg5_{1-513}$ (E_{1-513}) and microtubules (MT) were used as positive controls and motility buffer as negative control. For further details see Figure 3.17.

3.3.5 KIF5A and Eg5 chimeras with neck linker and/or neck regions interchanged

3.3.5.1 Chimeric KIF5A and Eg5 with neck linker and neck interchanged

The ATPase activities of the K-E(linker-neck) chimera, composed of the KIF5A catalytic core fused to the Eg5 neck linker and neck and a part of the Eg5 stalk (Figure 3.2), as well as of the complementary one, containing the Eg5 catalytic core fused to the KIF5A neck linker, neck and part of the KIF5A stalk were measured. The basal activities were 0.03 s^{-1} and 0.1 s^{-1}, respectively. The activity of both chimeras was substantially elevated upon microtubule binding (Figure 3.19 and Table 3.2).

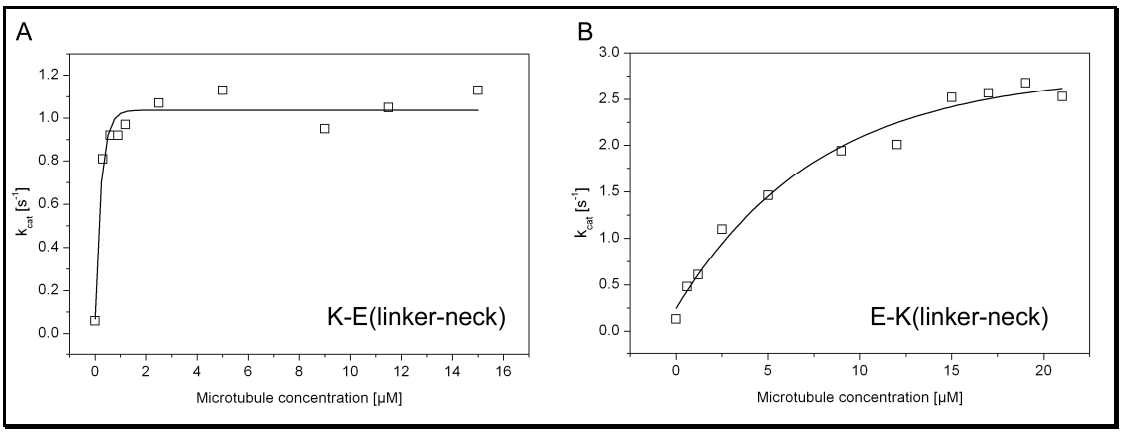

Figure 3.19 *ATPase activities of KIF5A- (A) and Eg5-based (B) chimeras with neck linker and neck interchanged.*

Though the ATPase of the K-E(linker-neck) chimera was significantly stimulated by microtubules, this protein was not able to generate motility. In contrast, the E-K(linker-neck) chimera was found to move at ~0.12 µm s^{-1} (Figure 3.20 and Table 3.2) under the same conditions. Remarkably, this velocity exceeds that of the control $Eg5_{1\text{-}513}$ by a factor of 3 (Figure 3.27 B).

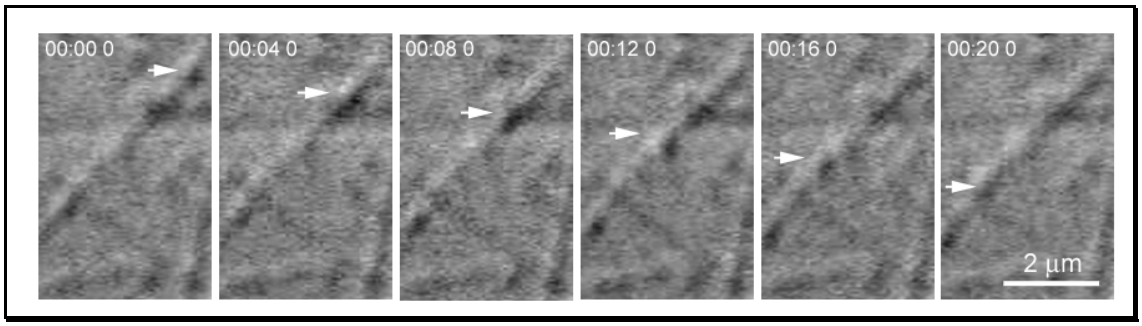

Figure 3.20 *Video sequence of bead transport by the E-K(linker-neck) chimera.*
The moving bead is indicated by an arrow; the time scale indicates minutes, seconds, and tenths of a second.

3.3.5.2 Chimeric KIF5A and Eg5 with neck interchanged

The chimeras K-E(neck) and E-K(neck) in which the neck regions were interchanged had a basal k_{cat} of 0.1 and 0.2 s^{-1}, respectively.

In the presence of microtubules, their k_{cat} values were elevated to 3.9 s^{-1}, and 4.4 s^{-1}, respectively (Figure 3.21 and Table 3.2).

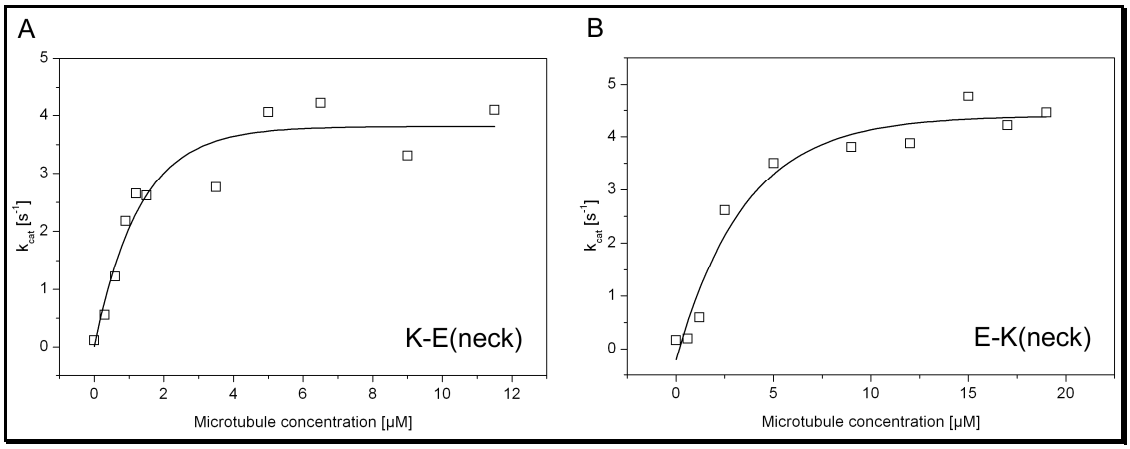

Figure 3.21 *ATPase activities of KIF5A- (A) and Eg5-based (B) chimeras with neck regions interchanged.*

The K-E(neck) construct, composed of the KIF5A core and linker fused to the Eg5 neck coiled-coil moved at a decreased velocity of about 0.54 μm s^{-1}, compared to the control $KIF5A_{1-560}$ (Figures 3.22, 3.27 A and Table 3.2). This decrease was found to be statistically significant (Student's t-test; P<0.0001). In contrast, the complementary E-K(neck) chimera moved with increased velocity of ~0.07 μm s^{-1} (Student's t-test; P<0.0001) in comparison to the control $Eg5_{1-513}$ (Figures 3.22, 3.27 B and Table 3.2).

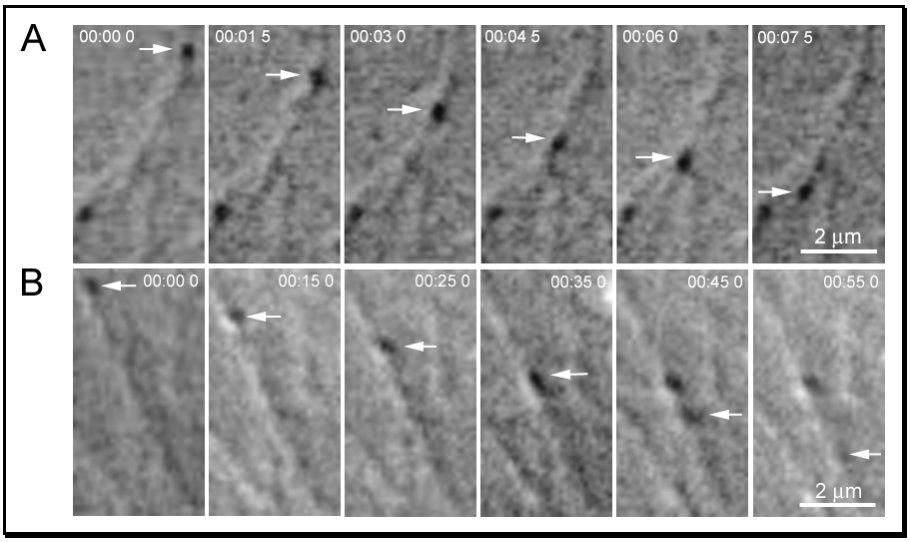

Figure 3.22 *Video sequences of bead transport by the K-E(neck) (A) and E-K(neck) (B) chimeras.* Moving beads are indicated by arrows; the time scale indicates minutes, seconds, and tenths of a second.

3.3.6 KIF5A proteins to study the role of the linker in motility generation

The truncated KIF5A$_{1-325}$ construct representing the KIF5A catalytic core without the linker was found to have a very low ATP hydrolysis rate (Figure 3.16 A and Table 3.2) in comparison to the control KIF5A$_{1-560}$. Additionally, the chimera composed of the KIF5A core fused to Eg5 linker and neck was found to be immotile despite microtubule-promoted ATPase activity. These results indicate that the KIF5A linker may play an essential role in ATPase activity and motility generation.

3.3.6.1 Truncated KIF5A with either the half or the full neck linker

To elucidate the role of the KIF5A linker in the ATPase activity, truncated KIF5A proteins containing either the first half of the linker (representing strand β9; Hwang *et al.* 2008) (KIF5A$_{1-330}$), or the full linker (KIF5A$_{1-336}$) were produced and their ATPase activities were compared to that of the KIF5A$_{1-325}$.

In contrast to KIF5A$_{1-325}$ (Figure 3.16 A), the KIF5A$_{1-330}$ and KIF5A$_{1-336}$ proteins showed an ATP turnover rate of ~25 s^{-1} and 28 s^{-1}, respectively (Figure 3.23 and Table 3.2).

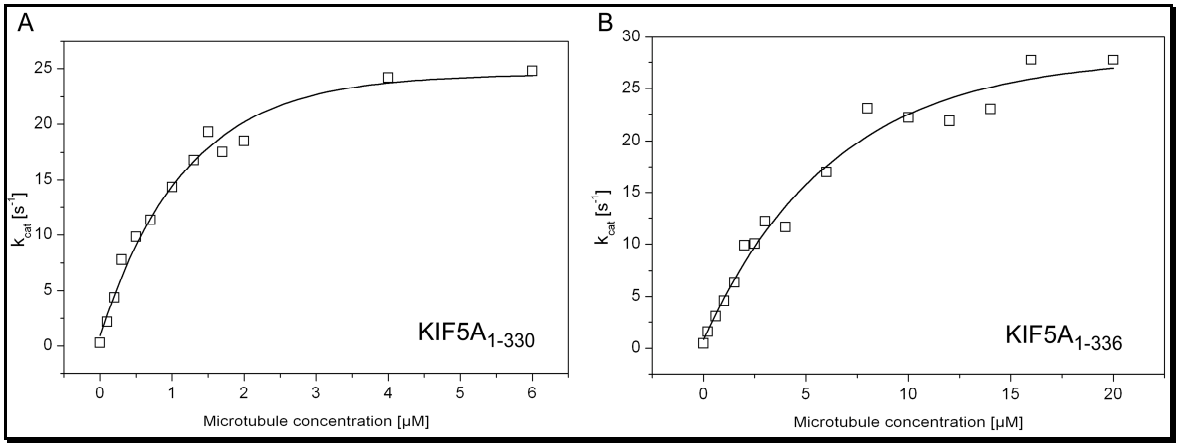

Figure 3.23 *ATPase activities of truncated KIF5A$_{1-330}$ (A) and KIF5A$_{1-336}$ (B) proteins.*

3.3.6.2 Chimeric KIF5A construct with half native linker fused to the Eg5 linker and neck

The results from the truncated KIF5A constructs (3.3.6.1) indicated that the first half of the KIF5A linker (representing strand β9) plays an essential role in ATP hydrolysis. Since the K-E(linker-neck) chimera was immotile, the question arises whether the strand β9 is essential for motility generation. To answer this question a chimeric

protein structurally very similar to K-E(linker-neck) construct was produced. This protein contains additionally the first half part of the native KIF5A linker (Figure 3.5).
It had a k_{cat} value of 7.7 s^{-1} (Figure 3.24 and Table 3.2), which corresponds well to the control $KIF5A_{1-560}$ protein and which is remarkably higher than that of the K-E(linker-neck) chimera (k_{cat} of 0.5 s^{-1}).

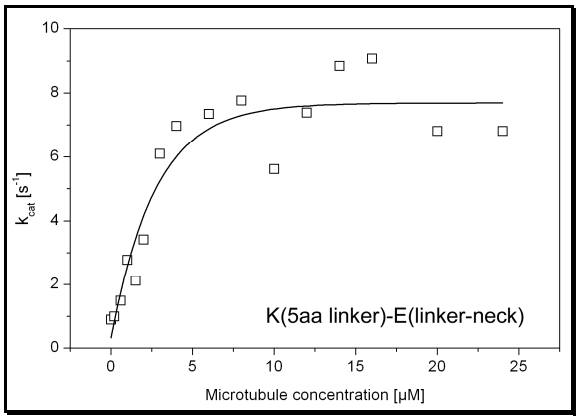

Figure 3.24 *ATPase activity of K(5aa linker)-E(linker-neck) chimera.*

The insertion of the first half of the KIF5A linker into the K-E(linker-neck) chimera restored motility. This protein moved with a velocity of about 0.3 µm s^{-1} (Figures 3.25, 3.28 and Table 3.2).

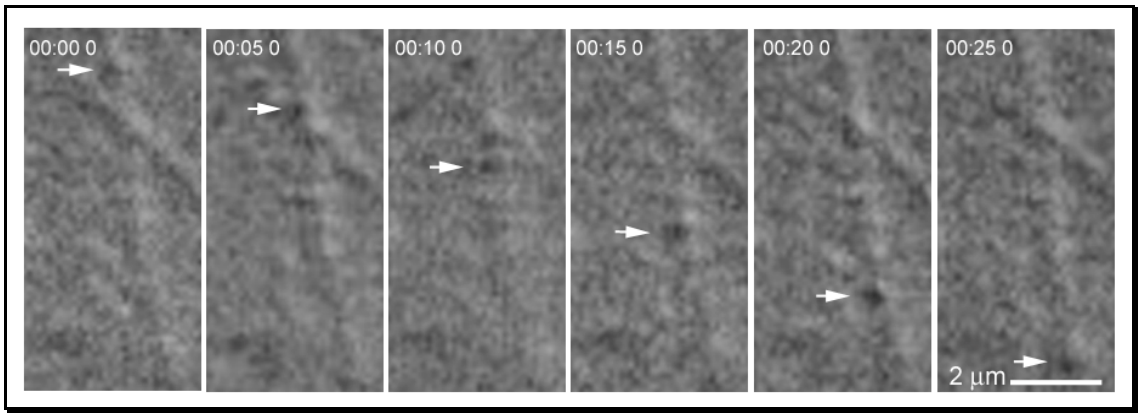

Figure 3.25 *Video sequence of bead transport by the K(5aa linker)-E(linker-neck) chimeric protein.*
The moving bead is indicated by an arrow; the time scale indicates minutes, seconds, and tenths of a second.

3.3.7 Summary of the results

Comparing the ATPase activities of the KIF5A and Eg5 constructs, it became evident that C-terminal shortening the KIF5A and Eg5 proteins increases the ATP hydrolysis rate (k_{cat}) (Figure 3.26 and Table 3.2). To achieve a maximal hydrolysis rate, KIF5A should include the catalytic core and at least the first half of the linker. These results indicate that KIF5A linker is an essential regulatory element of ATP hydrolysis. In the case of Eg5, the maximum ATP hydrolysis rate was observed for the $Eg5_{1-357}$ construct containing the Eg5 catalytic core, only. A further Eg5 construct containing the Eg5 core, neck linker and neck elements ($Eg5_{1-406}$) was found to have an ATP hydrolysis rate undistinguishable from that of the $Eg5_{1-357}$ (data not shown).

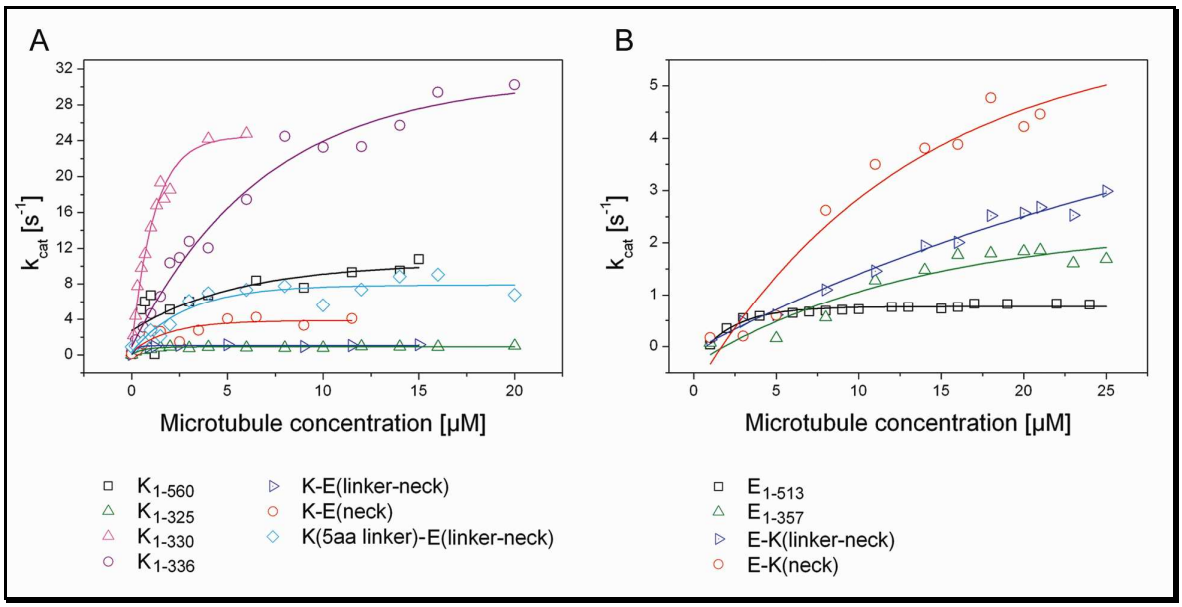

Figure 3.26 *Overview of the ATPase activities of truncated and chimeric kinesins.*
Constructs based on KIF5A (A) and Eg5 (B) catalytic cores, respectively. The k_{cat} values (see Table 3.2) are calculated on the basis of the steady state level of the exponential curves. Microtubule concentration is given as tubulin dimer concentration.

When the neck linker and/or neck of the fast-moving KIF5A were fused to the Eg5 core, the hydrolysis rates of the corresponding constructs increased in comparison to the control Eg5 protein. In contrast, fusing the neck linker and/or neck of the slow-moving Eg5 to the KIF5A core led to a decreased k_{cat} value compared to KIF5A control protein (Figure 3.26).

Protein	core elements		linker		neck		k_{cat} (s^{-1})		velocity (µm s^{-1})
	K	E	K	E	K	E	+ MT	- MT	
K_{1-560}	x		x		x		9.8 ± 0.47	0.10	1.08 ± 0.3
E_{1-513}		x		x		x	0.7 ± 0.01	0.04	0.04 ± 0.02
K_{1-325}	x						1.1 ± 0.05	0.03	NA
E_{1-357}		x					2.0 ± 0.08	0.07	NA
K_{1-330}	x		TIKNT				25 ± 0.8	0.20	NA
K_{1-336}	x		x				28 ± 1.4	0.40	NA
K_{1-304}	¥						0.02	0.02	NA
E_{1-341}		¥					0.02	0.01	NA
K_{1-295}	§						0.03	0.01	NA
E_{1-329}		§					0.05	0.02	NA
K-E(β8α6-linker-neck)	§	β8α6		x		x	0.01	0.01	NO
E-K(β8α6-linker-neck)	β8α6	§	x		x		0.01	0.02	NO
K-E(linker-neck)	x			x		x	0.5 ± 0.01	0.03	NO
K(5aa linker)-E(linker-neck)	x		TIKNT	x		x	7.7 ± 0.42	0.80	0.30 ± 0.09
E-K(linker-neck)		x	x		x		2.8 ± 0.19	0.10	0.12 ± 0.05
K-E(neck)	x					x	3.9 ± 0.22	0.10	0.54 ± 0.18
E-K(neck)		x		x	x		4.4 ± 0.23	0.20	0.07 ± 0.04

Table 3.2 *Summary of ATPase and motility activity of the kinesin constructs.*
K and E are used for KIF5A- and Eg5-derived structure elements. x depicts a complete structure - catalytic core, neck linker or neck elements. ¥ - core lacking α6; § - core lacking both β8 and α6; TIKNT - first five amino acids of the linker. In the case of the chimera K-E(β8α6-linker-neck) the β8 and α6 are taken from Eg5, and in the case of the chimera E-K(β8α6-linker-neck) from KIF5A, respectively. k_{cat} (s^{-1}) represents the maximal ATPase activity at saturating microtubule concentrations. NA: not applicable; NO: motility not observed.

The increase in the ATP hydrolysis rate was not found to correlate with the velocity of the corresponding protein. Though the k_{cat} value of the E-K(linker-neck) was lower than that of the E-K(neck) chimera, it moved significantly faster (Table 3.2, Figures 3.26 B and 3.27 B). These results indicate the essential role of the neck linker and neck elements in velocity regulation.

Fusing the KIF5A neck linker and neck to the Eg5 core, or the KIF5A neck to the Eg5 core and linker resulted in a velocity increase, compared to the control Eg5 (Figure 3.27 B). *Vice versa*, fusing the Eg5 neck to the KIF5A core and linker caused a decrease of the KIF5A velocity, while fusing both neck linker and neck of Eg5 to the KIF5A core even abolishes motility (Figure 3.27 A).

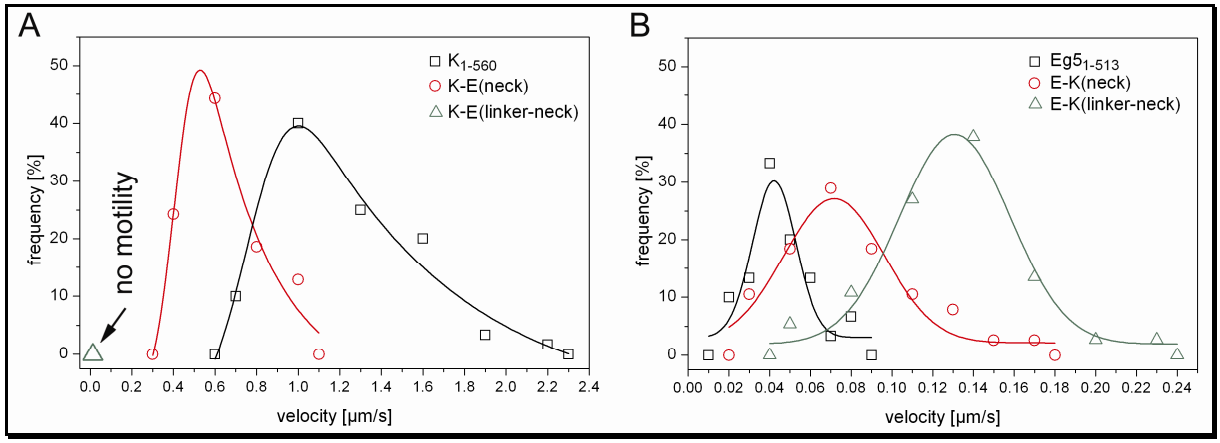

Figure 3.27 *Frequency diagram of velocity distributions of beads moved by:*
A) KIF5A control K_{1-560} and KIF5A-based chimeric proteins with interchanged neck linker and neck elements. Each single data point represents the percentage of beads moving at a velocity corresponding to the value indicated at the x-axis with: ± 0.1 µm s^{-1} for K-E(neck) (number of beads n=70) and ± 0.15 µm s^{-1} for K_{1-560} (n=60), respectively; B) Eg5 control E_{1-513} and Eg5-based chimeric proteins with interchanged neck linker and neck: ± 0.005 µm s^{-1} for E_{1-513} (n=30); ± 0.01 µm s^{-1} for E-K(neck) (n=38) and ± 0.015 µm s^{-1} for E-K(linker-neck) (n=37), respectively.

Introducing the first half of the KIF5A linker (representing strand β9) into the motility-inactive K-E(linker-neck) chimera resulted in a protein with restored motility (Figure 3.28). This result indicates the essential role of the KIF5A linker in motility generation.

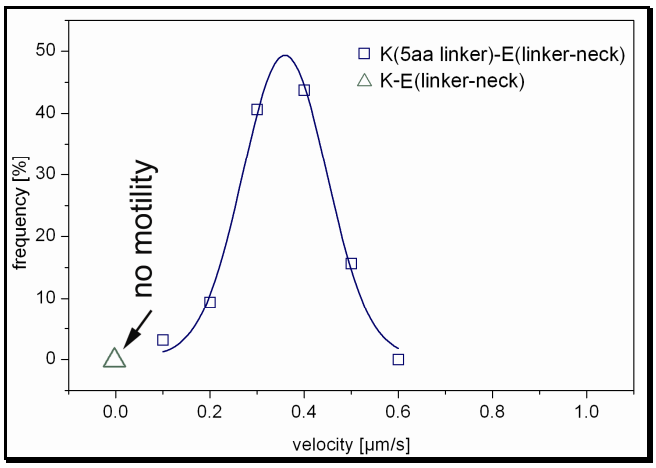

Figure 3.28 *Frequency diagram of velocity distributions of beads moved by K(5aa linker)-E(linker-neck) chimera.*
Each single data point represents the percentage of beads moving at a velocity corresponding to the value indicated at the x-axis with: ± 0.05 µm s^{-1} (number of beads n=36).

4. Discussion

The central goal was to gain insight into the mechanochemical mechanism of kinesin-mediated force generation, whereby this study is focused on the interaction between particular structural elements of the kinesin motor domain and on the effects this interaction exerts on motility generation in general and in velocity regulation. With this intention, C-terminally truncated KIF5A and Eg5 proteins were comparatively analyzed to define the structural organization of the catalytic core of both proteins required to represent activity. Based on these results, KIF5A and Eg5 chimeric proteins were constructed to investigate the elements involved in kinesin velocity regulation. Additionally, the functional role of the KIF5A neck linker region was studied by constructing and analyzing C-terminally truncated and chimeric proteins.

4.1 Control KIF5A and Eg5 constructs

The constructs used in this work as reference proteins differ from natural KIF5A and Eg5 as follows: They are C-terminally truncated at amino acid 560 for KIF5A, and 513 for Eg5, respectively, in order to increase their expression rates. Additionally, truncation prevents motor domain-to-tail interaction of KIF5A, leading to decreased ATPase activity (Verhey & Rapoport 2001; Cai *et al.* 2007). In the case of Eg5 tetramerization was disabled.

The velocity of ~1.0 µm s^{-1} measured for $KIF5A_{1-560}$ was comparable to that of the full-length KIF5A (Figure 3.15). Compared to the full-length KIF5A, the $KIF5A_{1-560}$ showed a five-fold increased hydrolysis rate. Nevertheless, this value is threefold lower than published for kinesin-1 proteins from *Drosophila*, rat and human, expressed in *E. coli* (k_{cat} ~20-30 s^{-1}) (Gilbert *et al.* 1998; Rice *et al.* 1999; Rosenfeld *et al.* 2002; Rosenfeld *et al.* 2003; Klumpp *et al.* 2003; Klumpp *et al.* 2004; Auerbach & Johnson 2005). Such high activities were obtained in this study for KIF5A only after further truncation. This might imply that in the case of the neuron-specific KIF5A not only the tail but additionally parts of the stalk are involved in self-inhibition of ATPase caused by motor domain-to-tail interaction (Coy *et al.* 1999; Verhey & Rapoport 2001; Cai *et al.* 2007) (see chapter 4.3)

The velocity of $Eg5_{1-513}$ (Figure 3.27 B) was ~0.04 µm s^{-1}, which is in agreement with values reported for various *Xenopus* full-length and truncated human Eg5 variants. Hydrolysis rates for Eg5 are available only for truncated constructs (Rosenfeld *et al.*

2005; Valentine *et al.* 2006; Krzysiak *et al.* 2006) and are comparable to those measured for $Eg5_{1-513}$ protein in this study (Figure 3.13 B).

4.2 KIF5A and Eg5 motor domains

4.2.1 The role of strand β8 and helix α6 in activity generation

Though Eg5 is known to share ~40% amino acid identity only, there is a high structural similarity to the motor domain of kinesin-1.

The catalytic core of kinesins is composed of eight β-strands surrounded by six α-helices (Figure 1.4). To answer the question of whether the motor domains of KIF5A and Eg5 require the same structural elements of their catalytic cores to generate activity (ATPase and microtubule-binding activity) $KIF5A_{1-325}$ and $Eg5_{1-357}$ motor domains were expressed. These constructs contain the complete catalytic core up to the end of helix α6, without the linker (Figure 3.1).

It is known that internal ATP-dependent shifts between helix α5 and its neighbouring loops are crucial for KIF5A and Eg5 activity (Turner *et al.* 2001). The functional role of the strand β8 and helix α6, which are parts of neither the microtubule- nor the ATP-binding site, is unclear. To elucidate if these core structures are essential for activity generation, or if they are only elements to maintain proper core conformation, truncated KIF5A and Eg5 motor domains lacking either α6 ($KIF5A_{1-304}$ and $Eg5_{1-341}$) or both β8 and α6 ($KIF5A_{1-295}$ and $Eg5_{1-329}$) were expressed.

The binding of kinesin motors to microtubules generally leads to increased ATPase activities. In contrast to $KIF5A_{1-325}$ and $Eg5_{1-357}$, the ATPase of the truncated proteins lacking α6 ($KIF5A_{1-304}$ and $Eg5_{1-341}$) or both α6 and β8 ($KIF5A_{1-295}$ and $Eg5_{1-329}$) was not stimulated by microtubules. In this context, the question arouse if these constructs were still able to bind to microtubules. To test if truncation of the KIF5A and Eg5 catalytic cores distorts microtubule binding, which in turn results in deficiency of ATPase activity, a microtubule-binding assay was performed at a kinesin-to-tubulin ratio of ~1.5:1. Parallel, the ATPase activities were determined for the corresponding constructs at the same ratio. In all cases, only the basal activity was measured. Noteworthy, the microtubule-binding assay demonstrated that the ATPase-inactive proteins had not lost their ability to interact with microtubules (Figure 3.17).

In the ATPase cycle of kinesins switch I and switch II elements play an important role as γ-phosphate sensors (Kull *et al.* 1996; Sack *et al.* 1997; Kikkawa *et al.* 2001).

Binding of ATP induces conformational changes and movements within the core which start in the switch I and II region and are transmitted and amplified to secondary movements, such as docking of the neck linker and increasing the microtubule-binding activity. Upon microtubule binding, switch I element has been shown to close the nucleotide pocket, thus priming the motor for hydrolysis, conformational changes in switch II, and consequently directed motion (Naber *et al.* 2003).

So far, there is a deficiency of information concerning kinesins with shortened catalytic cores. The results from the C-terminally truncated motor domain proteins in this study indicate an essential role of helix α6 and/or strand β8 in the conformational response of the core to nucleotide and microtubule binding. Helix α6 connects the flexible neck linker to the core. During the mechanochemical cycle of kinesin the neck linker zippers along a groove between helix α6 and loop 10 (the tip of the core) whereafter it becomes stabilized via hydrogen bond formation at this position.

The loss of ATPase activity upon binding to microtubules in the case of the truncated motor domains (lacking α6, or both α6 and β8) suggests that helix α6 might be involved in nucleotide-dependent movements, essential for hydrolysis. There is no evidence of a direct α6 movement within KIF5A and Eg5 core. But, this can be expected to some extent since the initial conformational change in switch I and II should induce other structures to be shifted to release the tension produced within the core upon ATP and microtubule binding. Moreover, in both KIF5A and Eg5 helix α6 is positioned very close to the highly flexible N-terminal elements of the core and to the ATP-binding loop (P-loop at the end of β3) (Figures 1.4 and 1.7).

The idea that helix α6 might make nucleotide-dependent movements is supported by some information taken from structural studies. Using cryo-electron microscopy a pathway for the mechanochemical cycle of the single-headed KIF1A kinesin has been proposed (Kikkawa & Hirokawa 2006). Like conventional kinesin, the KIF1A neck linker docks upon ATP binding to the catalytic core. The tension applied to the linker has been found to lead to core rotations which subsequently regulate the ATP cycle. In the KIF1A structure the nucleotide and the neck linker are proposed to be mechanically connected via the catalytic core. It has been shown that in the ADP state the core rotations lead to α6 movements, *i.e.*, α6 is shifted relative to switch II (helix 4) which occludes docking of the linker. In ATP state helix α6 moves again to allow the neck-linker docking.

Taken together, helix α6 might serve as a bridge that supports the binding and/or hydrolysis of ATP, and transmits the aroused movements into docking the neck linker.

For further characterization of the functional role of helix α6 and strand β8 the following two KIF5A- and Eg5-based chimeras were expressed: One contained the shortened Eg5 core without strand β8 and helix α6 fused to KIF5A starting at the strand β8 and helix α6 and followed by the KIF5A neck linker and neck. The second one comprises the KIF5A core, up to the end of α5 followed by the complementary elements of Eg5. For these chimeras homology modelling was performed on the basis of the crystal structures of kinesin-1 (PDB: 1BG2) (Kull *et al.* 1996) and Eg5 (PDB: 1II6) (Turner *et al.* 2001) using the interactive three-dimensional graphics program MAIN (Turk 1992). The result indicated that interchanging strand β8 and helix α6 should not disturb the proper conformation of the catalytic cores of the resulting proteins and thus should not alter their activity. However, these proteins were not able to stimulate ATP hydrolysis in the presence of microtubules though they had not lost their ability to bind to microtubules, indicated by ligand blotting (Figure 3.18). Corresponding to the failure of ATPase stimulation, the chimeric proteins were immotile.

These results strongly suggest that both KIF5A and Eg5 motor domains require the same minimal organization of the catalytic core, *i.e.*, to obtain ATPase activity the catalytic core up to helix α6 has to be preserved and must not be altered. Strand β8 and helix α6 do not only maintain proper core conformation. Helix α6 seems to be a functional structure involved in regulation of the ATP hydrolysis cycle and consequently motility generation of kinesins. Moreover, β8 and α6 of KIF5A and Eg5 are kinesin type-specific and cannot be replaced by each other.

4.2.2 The role of the half linker in KIF5A activity

Analysis of available kinesin crystal structures combined with molecular dynamics simulations have recently demonstrated that a nine amino acid long N-terminal region (strand β0), termed cover strand, is crucial for kinesin-1 force generation (Hwang *et al.* 2008). Upon ATP binding the cover strand forms a β-sheet with the first half (strand β9) of the linker and creates a cover-neck bundle. The cover-neck bundle is discussed to be a special conformation which forces the linker to dock to the core.

Thus, a new view on the kinesin mechanochemical cycle has been proposed, namely, the kinesin works by forming and breaking cover-neck bundles.

Helix α6 does also play an important role in power stroke generation. In nucleotide-free state with undocked linker, helix α6 reveals an unwind C-terminal portion which directly contacts the linker. This α6 conformation blocks the formation of the cover-neck bundle. Binding of ATP and retraction of switch II (helix α4) allow the formation of an extra helical turn of the α6 C-terminal portion (Hwang *et al.* 2008). Thus, the linker makes contact with the cover strand and the cover-neck bundle is formed, leading to the power stroke.

To approve experimentally this theoretical model of kinesin activity generation, KIF5A truncated constructs, including either the full linker ($KIF5A_{1-336}$) or the half linker only ($KIF5A_{1-330}$) (Figure 3.4), have been expressed and compared according their ATPase activity with the $KIF5A_{1-325}$ protein which lacks the linker.

Truncated KIF5A with the half linker ($KIF5A_{1-330}$) or with the full linker ($KIF5A_{1-336}$) showed hydrolysis rates of ~25-28 s^{-1}, which are in accordance to rates published for other kinesin-1 members (Gilbert *et al.* 1998; Rice *et al.* 1999; Rosenfeld *et al.* 2002; Rosenfeld *et al.* 2003; Klumpp *et al.* 2003; Klumpp *et al.* 2004; Auerbach & Johnson 2005). In contrast, the $KIF5A_{1-325}$ was found to have a significantly lower hydrolysis rate (~1.1 s^{-1}), indicating that the absence of linker sequences and consequently the inability to form a cover-neck bundle, affects the ATP hydrolysis. Therefore, the formation of the cover-neck bundle seems to be a crucial step in the mechanochemical cycle of KIF5A, which determines the rate of ATP hydrolysis.

4.3 The role of KIF5A and Eg5 C-terminal regions in the regulation of motor activity

In the present study the enzymatic characteristics of full-length KIF5A and Eg5, as well as, of KIF5A and Eg5 truncated proteins have been investigated. The results demonstrated that the microtubule-activated ATPase activity increases with shortening the sequence of the KIF5A and Eg5 constructs up to the motor domain (Figure 3.26 and Table 3.2). Such a correlation, reported for Eg5 (DeBonis *et al.* 2003) and *Drosophila* kinesin-1 (Jiang *et al.* 1997; Hackney & Stock 2000), has been explained by the so-called half-site reactivity model in which only one motor domain is being active at a time. Alternative explanations are based on the fact that longer constructs are more unstable and tend to aggregate.

However, the most probable explanation for the lower ATPase activities in the case of longer constructs might be the following. Within cells, the motor protein activity must be tightly regulated to prevent futile ATP hydrolysis. For kinesin-1 it has been shown that motor activity can be regulated by an autoinhibition mechanism based on the interaction of the N-terminal motor by C-terminal elements (Coy *et al.* 1999; Verhey & Rapoport 2001; Cai *et al.* 2007). Inactive kinesin-1 molecules have been found to be folded and autoinhibited in a fashion that the tails of the heavy chains block the initial interaction of the motor domain with the microtubule.

The results obtained in this study are in agreement with the model. The truncated $KIF5A_{1\text{-}560}$ and $Eg5_{1\text{-}513}$ lacking the tail and parts of the stalk regions possessed higher hydrolysis rates, compared to their full-length counterparts, but lower rates compared to the corresponding monomeric variants ($KIF5A_{1\text{-}336}$, $KIF5A_{1\text{-}330}$ and $Eg5_{1\text{-}357}$, respectively). This observation suggests that not only the tail regions, but also parts of the stalk regions of kinesin motors might be involved in the autoinhibitory regulation of motor activity.

4.4 The role of the neck linker and neck in KIF5A and Eg5 velocity regulation

To understand the complex mechanisms of kinesin-mediated motility and the role of the catalytic core and the neck linker and neck in this process, several studies have been performed, including the construction and expression of chimeric proteins consisting of parts of plus-end-directed and minus-end-directed kinesins (Henningsen & Schliwa 1997; Hirose *et al.* 2000), replacement of the kinesin linker with designed random coils (Case *et al.* 2000), and cross-linking studies to elucidate the effect of the neck linker on motor core kinetics (Hahlen *et al.* 2006).

Kinesin velocity can be regulated in cell-free environments by several factors, including the viscosity of the buffer solutions, the load implied, the temperature, ATP and Mg^{2+} concentration, or the number of kinesins involved in cargo transport (Hunt *et al.* 1994; Schnitzer *et al.* 2000; Böhm *et al.* 2000a; Böhm *et al.* 2000b). However, no information on velocity regulation by intrinsic kinesin properties has been available.

The question why kinesins with conserved catalytic cores and highly similar motor domain structures move at quite different velocities has been unsolved.

For both the truncated human $KIF5A_{1-560}$ and the human full-length KIF5A velocities of about 0.8-1.0 µm s^{-1} (Figure 3.15) were measured, which correspond well with the data published for other kinesin-1 members (see *e.g.*, Hancock & Howard 1998; Blasius *et al.* 2007).

The velocity of full-length tetrameric Eg5 has been measured so far only for the *Xenopus* Eg5 homologue (Kapitein *et al.* 2005). This tetrameric Eg5 moves at ~0.02 µm s^{-1} on each of both anti-parallel microtubules that are crosslinked by the same Eg5. Movement at such velocity results in relative sliding of both microtubules at ~0.04 µm s^{-1}.

The truncated human $Eg5_{1-513}$ expressed in this study moved at ~0.04 µm s^{-1}. Compared to KIF5A, it moves slower by a factor of about 25. The striking difference between the velocities of Eg5 and KIF5A provoked the question if structures outside the catalytic core might be involved in the velocity regulation.

The neck linker of kinesin motors is known to play an essential role in generation of motility. Depending on the nucleotide-bound state it switches between two conformational stages: The linker is docked to the catalytic core when ATP is bound, whereas in the ADP or nucleotide-free state it is flexible and undocked (Rice *et al.* 1999; Rice *et al.* 2003). Differing from that of kinesin-1, the neck linker of Eg5 was found in the ADP-bound state in a stable position, perpendicular to the core (Turner *et al.* 2001). On this basis, it can be hypothesized that the neck linker and/or its position in respect to the core might be involved in velocity regulation.

Case and co-workers (Case *et al.* 2000) showed that replacement of the native linker of human kinesin-1 with artificially designed random coils generated motors which were practically immotile (1.0-3.7 nm s^{-1} compared to 460 nm s^{-1} for the wild type construct). The effects of artificial coils on kinesin velocity may be completely different from those evoked by the replacement of the linker with natural, kinesin family-specific structures. Therefore, in this study, chimeric proteins were designed in which the native neck linker and neck elements of the fast-moving KIF5A and the slow-moving Eg5 were interchanged (Figure 3.3). This enables to check if it is possible not only to slow down a motor but also to speed up the slow Eg5 by substituting its native neck linker and neck by analogous structures taken from a fast-moving one.

4.4.1 The effect of the neck linker on KIF5A and Eg5 velocity

To study the effect of the linker on velocity the following chimeras were expressed: the K-E(linker-neck) construct containing the KIF5A catalytic core fused to the Eg5 neck linker, neck and part of the stalk, and the complementary E-K(linker-neck) construct, composed of the catalytic core of Eg5 fused to the KIF5A neck linker and neck and a part of the stalk. Both chimeras showed microtubule-stimulated ATPase activity. While the ATP turnover rate of E-K(linker-neck) was about fourfold higher than that of $Eg5_{1\text{-}513}$, the rate of the K-E(linker-neck) was about 20-fold lower in comparison to the $KIF5A_{1\text{-}560}$ control protein.

Though it had a microtubule-stimulated ATPase, the K-E(linker-neck) construct was immotile. Under the same conditions, the complementary chimera containing the Eg5 catalytic core fused to the KIF5A neck linker and neck moved significantly faster (threefold) than the $Eg5_{1\text{-}513}$ control protein (Figure 3.27 B). This is the first evidence for speeding up the slow Eg5 motor by exchanging its mechanical element (neck linker and neck) by complementary one, taken from a fast motor.

The mechanochemical cycle of dimeric Eg5 differs to some extent from that of kinesin-1 (Krzysiak *et al.* 2008). Upon microtubule binding, the one motor domain of Eg5 releases ADP rapidly, while the second one does it after a conformational change, only. This change proceeds slowly, probably reflecting the reorientation of the neck linker from its relatively stable perpendicular orientation to the core into a docked position (Krzysiak *et al.* 2008).

The perpendicular position of Eg5 linker is stabilized by hydrogen bonds within the linker and by structures of the gap between helix α6 and loop 10, which the linker docks with. This neck-linker stabilization is ascribed to several Eg5 family-specific residues. Turner *et al.* (2001) discussed that the Lys-364 and Pro-365 interact with the family-conserved Glu-49 and Thr-67 (Figure 4.1). Additionally, residues that might be involved in neck-linker docking during ATP hydrolysis include Val-303, Arg-327, Thr-328, Gly-252, Glu-253 and Glu-254.

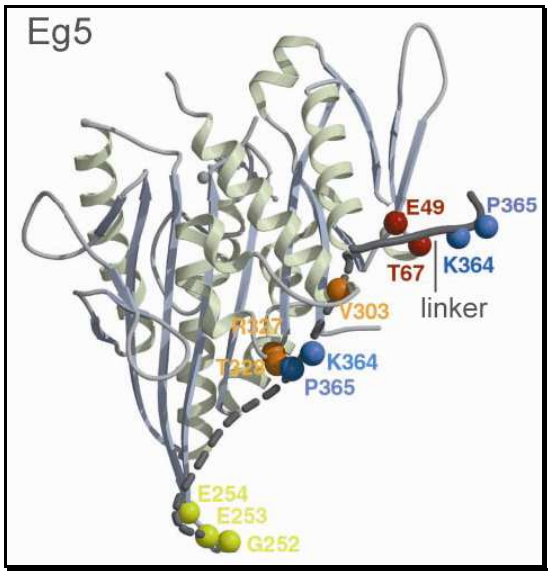

Figure 4.1 *Localization of the conserved Eg5 residues involved in stabilization of the neck-linker position.*
Lys-364 and Pro-365 (blue) in the neck linker interact with Glu-49 and Thr-67 (red) from the catalytic core to ensure the well ordered, perpendicular to the core, position of the linker in undocked state. Val-303, Arg-327, and Thr-328 (in orange) and Gly-252, Glu-253, and Glu-254 (in yellow) are suggested to be additionally involved in neck-linker docking. The Figure is taken from Turner *et al.* 2001.

The faster movement of the E-K(linker-neck) chimera suggests that fusing the KIF5A linker and neck to the Eg5 catalytic core might lead to alterations of the specific linker-core interactions during docking and undocking cycle. One can speculate that the stabilized linker position in the ADP state (specific for Eg5 only) is eliminated (see a hypothetical model in Figure 4.2 A), the switch between docked and undocked state might became faster which in turn might result in faster movement compared to the wild type Eg5.

There was no motility in the case of the K-E(linker-neck) chimera, where the Eg5 linker and neck were fused to KIF5A catalytic core. Within this protein, the meshwork of hydrogen bonds holding the linker in undocked/docked state might be changed in a fashion preventing motility generation. Alternatively, the absence of motility even in the case of ATPase activity might be explained assuming that docking and undocking of the neck linker depends on its relative position to helix α6 which connects it to the core. Another point is that the KIF5A-specific strand β9, which is not included in the K-E(linker-neck) chimera, might play a crucial role in the initiation of linker docking (see a hypothetical model in Figure 4.2 B).

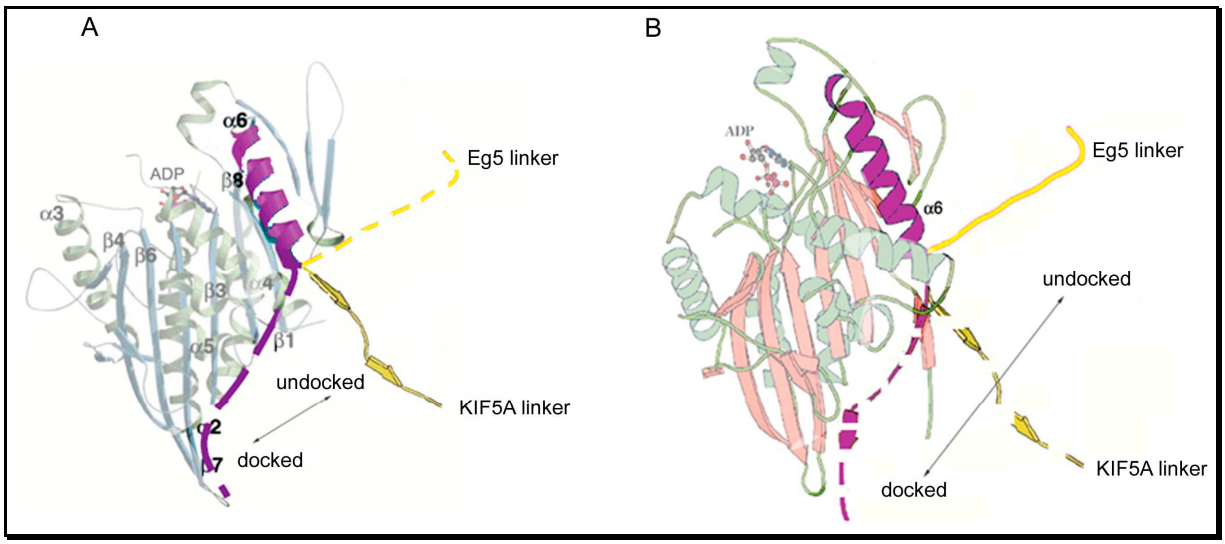

Figure 4.2 *Hypothetical model of neck-linker position in the chimeras with neck-linker and neck regions interchanged.*
A) core of Eg5. Yellow dashed line - the natural Eg5 linker in undocked state, purple dashed line - linker in docked state, respectively. In the E-K(linker-neck) chimera the KIF5A linker (added as yellow structure) might take a new position in undocked state, different from that of the natural Eg5 linker. The crystal structure is adapted from Turner *et al.* 2001 (PDB accession number: 1II6).
B) core of kinesin-1 (PDB number: 2KIN). Yellow dashed line: natural KIF5A linker in undocked state, purple dashed line - linker in docked state, respectively. In the immotile K-E(linker-neck) chimera the Eg5 linker (added as yellow line) or its position might reflect an disturbed docking/undocking mechanism. The structure is adapted from Mogilner *et al.* 2001.

The cover strand region (β0) of kinesins, studied by molecular dynamic simulations (Hwang *et al.* 2008), has been found to vary in length and sequence, whereby it is suggested to be sequence-conserved preferentially among the kinesin-1 family members. The experimental data presented in this study suggest that fusing the Eg5 linker to KIF5A core might lead to altered cover-neck bundle formation. In this case, the lack of motility even in the presence of microtubule-stimulated ATPase activity indicates the specificity of interaction between the N-terminal KIF5A part (strand β0) and the strand β9 of the linker. This result supports the hypothesis that kinesin moves by forming and breaking cover-neck bundles during its mechanochemical cycle. This hypothesis was further strengthened in this work by the expression of a chimeric protein composed of KIF5A core, including the first five amino acids of its native linker (representing strand β9), fused to Eg5 linker and neck (discussed in 4.4.3).

4.4.2 The effect of the neck on KIF5A and Eg5 velocity

It is commonly accepted that the kinesin neck coiled-coil region ensures kinesin dimerization (Jiang *et al.* 1997). As a part of the mechanical element it is essential for motility generation. To test if the observed effects on velocity are exclusively due to the linker or if the neck is also involved in kinesin velocity regulation, chimeras with the neck regions interchanged were expressed (Figure 3.3). While the K-E(neck) chimera moved at lower velocity than the control $KIF5A_{1\text{-}560}$ (Figure 3.27 A and Table 3.2), the E-K(neck) chimera was found to move at almost twofold increased velocity, compared to the control $Eg5_{1\text{-}513}$ (Figure 3.27 B and Table 3.2).

Recently, a mutation in the KIF5A gene has been identified as molecular cause of hereditary spastic paraplegia (Lo Giudice *et al.* 2006), which is a neurodegenerative disease caused by motor-neuron degeneration. This mutation is localized in the neck coiled-coil of KIF5A as an alanine-to-valine substitution (A361V). The alanine at position 361 is conserved in KIF5A of several vertebrate species (Lo Giudice *et al.* 2006). However, functional studies on recombinant mutant KIF5A proteins with A361V substitution have shown that this point mutation has no effect on the motility (Ebbing *et al.* 2008). In the study presented here, it is clearly shown that changes in the amino acid sequence of the neck can result in changed activity. The chimera composed of the KIF5A core and linker fused to the Eg5 neck moved with decreased velocity. The results indicate that the neck is also involved in velocity regulation. Moreover, the KIF5A neck seems to have a positive feedback on the velocity since the E-K(neck) chimera with KIF5A neck coiled-coil fused to the Eg5 core and linker was found to move faster than the control $Eg5_{1\text{-}513}$.

4.4.3 The effect of the first half of KIF5A linker on velocity

When the activities of the C-terminally truncated KIF5A proteins containing either the full linker ($KIF5A_{1\text{-}336}$) or the first half of the linker only ($KIF5A_{1\text{-}330}$) were compared with that of the KIF5A construct lacking linker sequences ($KIF5A_{1\text{-}325}$) it became evident that the N-terminal half of the linker (representing strand β9) is essentially involved in the process of ATP hydrolysis. The chimera in which the KIF5A core without its native linker was fused to Eg5-specific linker and neck sequences was immotile, despite the microtubule-stimulated ATPase activity. Taken together, these results suggest a crucial role of the first half (strand β9) of the KIF5A linker in motility generation, as predicted by the computer simulations (Hwang *et al.* 2008).

To gain insight into KIF5A motility generation the chimera K(5aa linker)-E(linker-neck) was expressed (Figure 3.5), which was structurally very similar to the motility-inactive K-E(linker-neck) construct, but additionally contained the first five amino acids (representing strand β9) of the native KIF5A linker. The insertion of the first half of the KIF5A linker was found to result in restored motility (Figure 3.28).

In Eg5, the cover strand (β0) is four amino acids longer than in kinesin-1 family members and differs in its sequence (Hwang *et al.* 2008). In the immotile chimera, in which the Eg5 linker has been fused to KIF5A catalytic core, the cover-neck bundle between the Eg5 half linker (strand β9) and the KIF5A cover strand might not form due to different length and the differences in the sequence of the cover strand. Inserting the half KIF5A linker seems to be sufficient to form the cover-neck bundle which in turn generates the force for motility (see hypothetical model in Figure 4.3).

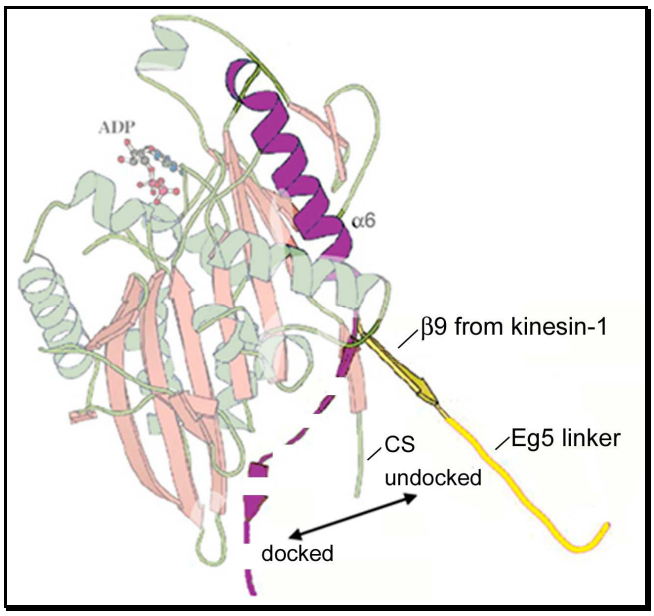

Figure 4.3 *Hypothetical model of the neck-linker structure in the K(5aa linker)-E(linker-neck) chimera.*
The core structure is that of kinesin-1 (PDB accession number: 2KIN). The helix α6 and the docked natural linker (dashed line) are depicted in purple. The modified linker composed of KIF5A strand β9 and the full Eg5 linker is depicted in yellow. The N-terminal cover strand (CS) and strand β9 from KIF5A linker might interact to form the cover-neck bundle. The Figure is adapted from Mogilner *et al.* 2001.

Up-to-date, no experimental data have been available on recombinant kinesin family members with altered β9 strands to support the “cover-neck bundling” model of kinesin force generation worked out by Hwang *et al.* (2008). The results obtained in

this study for the K(5aa linker)-E(linker-neck) chimera and for the KIF5A constructs with or without the half linker strongly support the theoretical model on kinesin motility generation by forming and breaking cover-neck bundles.

4.5 Conclusions

Although both kinesin-1 and Eg5 bear a conserved catalytic core and have a very similar motor domain organization, they have evolved quite different biological functions. Kinesin-1, including the neuron-specific KIF5A as axonal transporter protein, is required to deliver different intracellular cargoes over long distances to specialized cellular locations. The velocity of kinesin-1 must be high enough to ensure fast intracellular transport functions, *e.g*., the fast neuronal transport. Eg5 participates in the formation of the bipolar mitotic spindle by sliding the anti-parallel microtubules apart. Its velocity, which is comparable to the spindle pole separation rates *in vivo* (Brust-Mascher & Scholey 2002), has to be kept on a low level to ensure proper spindle organization and consequently correct chromosome alignment and segregation. The neck linker and neck of KIF5A and Eg5 are crucial not only for motility generation in general. The present study provides first evidence that the neck linker and neck elements are also involved in determination and regulation of the velocity at which kinesin motors move. Thus, evolutionary the neck linker and neck might have evolved to adapt the variety of cellular motors to their different biological functions.

5. References

Aizawa H, Sekine Y, Takemura R, Zhang Z, Nangaku M, Hirokawa N (1992) Kinesin family in murine central nervous system. J Cell Biol 119:1287-1296

Alberts B, Bray D, Lewis J, Raff M, Roberts K, Watson JD Molecular biology of the cell. Garland Publishing, Inc., New York, 2002 (4th ed.)

Asbury CL, Fehr AN, Block SM (2003) Kinesin moves by an asymmetric hand-over-hand mechanism. Science 302: 2130-2134

Auerbach SD & Johnson KA (2005) Alternating site ATPase pathway of rat conventional kinesin. J Biol Chem 280: 37048-37060

Blair MA, Ma S, Hedera P (2006) Mutation in KIF5A can also cause adult-onset hereditary spastic paraplegia. Neurogenetics 7: 47-50

Blangy A, Lane HA, d'Herin P, Harper M, Kress M, Nigg EA (1995) Phosphorylation by p34cdc2 regulates spindle association of human Eg5, a kinesin-related motor essential for bipolar spindle formation in vivo. Cell 83: 1159-1169

Blasius TL, Cai D, Jih GT, Toret CP, Verhey KJ (2007) Two binding partners cooperate to activate the molecular motor Kinesin-1. J Cell Biol 176: 11-17

Bloom GS, Wagner MC, Pfister KK, Brady ST (1988) Native structure and physical properties of bovine brain kinesin and identification of the ATP-binding subunit polypeptide. Biochemistry 27: 3409-3416

Böhm KJ, Stracke R, Baum M, Zieren M, Unger E (2000)a Effect of temperature on kinesin-driven microtubule gliding and kinesin ATPase activity. FEBS Lett 466: 59-62

Böhm KJ, Stracke R, Unger E (2000)b Speeding up kinesin-driven microtubule gliding in vitro by variation of cofactor composition and physicochemical parameters. Cell Biol Int 24: 335-341

Brady ST (1985) A novel brain ATPase with properties expected for the fast axonal transport motor. Nature 317: 73-75

Brust-Mascher I & Scholey JM (2002) Microtubule flux and sliding in mitotic spindles of Drosophila embryos. Mol Biol Cell 13: 3967-3975

Cai D, Hoppe AD, Swanson JA, Verhey KJ (2007) Kinesin-1 structural organization and conformational changes revealed by FRET stoichiometry in live cells. J Cell Biol 1: 51-63

Case RB, Pierce DW, Hom-Booher N, Hart CL, Vale RD (1997) The directional preference of kinesin motors is specified by an element outside of the motor catalytic domain. Cell 90: 959-966

Case RB, Rice S, Hart CL, Ly B, Vale RD (2000) Role of the kinesin neck linker and catalytic core in microtubule-based motility. Curr Biol 10: 157-160

Cochran JC, Sontag CA, Maliga Z, Kapoor TM, Correia JJ, Gilbert SP (2004) Mechanistic analysis of the mitotic kinesin Eg5. J Biol Chem 279: 38861-38870

Cochran JC, Krzysiak TC, Gilbert SP (2006) Pathway of ATP hydrolysis by monomeric kinesin Eg5. Biochemistry 45: 12334-12344

Cole DG, Cande WZ, Baskin RJ, Skoufias DA, Hogan CJ, Scholey JM (1992) Isolation of a sea urchin egg kinesin-related protein using peptide antibodies. J Cell Sci 101: 291-301

Coy DL, Hancock WO, Wagenbach M, Howard J (1999) Kinesin's tail domain is an inhibitory regulator of the motor domain. Nat Cell Biol 5: 288-292

Crevel IM, Lockhart A, Cross RA (1997) Kinetic evidence for low chemical processivity in ncd and Eg5. J Mol Biol 273: 160-170

Cross RA (2004) The kinetic mechanism of kinesin. Trends Biochem Sci 29: 301-309

DeBonis S, Simorre JP, Crevel I, Lebeau L, Skoufias DA, Blangy A, Ebel C, Gans P, Cross R, Hackney DD, Wade RH, Kozielski F (2003) Interaction of the mitotic inhibitor monastrol with human kinesin Eg5. Biochemistry 42: 338-349

De La Cruz EM, Ostap EM, Sweeney HL (2001) Kinetic mechanism and regulation of myosin VI. J Biol Chem 276: 32373-32381

Diefenbach RJ, Mackay JP, Armati PJ & Cunningham AL (1998) The C-terminal region of the stalk domain of ubiquitous human kinesin heavy chain contains the binding site for kinesin light chain. Biochemistry 37: 16663-16670

Duhl DM & Renhowe PA (2005) Inhibitors of kinesin motor proteins - research and clinical progress. Curr Opin Drug Discov Devel 8: 431-436

Ebbing B, Mann K, Starosta A, Jaud J, Schöls L, Schüle R, Woehlke G (2008) Effect of spastic paraplegia mutations in KIF5A kinesin on transport activity. Hum Mol Genet 17: 1245-1252

Endow SA (1999) Determinants of molecular motor directionality. Nat Cell Biol 1: 163-167

Endow SA & Barker DS (2003) Processive and nonprocessive models of kinesin movement. Annu Rev Physiol 65: 161-175

Enos AP & Morris NR (1990) Mutation of a gene that encodes a kinesin-like protein blocks nuclear division in A. nidulans. Cell 60: 1019-1027

Fichera M, Lo Giudice M, Falco M, Sturnio M, Amata S, Calabrese O, Bigoni S, Calzolari E, Neri M (2004) Evidence of kinesin heavy chain (KIF5A) involvement in pure hereditary spastic paraplegia. Neurology 63: 1108-1110

Goldstein LSB (2001) Molecular motors: from one motor many tails to one motor many tales. Trends Cell Biol 11: 477-482

Gilbert SP, Moyer ML, Johnson KA (1998) Alternating site mechanism of the kinesin ATPase. Biochemistry 37: 792-799

Gindhart JG Jr, Desai CJ, Beushausen S, Zinn K, Goldstein LS (1998) Kinesin light chains are essential for axonal transport in Drosophila. J Cell Biol 141: 443-454

Grant BJ, McCammon JA, Caves LS, Cross RA (2007) Multivariate analysis of conserved sequence-structure relationships in kinesins: coupling of the active site and a tubulin-binding sub-domain. J Mol Biol 368: 1231-1248

Hackney DD (1994) Evidence for alternating head catalysis by kinesin during microtubule-stimulated ATP hydrolysis. Proc Natl Acad Sci U S A 91: 6865-6869

Hackney DD (1995) Highly processive microtubule-stimulated ATP hydrolysis by dimeric kinesin head domains. Nature 377: 448-450

Hackney DD & Stock MF (2000) Kinesin's IAK tail domain inhibits initial microtubule-stimulated ADP release. Nat Cell Biol 5: 257-260

Hagan I &Yanagida M (1990) Novel potential mitotic motor protein encoded by the fission yeast cut7+ gene. Nature 347: 563-566

Hahlen K, Ebbing B, Reinders J, Mergler J, Sickmann A, Woehlke G (2006) Feedback of the kinesin-1 neck-linker position on the catalytic site. J Biol Chem 281: 18868-18877

Hancock WO & Howard J (1998) Processivity of the motor protein kinesin requires two heads. J Cell Biol 140: 1395-13405

Hancock WO & Howard J (1999) Kinesin's processivity results from mechanical and chemical coordination between the ATP hydrolysis cycles of the two motor domains. Proc Natl Acad Sci U S A 96: 13147-13152

Heck MM, Peereira A, Pesavento P, Yannoni Y, Spradling AC, Goldstein LS (1993) The kinesin-like protein KLP61F is essential for mitosis in Drosophila. J Cell Biol 123: 655-679

Henningsen U & Schliwa M (1997) Reversal in the direction of movement of a molecular motor. Nature 389: 93-96

Hirokawa N (1993) Mechanism of axonal transport. Identification of new molecular motors and regulations of transports. Neurosci Res 18: 1-9

Hirokawa N (1998) Kinesin and dynein superfamily proteins and the mechanism of organelle transport. Science 279: 519-526

Hirokawa N & Takemura R in Molecular Motors (ed. Schliwa, M.) 79-109 (Wiley-VCH, Weinheim, 2003)

Hirokawa N & Takemura R (2004) Kinesin superfamily proteins and their various functions and dynamics. Exp Cell Res 301: 50-59

Hirokawa N & Takemura R (2005) Molecular motors and mechanisms of directional transport in neurons. Nat Rev Neurosci 6: 201-214

Hirokawa N & Noda Y (2008) Intracellular transport and kinesin superfamily proteins, KIFs: Structure, Function, and Dynamics. Physiol Rev 88: 1089-1118

Hirose K, Henningsen U, Schliwa M, Toyoshima C, Shimizu T, Alonso M, Cross RA, Amos LA (2000) Structural comparison of dimeric Eg5, Neurospora kinesin (Nkin) and Ncd head-Nkin neck chimera with conventional kinesin. EMBO J 19: 5308-5314

Ho SN, Hunt HD, Horton RM, Pullen JK, Pease LR (1989) Site-directed mutagenesis by overlap extension using the polymerase chain reaction. Gene 77: 51-59

Hoenger A, Sack S, Thormählen M, Marx A, Müller J, Gross H, Mandelkow E (1998) Image reconstructions of microtubules decorated with monomeric and dimeric kinesins: comparison with x-ray structure and implications for motility. J Cell Biol 141: 419-430

Hoenger A, Thormählen M, Diaz-Avalos R, Doerhoefer M, Goldie KN, Müller J, Mandelkow E (2000) A new look at the microtubule binding patterns of dimeric kinesins. J Mol Biol 297: 1087-1103

Hoyt MA, He L, Loo KK, Saunders WS (1992) Two Saccharomyces cerevisiae kinesin-related gene products required for mitotic spindle assembly. J Cell Biol 118: 109-120

Hua W, Young EC, Fleming ML, Gelles J (1997) Coupling of kinesin steps to ATP hydrolysis. Nature 388: 390-393

Hua W, Chung J, Gelles J (2002) Distinguishing inchworm and hand-over-hand processive kinesin movement by neck rotation measurements. Science 295: 844-848

Hunt AJ, Gittes F, Howard J (1994) The force exerted by a single kinesin molecule against a viscous load. Biophys J 2: 766-781

Hwang W, Lang MJ, Karplus M (2008) Force generation in kinesin hinges on cover-neck bundle formation. Structure 16: 62-71

Jiang W, Stock MF, Li X, Hackney DD (1997) Influence of the kinesin neck domain on dimerization and ATPase kinetics. J Biol Chem 272: 7626-7632

Kanai Y, Okada Y, Tanaka Y, Harada A, Terada S, Hirokawa N (2000) KIF5C, a novel neuronal kinesin enriched in motor neurons. J Neurosci 20: 6374-6384

Kapitein LC, Peterman EJ, Kwok BH, Kim JH, Kapoor TM, Schmidt CF (2005) The bipolar mitotic kinesin Eg5 moves on both microtubules that it crosslinks. Nature 435: 114-118

Kaseda K, Higuchi H, Hirose K (2003) Alternate fast and slow stepping of a heterodimeric kinesin molecule. Nat Cell Biol 5: 1079-1082

Kashina AS, Baskin RJ, Cole DG, Wedman KP, Saxton WM, Scholey JM (1996) A bipolar kinesin. Nature 379: 270-272

Kikkawa M, Sablin EP, Okada Y, Yajima H, Fletterick RJ, Hirokawa N (2001) Switch-based mechanism of kinesin motors. Nature 411: 439-445

Kikkawa M & Hirokawa N (2006) High-resolution cryo-EM maps show the nucleotide binding pocket of KIF1A in open and closed conformations. EMBO J 25: 4187-94

Klumpp LM, Mackey AT, Farrell CM, Rosenberg JM, Gilbert SP (2003) A kinesin switch I arginine to lysine mutation rescues microtubule function. J Biol Chem 278: 39059-39067

Klumpp LM, Hoenger A, Gilbert SP (2004) Kinesin's second step. Proc Natl Acad Sci U S A 101: 3444-3449

Korneev MJ, Lakämper S, Schmidt CF (2007) Load-dependent release limits the processive stepping of the tetrameric Eg5 motor. Eur Biophys J 36: 675-681

Kozielski F, DeBonis S, Skoufias DA (2007) Screening for inhibitors of microtubule-associated motor proteins. Methods Mol Med 137: 189-207

Krzysiak TC & Gilbert SP (2006) Dimeric Eg5 maintains processivity through alternating-site catalysis with rate-limiting ATP hydrolysis. J Biol Chem 281: 39444-39454

Krzysiak TC, Wendt T, Sproul LR, Tittmann P, Gross H, Gilbert SP, Hoenger A (2006) A structural model for monastrol inhibition of dimeric kinesin Eg5. EMBO J 25: 2263-22673

Krzysiak TC, Grabe M, Gilbert SP (2008) Getting in Sync with Dimeric Eg5: Initiation and regulation of the processive run. J Biol Chem 283: 2078-2087

Kull FJ, Sablin EP, Lau R, Fletterick RJ, Vale RD (1996) Crystal structure of the kinesin motor domain reveals a structural similarity to myosin. Nature 380: 550-555

Kwok BH, Kapitein LC, Kim JH, Peterman EJ, Schmidt CF, Kapoor TM (2006) Allosteric inhibition of kinesin-5 modulates its processive directional motility. Nat Chem Biol 2: 480-485

Laemmli UK (1970) Cleavage of structural proteins during the assembly of the head of bacteriophage T4. Nature 356: 722-725

LeGuellec R, Paric J, Couturier A, Roghi C, Philippe M (1991) Cloning by differential screening of a Xenopus cDNA that encodes a kinesin-related protein. Mol Cell Biol 11: 3395-3398

Lockhart A, & Cross RA (1996) Kinetics and motility of the Eg5 microtubule motor. Biochemistry 35: 2365-2373

Lowry OH, Rosebrough NJ, Farr AL, Randall RJ (1951) Protein measurement with the Folin-Phenol reagents. J Biol Chem 193: 265-275

Lo Giudice M, Neri M, Falco M, Sturnio M, Calzolari E, Di Benedetto D, Fichera M (2006) A missense mutation in the coiled-coil domain of the KIF5A gene and late-onset hereditary spastic paraplegia. Arch Neurol 63: 284-287

Ma YZ & Taylor EW (1997) Interacting head mechanism of microtubule-kinesin ATPase. J Biol Chem 272: 724-730

Mandelkow E & Johnson KA (1998) The structural and mechanochemical cycle of kinesin. Trends Biochem Sci 23: 429-433

Marston FA (1986) The purification of eukaryotic polypeptides synthesized in *Escherichia coli*. J Biochem 240: 1-12

Martin B, Pallen CJ, Wang JH, Graves DJ (1985) Use of fluorinated tyrosine phosphates to probe the substrate specificity of the low molecular weight phosphatase activity of calcineurin. J Biol Chem 260: 14932-14937

Mayer TU, Kapoor TM, Haggarty SJ, King RW, Schreiber SL, Mitchison TJ (1999) Small molecule inhibitor of mitotic spindle bipolarity identified in a phenotype-based screen. Science 286: 971-974

Miki H, Setou M, Kaneshiro K, Hirokawa N (2001) All kinesin superfamily protein, KIF, genes in mouse and human. Proc. Natl Acad Sci U S A 98: 7004-7011

Miki H, Okada Y, Hirokawa N (2005) Analysis of the kinesin superfamily: insights into structure and function. Trends Cell Biol 15: 467-476

Mogilner A, Fisher AJ, Baskin RJ (2001) Structural changes in the neck linker of kinesin explain the load dependence of the motor's mechanical cycle. J Theor Biol 2: 143-157

Mori T, Vale RD, Tomishige M (2007) How kinesin waits between steps. Nature 450: 750-754

Moyer ML, Gilbert SP, Johnson KA (1996) Purification and characterization of two monomeric kinesin constructs. Biochemistry 35: 6321-6329

Moyer ML, Gilbert SP, Johnson KA (1998) Pathway of ATP hydrolysis by monomeric and dimeric kinesin. Biochemistry 37: 800-813

Naber N, Minehardt TJ, Rice S, Chen X, Grammer J, Matuska M, Vale RD, Kollman PA, Car R, Yount RG, Cooke R, Pate E (2003) Closing of the nucleotide pocket of kinesin-family motors upon binding to microtubules. Science 300: 798-801

Nakagawa T, Tanaka Y, Matsuoka E, Kondo S, Okada Y, Noda Y, Kanai Y, Hirokawa N (1997) Identification and classification of 16 new kinesin superfamily (KIF) proteins in mouse genome. Proc Natl Acad Sci U S A 94: 9654-9659

Navone F, Niclas J, Hom-Booher N, Sparks L, Bernstein HD, McCaffrey G, Vale RD (1992) Cloning and expression of a human kinesin heavy chain gene: interaction of the COOH-terminal domain with cytoplasmic microtubules in transfected CV-1 cells. J Cell Biol 117: 1263-1275

Niclas J, Navone F, Hom-Booher N, Vale RD (1994) Cloning and localization of a conventional kinesin motor expressed exclusively in neurons. Neuron 12: 1059-1072

Ray S, Meyhöfer E, Milligan RA, Howard J (1993) Kinesin follows the microtubule's protofilament axis. J Cell Biol 121: 1083-1093

Reid E, Kloos M, Ashley-Koch A, Hughes L, Bevan S, Svenson IK, Graham FL, Gaskell PC, Dearlove A, Pericak-Vance MA, Rubinsztein DC, Marchuk DA (2002) A kinesin heavy chain (KIF5A) mutation in hereditary spastic paraplegia (SPG10). Am J Hum Genet 71: 1189-1194

Rice S, Lin AW, Safer D, Hart CL, Naber N, Carragher BO, Cain SM, Pechatnikova E, Wilson-Kubalek EM, Whittaker M, Pate E, Cooke R, Taylor EW, Milligan RA, Vale RD (1999) A structural change in the kinesin motor protein that drives motility. Nature 402: 778-784

Rice S, Cui Y, Sindelar C, Naber N, Matuska M, Vale R, Cooke R (2003) Thermodynamic properties of the kinesin neck-region docking to the catalytic core. Biophys J 84: 1844-1854

Rosenfeld SS, Rener B, Correia JJ, Mayo MS, Cheung HC (1996) Equilibrium studies of kinesin-nucleotide intermediates. J Biol Chem 271: 9473-9482

Rosenfeld SS, Xing J, Jefferson GM, Cheung HC, King PH (2002) Measuring kinesin's first step. J Biol Chem 277: 36731-36739

Rosenfeld SS, Fordyce PM, Jeffereson GM, King PH, Block SM (2003) Stepping and stretching: how kinesin uses internal strain to walk processively. J Biol Chem 278: 18550-18556

Rosenfeld SS, Xing J, Jefferson GM, King PH (2005) Docking and rolling, a model of how the mitotic motor Eg5 works. J Biol Chem 280: 35684-35695

Sablin EP, Kull FJ, Cooke R, Vale RD, Fletterick RJ (1996) Crystal structure of the motor domain of the kinesin-related motor ncd. Nature 380: 555-559

Sack S, Müller J, Marx A, Thormählen M, Mandelkow EM, Brady ST, Mandelkow E (1997) X-ray structure of motor and neck domains from rat brain kinesin. Biochemistry 36: 16155-16165

Sack S, Kull FJ, Mandelkow E (1999) Motor proteins of the kinesin family. Structures, variations, and nucleotide binding sites. Eur J Biochem 262: 1-11

Sakamoto T, Wang F, Schmitz S, Xu Y, Xu Q, Molloy JE, Veigel C, Sellers JR (2003) Neck length and processivity of myosin V. J Biol Chem 278: 29201-29207

Sambrook J, Fritsch EF, Maniatis T (1989) Molecular cloning: a laboratory manual. Cold Spring Habor Laboratory Press

Schief WR & Howard J (2001) Conformational changes during kinesin motility. Curr Opin Cell Biol 13: 19-28

Schief WR, Clark RH, Crevenna AH, Howard J (2004) Inhibition of kinesin motility by ADP and phosphate supports a hand-over-hand mechanism. Proc Natl Acad Sci U S A 101: 1183-1188

Schliwa M & Woehlke G (2003) Molecular motors. Nature 422: 759-765

Schnitzer MJ & Block SM (1997) Kinesin hydrolyses one ATP per 8-nm step. Nature 388: 386-390

Schnitzer MJ, Visscher K, Block SM (2000) Force production by single kinesin motors. Nat Cell Biol 2: 718-723

Shao Q & Gao YQ (2006) On the hand-over-hand mechanism of kinesin. Proc Natl Acad Sci U S A 103: 8072-8077

Sharp DJ, McDonald KL, Brown HM, Matthies HJ, Walczak C, Vale RD, Mitchison TJ, Scholey JM (1999) The bipolar kinesin, KLP61F, cross-links microtubules within interpolar microtubule bundles of Drosophila embryonic mitotic spindles. J Cell Biol 144: 125-138

Sharp DJ, Rogers GC, Scholey JM (2000) Microtubule motors in mitosis. Nature 407: 41-47

Shelanski ML, Gaskin F, Cantor CR (1973) Microtubule assembly in the absence of added nucleotides. Proc Natl Acad Sci U S A 70: 765-768

Sindelar CV, Budny MJ, Rice S, Naber N, Fletterick R, Cooke R (2002) Two conformations in the human kinesin power stroke defined by X-ray crystallography and EPR spectroscopy. Nat Struct Biol 9: 844-848

Song YH, Marx A, Müller J, Woehlke G, Schliwa M, Krebs A, Hoenger A, Mandelkow E (2001) Structure of a fast kinesin: implications for ATPase mechanism and interactions with microtubules. EMBO J 20: 6213-6625

Stenoien DL & Brady ST (1997) Immunochemical analysis of kinesin light chain function. Mol Biol Cell 8: 675-689

Svoboda K, Schmidt CF, Schnapp BJ, Block SM (1993) Direct observation of kinesin stepping by optical trapping interferometry. Nature 365: 721-727

Swain KE, LeGuellec K, Philippe M, Mitchison TJ (1992) Mitotic spindle organization by a plus-end-directed microtubule motor. Nature 359: 540-543

Swain KE & Mitchison TJ (1995) Mutations in the kinesin-like protein Eg5 disrupting localization to the mitotic spindle. Proc Natl Acad U S A 92: 4289-4293

Tabish M, Siddiqui ZK, Nishikawa K, Siddiqui SS (1995) Exclusive expression of C. elegans osm-3 kinesin gene in chemosensory neurons open to the external environment. J Mol Biol 247: 377-389

Tomishige M & Vale RD (2000) Controlling kinesin by reversible disulfide cross-linking. Identifying the motility-producing conformational change. J Cell Biol 151: 1081-1092

Turk D (1992) Weiterentwicklung eines Programms für Molekülgraphik und Elektrondichte-Manipulation und seine Anwendung auf verschiedene Protein-Strukturaufklärungen. Ph.D. Thesis, Technische Universität, München.

Turner J, Anderson R, Guo J, Beraud C, Fletterick R, Sakowicz R (2001) Crystal structure of the mitotic spindle kinesin Eg5 reveals a novel conformation of the neck-linker. J Biol Chem 276: 25496-25502

Vale RD, Reese TS, Sheetz MP (1985) Identification of a novel force-generating protein, kinesin, involved in microtubule-based motility. Cell 42: 39-50

Vale RD & Fletterick RJ (1997) The design plan of kinesin motors. Annu Rev Cell Dev Biol 13: 745-777

Vale RD & Milligan RA (2000) The way things move: looking under the hood of molecular motor proteins. Science 288: 88-95

Valentine MT, Fordyce PM, Krzysiak TC, Gilbert SP, Block SM (2006) Individual dimers of the mitotic kinesin motor Eg5 step processively and support substantial loads in vitro. Nat Cell Biol 8: 470-476

Valentine MT & Gilbert SP (2007) To step or not to step? How biochemistry and mechanics influence processivity in Kinesin and Eg5. Curr Opin Cell Biol 19: 75-81

Verhey KJ, Lizotte DL, Abramson T, Barenboim L, Schnapp BJ, Rapoport TA (1998) Light chain-dependent regulation of Kinesin's interaction with microtubules. J Cell Biol 143: 1053-1066

Verhey KJ & Rapoport TA (2001) Kinesin carries the signal. Trends Biochem Sci 9: 545-550

Weingarten MD, Lockwood AH, Hwo SY, Kirschner MW (1975) A protein factor essential for microtubule assembly. Proc Natl Acad Sci U S A 72: 1858-1862

Woehlke G, Ruby AK, Hart CL, Ly B, Hom-Booher N, Vale RD (1997) Microtubule interaction site of the kinesin motor. Cell 90: 207-216

Xia CH, Roberts EA, Her LS, Liu X, Williams DS, Cleveland DW, Goldstein LS (2003) Abnormal neurofilament transport caused by targeted disruption of neuronal kinesin heavy chain KIF5A. J Cell Biol 161: 55-66

Yan Y, Sardana V, Xu B, Homnick C, Halczenko W, Buser CA, Schaber M, Hartman GD, Huber HE, Kuo LC (2004) Inhibition of a mitotic motor protein: where, how, and conformational consequences. J Mol Biol 335: 547-554

Yang JT, Saxton WM, Stewart RJ, Raff EC, Goldstein LS (1990) Evidence that the head of kinesin is sufficient for force generation and motility in vitro. Science 249: 42-47

Yang Z, Hanlon DW, Marszalek JR, Goldstein LS (1997) Identification, partial characterization, and genetic mapping of kinesin-like protein genes in mouse. Genomics 45: 123-131

Yildiz A, Tomishige M, Vale RD, Selvin PR (2004) Kinesin walks hand-over-hand. Science 303: 676-678

Acknowledgements

First, I would like to thank Prof. Frank Große for his permanent interest in my work and its representation at the Faculty of Biology and Pharmacy, University Jena.

I thank Prof. Karl Otto Greulich for giving me the opportunity to work in his research group.

I am grateful to Prof. Eberhard Unger for the challenging topic and motivating discussions.

I would especially like to thank Dr. Konrad J. Böhm for introducing me to the “kinesin-microtubule-world”. I thank for his continuous support, on which I always could trust, for time and patience, and for the helpful critical reviews and discussions. I have spent about four years in his lab and I would happily do it again.

I thank Marina Wollmann for her skilful technical support, Roland Stracke for the electron microscopy images and Kerstin Dreblow for willingness to discuss problems according practical work and life in general.

I wish to thank Dr. Karl-Heinz Gührs, Dr. Oliver Ohlenschläger and Dr. Manuel Than for practical advices and for helping me with homology modelling programs.

I would like to acknowledge my past and present colleagues and all my friends helped a lot to keep going, to forget disappointments, and to enjoy the time in Jena.

I thank my husband for his love, support, motivation and appreciation of my work.

Last but not least, I thank my parents and my sister for all of their love and unlimited support.

This study has been generously supported by research projects of the European commission within the Sixth EU Framework Programme, Contract No. NMP4-CT-2004-516989, and of the Zentaris GmbH Frankfurt/Main.

Curriculum vitae

Personal data

Name: Nikolina Dimitrova Kalchishkova

Day of birth: 10.05.1975

Place of birth: Yambol, Bulgaria

Nationality: Bulgarian

Family status: married

Education

March 2004 - July 2008	PhD thesis in the Molecular Motors Laboratory of Dr. Konrad J. Böhm, Research Group of Prof. Karl Otto Greulich, Leibniz Institute for Age Research, Fritz Lipmann Institute Jena (FLI Jena)
June 2002 - March 2004	Research work in Virus-Cell-Interaction Group of Dr. M. Messerle, Martin-Luther University, Halle-Wittenberg, Halle (Saale)
Sept. 2001 - May 2002	Research work in the Department of Medical Genetics, Medical University, Sofia, Bulgaria
Sept. 2000 - Sept. 2001	Diploma work at the Department of Medical Genetics, Medical University, Sofia
1996 - 2001	Studies of molecular biology at the University of Sofia, Bulgaria
1989 - 1994	Graduation of a language high school, Yambol, Bulgaria
1983 - 1989	Primary School, Yambol, Bulgaria

Publications:

- **Kalchishkova N**, Böhm, KJ (2008): The role of kinesin neck linker and neck in velocity regulation. *J. Mol. Biol.* 382: 127-135
- **Kalchishkova N**, Böhm, KJ: On the relevance of the core helix alpha 6 to kinesin activity generation. *Biophysical Reviews and Letters (in press)*
- Dreblow K, **Kalchishkova N**, Böhm KJ: Kinesin bypassing blockages on microtubule. *Biophysical Reviews and Letters* (*in press*)

Presentations:

Kalchishkova N: Internal structures of kinesin contributing to its velocity regulation. STREP Workshop, Potsdam, Sept. 10-11, 2007

Meeting abstracts:

- **Kalchishkova N**, Böhm KJ: Regulation of kinesin velocity by neck linker and neck structure. SFB523 International Symposium on Intracellular Trafficking and Transport, Göttingen 2008. Abstracts p.48.
- **Kalchishkova N**, Böhm KJ: Expression and characterization of human full-length Eg5 kinesin. 31st Annual Meeting of the German Society for Cell Biology, Marburg 2008. European Journal of Cell Biology, Vol. 87 (Suppl. 58), p. 24
- **Kalchishkova N**, Böhm KJ: Internal structures of kinesin contributing to its velocity regulation. GBM Fall Meeting - Molecular Life Science, Hamburg 2007. Abstracts p.38
- **Kalchishkova N**, Unger E, Böhm KJ: Effects of kinesin motor domain on kinesin activity. Abstracts 32nd FEBS Congress Molecular Machines, Vienna 2007. FEBS J., Vol. 274 (Suppl. 1), p. 99
- Dreblow K, Jayamani A, **Kalchishkova N**, Böhm KJ: Molecular mechanisms of kinesin movement along overcrowded microtubules. GBM Fall Meeting - Molecular Life Science, Hamburg, 2007. Abstracts p.36
- Dreblow K, **Kalchishkova N**, Jayamani A, Böhm KJ: Molecular mechanisms of kinesin bypassing roadblocks. Minerva-Weizman Workshop Moving Cells - From Molecules to Animals, Rehovot (Israel) 2007. Abstracts p.12
- Arsov T, Zaharieva B, **Kalchishkova N**, Damianov C, Tabakov V, Tzingilev B, Georgiev C, Todorov T, Toncheva D: Molecular cytogenetic profile of invasive transitional cell urinary bladder cancer determined by comparative genomic hybridization. European Congress of Human Genetics, Strasbourg 2002. European Journal of Human Genetics, Vol. 10 (Suppl. 1), p. 107-108

Selbstständigkeitserklärung

Die geltende Promotionsordnung der Biologisch-Pharmazeutischen Fakultät der Friedrich-Schiller-Universität ist mir bekannt. Die vorliegende Dissertation habe ich selbständig verfasst und keine anderen als die von mir angegebenen Quellen, persönlichen Mitteilungen und Hilfsmittel benutzt.

Bei der Auswahl und Auswertung des Materials sowie bei der Herstellung des Manuskripts hat mich Dr. Konrad J. Böhm unterstützt. Weitere Personen, die meine Arbeit gefördert haben, sind in der Danksagung genannt.

Ich habe nicht die Hilfe eines Promotionsberaters in Anspruch genommen und Dritte haben weder mittelbar noch unmittelbar geldwerte Leistungen von mir für Arbeiten erhalten, die im Zusammenhang mit dem Inhalt der vorliegenden Dissertation stehen.

Ich versichere außerdem, dass ich mich mit der vorliegenden Arbeit an keiner anderen Hochschule um den akademischen Grad *Doctor rerum naturalium* beworben habe und dass ich weder früher noch gegenwärtig die Eröffnung eines Verfahrens zum Erwerb des o.g. akademischen Grades an einer anderen Hochschule beantragt habe.

Jena, den 28.08.2008

Nikolina Kalchishkova